Temperature-dependant smart bead adhesion

A versatile platform for biomolecular immobilization in microfluidic devices

Noah Malmstadt

A dissertation submitted in partial fulfillment of the requirements for the degree of

Doctor of Philosophy

University of Washington
2003

Program authorized to offer degree: Department of Bioengineering

UMI Number: 3102677

ProQuest Information and Learning Company
300 North Zeeb Road
P.O. Box 1346
Ann Arbor, MI 48106-1346

In presenting this dissertation in partial fulfillment of the requirements for the Doctoral degree at the University of Washington, I agree that extensive copying of the dissertation is allowable only for scholarly purposes, consistent with "fair use" as prescribed in the U.S. Copyright Law. Requests for copying or reproduction of this dissertation may be referred to Proquest Information and Learning, 300 North Zeeb Road, Ann Arbor, MI 48106-1346, to whom the author has granted "the right to reproduce and sell (a) copies of the manuscript in microform and/or (b) printed copies of the manuscript made from microform."

Signature 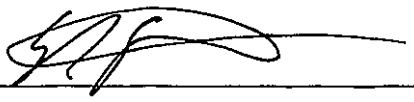

Date 8/14/03

University of Washington
Graduate School

This is to certify that I have examined this copy of a doctoral dissertation by

Noah Malmstadt

and have found that it is complete and satisfactory in all respects, and that any and all revisions requested by the final examining committee have been made.

Co-chairs of Supervisory Committee:

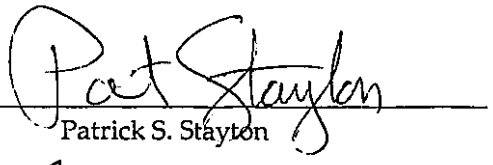

Patrick S. Stayton

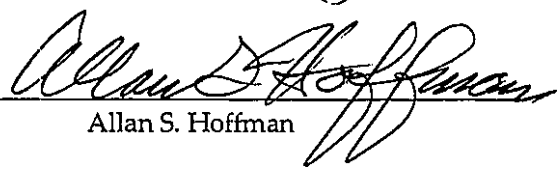

Allan S. Hoffman

Reading Committee:

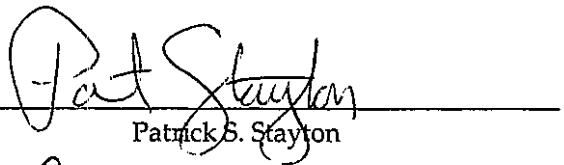

Patrick S. Stayton

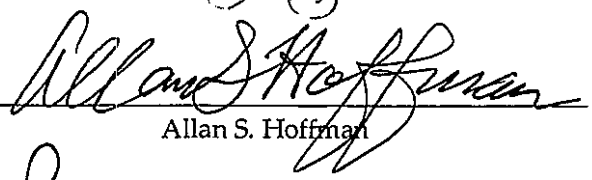

Allan S. Hoffman

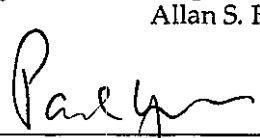

Paul Yager

Date: 8/14/03

University of Washington

Abstract

Temperature-dependant smart bead adhesion: A versatile platform for biomolecular immobilization in microfluidic devices

Noah Malmstadt

Co-chairs of the Supervisory Committee:
Professor Patrick S. Stayton and Professor Allan S. Hoffman
Department of Bioengineering

Microfluidic systems for chemical and biochemical analysis promise increased process portability, speed, and efficiency as well as decreased waste. One important aspect of microfluidic design is the incorporation of immobilized biomolecules in microfluidic devices. Of the methods that have been proposed for the microfluidic immobilization of biomolecules, few allow for reversible immobilization or end-user control over the immobilization process. The absence of these capabilities limits device flexibility and reusability.

Presented in this dissertation is a method for achieving the reversible, controlled immobilization of biomolecules in microfluidic devices. This method is based on so called "smart beads": latex nanobeads coated with the temperature-responsive smart polymer poly(*N*-isopropylacrylamide) (PNIPAAm). PNIPAAm exhibits lower critical solution temperature (LCST) behavior: soluble in aqueous solutions at room temperature, but becoming hydrophobic and reversibly aggregating at temperatures greater than ~32 °C. Similarly, 100 nm diameter polystyrene latex beads coated with PNIPAAm form a

suspension that flows easily through a microfluidic channel constructed from poly(ethylene terephthalate) (PET) at room temperature, but when the temperature of the channel is elevated above the polymer LCST, the beads aggregate and adhere to the channel walls. This adhesion is stable in the presence of flow, and reversible upon return of the channel temperature to below the polymer LCST. By co-modifying PNIPAAm-coated beads with biotinylated poly(ethylene glycol), we have made possible the controlled, reversible immobilization of diverse biomolecules.

Experiments preliminary to the development of the smart bead system described in this dissertation include the study of a PNIPAAm-based bioseparation scheme as well as the investigation of the behavior of PNIPAAm in microfluidic channels. Smart bead applications include an affinity chromatography system, in which the biotinylated beads serve as a chromatographic matrix for the separation of streptavidin from a flow stream, and an immunoassay system, in which beads modified with an antibody for the drug digoxin serve as the substrate for a competitive digoxin immunoassay. Further prospective applications of the smart bead system, such the facilitation of multiple parallel bioseparations in a single microfluidic channel, are also presented.

Table of Contents

List of Figures

List of Tables

Acknowledgements

I wish to express my gratitude to my advisors, Professors Patrick Stayton and Allan Hoffman, who, in addition to providing scientific guidance, have expressed unwavering confidence in my work and abilities. I'd also like to thank Professor Paul Yager, who introduced me to the field of microfluidics and has encouraged me to take advantage of his research group's considerable resources, both material and intellectual. The work described herein would have been impossible without those resources.

I also owe a debt of gratitude to current and former members of the Stayton, Hoffman, and Yager groups, who have, over the past six years, listened to my talks, critiqued my work, provided me with advice and material support, and consoled me when experiments failed. In particular, I'd like to thank Drs. David Hyre and Zhongli Ding in the Stayton/Hoffman group, who made essential material contributions to this dissertation in the form of protein engineering and polymer synthesis, respectively. I'd also like to single out Samarth Kulkarni and Dr. Andrew Kamholz, with whom I had early conversations regarding the potential applications of smart polymers to microfluidic devices; Dr. Catherine Cabrera, who enthusiastically encouraged me to take advantage of the resources of the Yager group; and Matthew Munson, with whom I have had countless valuable conversations about the practical and theoretical aspects of microfluidic devices.

I would also like to acknowledge several people with whom I worked on an earlier project that, while not described in this dissertation, was an important part of my graduate education: a study of two-dimensional crystallization of the protein streptavidin. The researchers at the University of Washington with whom I first began to work as a graduate student in the Stayton research group were Drs. Todd Edwards and Sandy Koppenol. They provided valuable guidance to me early in my graduate school career. I'd also like to thank Professor Masahiko Hara at the RIKEN Institute of Chemistry and Physics in Waco, Japan, who graciously invited me into his laboratory to continue the crystallization project. At RIKEN, Drs. Ken Nakajima and Keita Mitsui provided essential scientific and practical guidance.

I would like to thank the National Institutes of Health, the National Science Foundation, and the National Aeronautics and Space Administration for providing me with funding at various points in my graduate school career.

Finally, I would like to gratefully acknowledge the support and encouragement provided by my family throughout my formal education, the culmination of which is represented by this document.

Dedication

To Vandana

Chapter 1: Background and Literature Review

1.1 Summary

The research projects described in this dissertation have come about at the intersection of two emerging technologies: microfluidics and smart polymers. This chapter seeks to contextualize the research by providing the reader with a brief review of recent developments in both fields. Section 1.2 investigates recent developments in microfluidic integrated systems, including a survey of the range of laboratory operations that have been adapted to microfluidic devices and a focus on the problem of bioimmobilization in microfluidic devices, which is the major theme of chapters 4 and 5. Section 1.3 introduces smart polymer technology, with emphases on both the physics of a specific smart polymer—poly(*N*-isoproylacrylamide)—and on the practical applications of smart polymers in general. Finally, section 1.4 examines a third important technology used throughout the research described in this document: the streptavidin-biotin system.

1.2 Microfluidic Technology

1.2.1 The promise of the lab-on-a-chip

Recent decades have witnessed a revolution in computing and electronics brought about in part by microfabrication technologies capable of mass-producing integrated circuits and microprocessors. The capacity to put complete electronic circuits onto silicon chips has had an impact throughout society, and has greatly increased productivity across a broad

range of scientific and industrial fields. Now, an emerging technology promises to bring the power of microfabrication and on-chip integration to fluidic circuits for chemical and biochemical analysis. This technology—termed the lab-on-a-chip, or micro total analysis system (μTAS)—offers the concept of a complete laboratory analysis process integrated on a single microfabricated platform, in the manner of an electronic integrated circuit.[1] Several authors have recently reviewed the progress and potential of this technology.[2-6]

Microfabricated chemical analysis systems offer many advantages over conventional laboratory analysis technologies. Transport in a miniaturized fluidic (termed microfluidic) system becomes greatly simplified: the small distances involved allow for fast operation-to-operation transport with minimal void spaces, and the small scale ensures a laminar flow. Aside from fluid transport considerations, many chemical and biochemical processes are faster and more efficient on a small scale. The small volumes involved allow for relatively high concentrations of scarce reagents, and separation processes tend to be more efficient in small physical spaces[7]. Portability is also an immediate advantage of the lab-on-a-chip. A portable analysis device can be used to get immediate results in the field: medical diagnostic screening, quantification of environmental contamination, biological warfare agent detection, and biotechnology quality control are all important fields where the immediate results available from an on-site analytical device would be invaluable. There are also potential preparative applications of the lab-on-a-chip: the small size of microfluidic devices makes scale-up possible via simple parallel operation, and a parallel array of microfluidic devices could produce industrially relevant amounts of product.

1.2.2 Microfluidic unit operations and integrated applications

The development of complete on-chip integrated microfluidic laboratories depends upon the development of techniques to adapt standard laboratory operations onto microfluidic platforms; a wide range of unit operations has therefore been incorporated into μTAS devices. In this subsection, the breadth of microfluidic unit operation development will be explored, along with technologies used to drive and control flow through microfluidic devices and microfluidic fabrication techniques. Several authors have recently reviewed these issues in more detail.[8-11]

One key area of development of microfluidic unit operations has been separations technology. By far the most prominent microfluidic separation technology is capillary electrophoresis (CE).[12-14] Microchip CE involves the separation of charged biomolecules in a narrow (10-100 μm) channel according to differential mobility in an electric field (typically 1-30 kV). Standard CE in microfluidic channels is valuable for separating proteins, which carry a variety of mass-to-charge ratios[15]; separation of oligonucleotides requires capillary gel electrophoresis, which has also been implemented in a microfabricated on-chip platform[16,17]. Various chromatographic schemes have also been devised for use in microfluidic devices[18-22], allowing for separations according to various physiochemical properties and biochemical affinity interactions. Physiochemical chromatography schemes are typically based on the interaction between and immobilized stationary phase and a flowing mobile phase. The fabrication of physically immobilized phases has proven to be a challenge; however, recent work in micellar chromatography, which is based on the interaction between a mobile phase and micelles of an amphiphilic compound suspended in that phase, has the potential to

ameliorate some of these difficulties for hydrophobic interaction chromatography systems.[23] Affinity chromatography requires immobilization of biochemically active affinity moieties in microfluidic channels: this issue is explored in greater detail in section 1.2.3. Schemes for separating magnetic particles from a flow stream have also been proposed[24], raising the prospect of separation of biomolecules via binding to affinity-modified magnetic beads.

In addition to these batch separation techniques, which separate species in the direction of flow, several techniques have been developed to separate species in the direction transverse to flow. One such scheme relies on differences in rates of diffusion[25] of biomolecules.[25] Flow in microfluidic systems is laminar. Therefore, after a flow has developed, there is no convective transport in the direction perpendicular to the flow. Since transport in this direction is strictly diffusive (in the absence of an external field), the distance that a molecule travels in this direction over a fixed length of time is determined entirely by its rate of diffusion. Molecules can therefore be separated along the direction perpendicular to flow according to differential diffusion distances over a fixed residence time. Another system for separating molecules and particles in the direction transverse to flow relies on an electric field oriented perpendicular to the flow axis.[26,27] Isoelectric focusing of proteins[28] and bacteria[29] has been demonstrated in such a system.

Outside of separation systems, a wide variety of unit operations have been developed for microfluidic devices. Microfluidic reactors include heterogeneous phase immobilized enzyme bioreactors [30-35], enzymatic flow reactors for protein digestion[36,37] and enzyme inhibition[38-40] and kinetics[41] assays, and temperature-controlled microreaction chambers and channels for polymerase chain reaction (PCR)[42-45]. Mixing of fluid streams has proven to be a nontrivial problem in microfluidic devices: turbulent mixing cannot be relied

on due to the low-Reynolds-number environment, and it's a difficult microfabrication problem to insert an impeller or stir bar[46] into a microfluidic channel. Consequentially, several microfluidic constructs have been developed to facilitate the mixing of fluid streams.[47-50] Methods for temperature control in microfluidic channels have also been developed.[51] Detection of chemical species in microfluidic devices has focused on fluorescence[52,53] and electrochemical[54,55] methods, but other approaches, such as surface plasmon resonance (SPR)-based detection[56] have also received much recent attention.

Several device fabrication technologies have been explored; along with traditional silicon lithography[57] (also used for glass and quartz device fabrication), researchers have investigated polymer molding[58,59] and polymer laser ablation[60] approaches. There are also a number of options for driving the flow through a μTAS device, such as microsyringe pumping, electrokinetic flow[61,62], gravitationally driven flow, and centrifugally driven flow[63]. There has also been much recent interest in microelectromechanical pumping systems, which allow for pumps to be integrated directly onto microfluidic devices, further improving μTAS integration and portability.[64,65] Several approaches to controlling flow through microfluidic devices have been explored. Microelectromechanical valves—both passive and actively actuated—have been developed; such valves have been most prominently deployed in devices fabricated from silicon.[65] A related valve technology, more useful in polymeric devices, relies on separate control channels that interface with the microfluidic channels at flexible (but impermeable) polymer junctions. Increasing pressure in a control channel pushes out the polymer junction material into the microfluidic channel, closing the channel off.[66,67] There have also been recent publications describing the incorporation of stimulus-responsive polymer gels into microfluidic devices as valves: when the polymer is stimulated,

the gel expands, closing off the channel.[68,69] A final valve technology that has received recent attention relies on channel surface hydrophobicity or fluid surface tension resulting from an unusual channel geometry to retain fluid.[63,70] The hydrophobic or high-surface-tension region is impassible at low fluid pressures, but fluid can be forced past at higher driving pressures—valves of this type allow flow to be actively controlled simply through control of the driving pressure.

Despite the relative youth of μTAS technology, several complete integrated systems with discrete applications have been presented in the literature. Prominent among these are systems to perform sample pre-processing for mass spectrometry: microfluidic technology allows for improved automation of mass spectrometers, contributing to the development of proteomic research.[36,71-73] Reactors for performing PCR have already been mentioned; some of these have been integrated with CE units to yield complete DNA analysis devices.[44] Multiple integrated microfluidic systems for performing high-throughput enzyme inhibition assays have been developed[38,63], as have a number of immunoassay devices[74-78]. Microfluidic devices have also found recent application in the high-throughput screening of conditions for protein crystallization.[79,80]

1.2.3 Biomolecular immobilization in microfluidic devices

1.2.3.1 The importance of biomolecular immobilization to microfluidic technology

The technology described in chapters 4 and 5 of this document addresses an issue of paramount importance to the continuing development of integrated microfluidic systems: the issue of biomolecular immobilization. Immobilized biomolecules have long played a key role

in biotechnology and molecular biology research. Affinity chromatography and microtiter plate-based immunoassays are fundamental laboratory techniques that require an immobilized, biochemically active, phase. Many emerging technologies—including microarray analysis of genomic[81] and proteomic[82,83] material, micro/nanobead-based assays and separation processes, and various surface patterning-based approaches to tissue culture and tissue engineering—also require the immobilization of biomolecules onto a solid surface. As microfluidic analytical systems mature, many of these technologies will be adapted to microfluidic platforms. This adaptation will require the development of flexible, generally applicable techniques for immobilizing biomolecules in microfluidic devices.

The system described in this dissertation promises to deliver this generality and flexibility by providing the means to reversibly and controllably modify the walls of microfluidic channels with arbitrary biomolecules on an on-demand basis. The benefits of this system are best understood in the context of an examination of current approaches to biomolecular immobilization in microfluidic devices. There are currently three broad categories of microfluidic immobilization techniques: surface modification of microfluidic channel walls, packing of microfluidic channels with biomolecule-bearing beads, and packing of microfluidic channels with biomolecule-bearing porous monolithic slabs. This section contains an enumeration of the advantages and disadvantages of each of these three approaches, as well as a brief summary of specific implementations of each approach in the literature.

1.2.3.2 Surface modification

The approach to biomolecular immobilization described in chapters 4 and 5 is essentially a surface modification technique. Surface modification involves the chemical attachment or physical adsorption of molecules of interest to the walls of a microfluidic channel. Fluid flowing through the channel comes into contact with the modified surfaces and components of this fluid can interact with the immobilized molecules. The key advantages of surface modification for biochemical immobilization are its relative simplicity in implementation and its minimal impact on flow behavior. Surface modification does not require the microfabrication of any special features in channels, such as the frets or weirs required by packed-bead approaches. A channel of any size or geometry can be modified. Of course, specific materials require specific modification approaches; however, a wide range of modification techniques has been developed, accommodating all commonly used microfluidic device materials (specific examples are given below). Since surface modification does not affect device geometry, there is no additional pressure drop associated with a modified channel segment, and no danger of the formation of void spaces as a result of modification.

Since the surface chemistry of microfluidic channels has a significant impact on electroosmotic flow (EOF) through those channels, much work in microfluidic surface modification focused not on coating channel walls with active moieties for chemical and biochemical processes, but on the optimization of the EOF properties of channels.[84-87] Similarly, modification of surfaces with biomolecules can have an unpredictable or detrimental effect on EOF through the modified channels; consider, for example, the dampening of EOF mobility observed by Dodge *et al.* in silanized and protein-coated glass

channels.[76] Surface modification approaches to biomolecular immobilization are therefore often incompatible with electroosmotically-driven flow.

In contrast to other approaches to biomolecular immobilization (packing with beads or porous slabs), surface modification approaches suffer from a relatively low surface-area-to-volume ratio. Molecules in a flow stream must diffuse to the walls of the channel in order to interact with the chemical moieties immobilized there. This is an especially important concern for biochemical applications, which may involve large macromolecules with low rates of diffusion. Fortunately, the small size of microfluidic channels brings the entire flow stream close to the walls, requiring diffusion over only short distances. Given sufficient knowledge of the properties of the fluids and molecules involved in a given microfluidic process, it is possible to engineer a device such that the issue of diffusion is taken into account and sufficient transport of molecules to the channel surface is allowed.

Many studies of the biochemical modification of microfluidic channel surfaces have relied on nonspecific physisorption of proteins. Linder et al.[88] demonstrated the adsorption of biotinylated IgG to poly(dimethyl siloxane) (PDMS) channels, followed by binding to avidin and biotinylated dextran. Polymer channels have also been treated by laser ablation to increase their surface roughness and promote protein adsorption.[89] For channels made of materials not amenable to protein adsorption, surfaces have been modified: treatments include silane coatings on silicon[90] and glass[76] surfaces, and alkanethiol coatings on gold surfaces[90]. In these studies, treated surfaces demonstrated nonspecific protein adsorption. Physical adsorption of DNA to polycarbonate microchannels, modified with UV radiation to bear surface carboxylate groups, has been used to purify DNA sequencing reaction products in preparation for electrophoresis.[91] In addition to these nonspecific approaches, surfaces

have been modified with affinity moieties to accommodate specific protein binding. Affinity approaches include coating of PDMS surfaces with a lipid bilayer functionalized with an antigen for IgG binding[75] or with biotin for subsequent binding of avidin and a biotinylated enzyme [32]. A photoactive biotin derivative has also been pattered onto PDMS microfluidic surfaces via lithographic techniques.[92] Finally, microfluidic channel surfaces have been modified with reactive moieties to allow for the covalent immobilization of proteins. Such modifications include the coating of glass and silicon channels with organosilanes containing reactive pendant groups[77,93] and chemical vapor deposition of reactive polymer thin films onto PDMS[94].

1.2.3.3 Bead packing

Affinity chromatography is typically performed on columns that have been packed with beads modified to bear the affinity moiety of interest. Using such systems as a model, several researchers have packed microfluidic channels with biochemically-modified beads to create columns for affinity bioseparations or bioreactions. The central advantage of such an approach is that bead-packed channels have an enormous surface-area-to-volume ratio, maximizing the opportunity for interactions between the immobilized biomolecule and components of the fluid flowing through the packed channel. The smaller the beads, the more tightly packed the channel; tighter packing decreases the distance that components of the fluid must diffuse in order to reach the active surface.

Unfortunately, tightly packed columns are associated with large pressure drops. In fact, the pressure drop over a bead-packed column scales as the inverse of the square of the bead diameter. Consider, for example, a column with typically microfluidic dimensions of

0.3 mm × 0.1 mm × 20 mm, and beads of 5 μm diameter. This column would be expected theoretically to produce a pressure drop of 1.28 atm at a flow rate of 344 nL/min; pressure would be expected to increase with narrower channels, smaller beads, and faster flow rates.[95] In the context of microfabricated mechanical pumps, this is an unusually high pressure: a recent review of microfabricated pumps found only two reports of pumps capable of generating static pressure heads of greater than 1 atm out of approximately 45 reports reviewed.[64] Electroosmotic pumping is capable of generating significantly more pressure—up to 140 atm[96]—and standard lab-scale pumping systems can be coupled to microfluidic devices to provide arbitrarily high pressures. Nevertheless, the high back pressure generated by packed bead columns places a severe restriction on the flow-generating technology available to devices incorporating such columns.

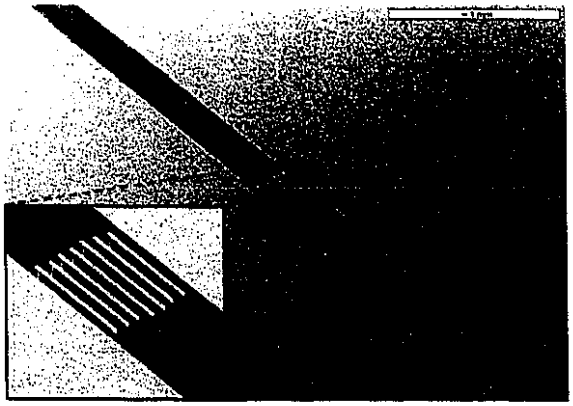

Figure 1.1: A scanning electron micrograph (SEM) of a frit in a microfluidic channel. Scale bar (white, upper right) is 1 mm long. Reproduced with permission from reference 97.

In addition to limits imposed by their high back pressure, packed bead columns demand specialized fabrication steps. In order to hold beads in place in a microfluidic channel, special microstructures must be fabricated at the exit of the channel. One such restraining structure is a frit: a series of ridges at the end of a column spaced more closely than the diameter of the beads to be restrained (Figure 1.1). Microfluidic frits have been manufactured in silicon[70,97,98], PDMS[22,33], and SU-8 photoresist[34]. Another option is a weir: a constriction (typically a in the form of a raised platform) in a channel that narrows the

channel width to below the bead diameter (Figure 1.2). Microfluidic weirs have been manufactured in silicon[99,100] and glass[41,78,101,102]. In addition to increasing the complexity of fabrication, these approaches limit the reversibility of the packing step: beads held in place by a microfabricated fret or weir cannot be easily removed and replaced, limiting the lifetime and reusability of packed bead columns. Furthermore, frits and weirs both distort the flow profile through channels, leading to dispersion and band-broadening[97]; this effect is amplified for eletroosmotically-driven flow, in which these structures distort the electric field, further disrupting the flow. Frits introduce special problems: they can be fragile, leading to failures of column packing, and their many sharp edges can serve as nucleation points for bubble formation.[103] Another approach to column packing is so-called "keystone" packing, which involves flowing beads into a tapered column in such a manner that they crowd together at the point of constriction and form a plug in the channel.[103] While this approach does avoid the fabrication issues raised by frits and weirs, it is similarly irreversible and it generates the high back-pressure typical of bead-packed columns. Another, ingenious, method for trapping beads in microfluidic channels was recently reported: pump-driven and electroosmotic flows are operated against one another, generating a recirculating flow that holds beads in place in a channel while analyte fluids are pumped through the same channel.[104] While this technique does allow for column packing without special microstuctures, as well as for controlled

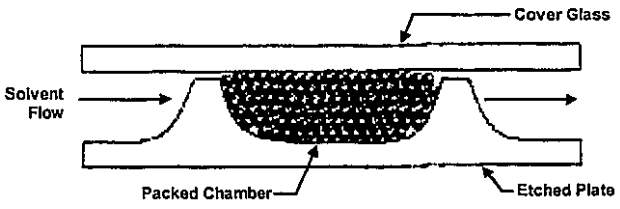

Figure 1.2: A cross-sectional diagram of a microfluidic chamber packed with beads, retained on either side by a weir. Reproduced with permission from reference 101. © Copyright 2000 American Chemical Society.

reversibility of packing, it requires a highly specialized flow pattern and therefore may not be generally applicable.

1.2.3.4 Monolithic slab packing

Several researchers have reported packing microfluidic channels with porous monolithic polymer slabs. Biomolecules immobilized in these slabs are exposed to fluid flowing through the pores. Like bead-packed columns, monolithic polymer-packed columns provide for a high surface-area-to-volume ratio. At the same time, they avoid many of the difficulties associated with packing a microfluidic column with beads. No frits or weirs are required to hold a monolith in place: a reactive monomer solution is simply flowed into the channel and polymerization is performed *in situ*, completely filling the channel with polymer, which can be bonded chemically to the channel walls or merely held in place by the geometry of the channel. Columns packed in this manner do share some disadvantages with packed bead columns, however. Since fluids passing though such columns must perfuse through a system of pores, there can be a considerable pressure drop across the polymer monolith. For example, Rohr et al. reported a back pressure of 8.9 atm for a 10 mm × 0.2 mm × 0.5 mm column packed with a monolithic slab of 50% porosity with a median pore diameter of 1 μm, at a flow rate of 1 μL/min.[105] Of course, the pressure drop over the column is highly dependant on the pore diameter and porosity of the column: increasing both of these parameters decreases the pressure drop. Techniques have been developed for producing a wide range of pore sizes, porosities, and, consequentially, column fluidic properties.[105,106] Another disadvantage monolithic slabs share with packed bead columns is the irreversibility of the packing procedure. Once the polymerization has been performed,

the polymer cannot be removed from the column. Finally, while porous monolithic polymer columns seem like an appropriate substrate for biomolecular immobilization (and, in fact, protein immobilization to such materials has been thoroughly explored on larger scales[107]), microfluidic demonstrations of such immobilization have been limited. While porous slabs have been used as substrates for microfluidic ion-exchange[108] and hydrophobic-interaction[109,110] chromatography, as well as for microfluidic mixing[105], there has been only one microfluidic demonstration of protein immobilization to such a substrate: Peterson et al. demonstrated the immobilization of trypsin to a porous polymer monolith to form a microfluidic enzymatic bioreactor[30].

1.3 Smart Polymers

1.3.1 The physiochemical properties of PNIPAAm and similar smart polymers

"Smart", or "intelligent", or "stimuli-responsive" polymers are synthetic polymers that undergo a drastic and reversible hydrophobic-hydrophilic phase transition in response to a change in a specific environmental condition (the

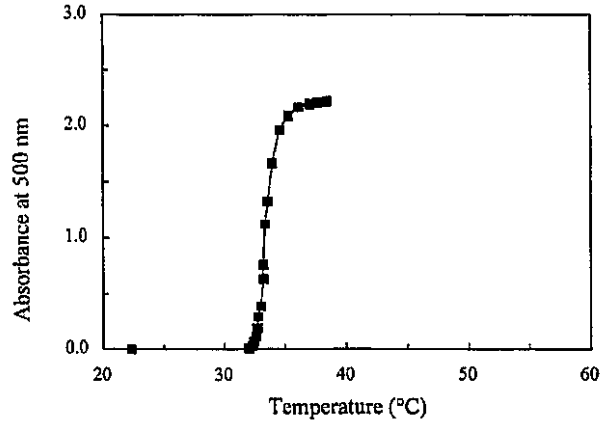

Figure 1.3: A typical PNIPAAm cloud-point diagram, showing the polymer's phase transition. As PNIPAAm transitions from hydrophilic to hydrophobic, it aggregates and the optical absorbance of the polymer solution increases. Note the sharpness of the phase transition. Reproduced from reference 126, © Copyright 2000, with permission from Elsevier.

stimulus). This transition is typically very sharp—a complete phase change is observed over a very short range of values of the stimulus condition. Consider, for example, the phase transition of poly(*N*-isopropylacrylamide) (PNIPAAm) in response to a temperature change shown in Figure 1.3: the phase transition begins and is completed over a range of less than 5 degrees centigrade. This sharp response to environmental stimulus is the key to the utility of smart polymers, since it allows these polymers to operate as an easily controlled binary switch. The phase transition behavior of smart polymers is further valuable because of the simplicity of the properties to which various smart polymers are responsive: there are smart polymers which respond to temperature, pH, ionic strength, and specific wavelengths of light.[111] Since smart polymers allow for the coupling of controlled macroscopic system properties to the microscopic behavior of the system, they are valuable molecular engineering tools.

The projects described in this dissertation rely on PNIPAAm as a means of separation and adhesion via aggregation upon hydophilic-hydrophobic phase transition. PNIPAAm (Figure 1.4) is possibly the best-studied smart polymer, with work on its temperature-sensitive behavior performed as early as 1968.[112] Schild published a thorough review of work on PNIPAAm in 1992.[113] PNIPAAm exhibits lower critical solution temperature (LCST) behavior: it is soluble in aqueous conditions below a certain temperature; above that temperature it undergoes a transition to a hydrophobic phase and aggregates out of solution. Two approaches have been applied to determining the LCST of PNIPAAm: observation of solution turbidity upon polymer aggregation[112] and calorimetry to detect the heat of phase

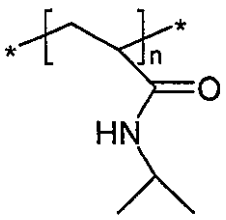

Figure 1.4: The chemical structure of the repeating unit of PNIPAAm.

transition[114]. The LCST of PNIPAAm is dependent on the ionic strength of the solution. In pure water, PNIPAAm has an LCST between 31 °C and 32 °C.[112] At 500 mM NaCl, the LCST is lowered to 27-28 °C, and the LCST drops to below room temperature at NaCl concentrations approaching 1M.[115] This dependence on ionic strength is similar to the salting-out effect commonly observed in aqueous protein solutions. The LCST is also dependent on pressure, increasing to 35°C at 400 atm.[116] PNIPAAm LCST decreases slightly with increasing polymer concentration at low polymer concentrations, though it is constant with increasing concentration above about 5 wt% polymer.[116] There is no strong dependence of LCST upon polymer molecular weigh.t[117] Conjugation of PNIPAAM to various biomolecules has also been shown to have very little effect on its LCST.[118]

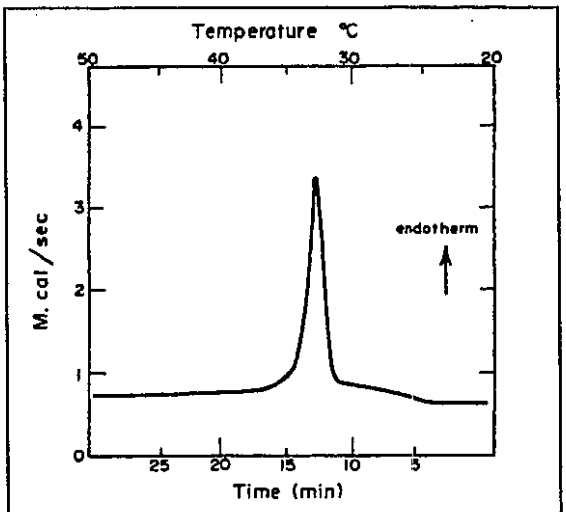

Figure 1.5: Calorimetry of PNIPAAm phase transition. As the temperature of the solution is increased, an endothermic peak is apparent near the LCST. Reproduced from reference 112.

The mechanism of PNIPAAm phase transition is a matter of some contention. Early calorimetric work established that the phase transition is endothermic, implying that it is an entropically driven process (Figure 1.5).[112] The polymer-solvent system can therefore be described as in balance between enthalpic forces favoring the solvated configuration and an entropic penalty associated with this configuration and favoring phase separation. It is clear that the source of the entropy gained upon hydrophobic polymer aggregation is the disordering of structured waters about the hydrophobic groups on the polymer; this conclusion is supported by several studies of

PNIPAAm and similar polymers[119,120]. The source of the countervailing enthalpy, however, is less clear. One possible source is the heat of dissociation of the hydrogen bonds between the hydrophilic groups on the polymer and water molecules; early conjecture favored this source.[112] However, there is evidence that the polymer is highly hydrated in its phase-separated state, implying that not many of these hydrogen bonds are actually broken upon phase transition.[112,121-123] The other potential source of the enthalpy of phase transition, suggested by a number of calorimetric studies, is the breaking of hydrogen bonds in the ordered water network surrounding the hydrophobic polymer groups in the solvated phase.[114,124] A related controversy is the source of the temperature dependence of phase separation. Those who suggest that the enthalpy of phase separation is related to the breaking of solvent-polymer hydrogen bonds argue that these bonds are destabilized as the temperature increases until the entropic pressure towards phase separation overcomes the enthalpic penalty of breaking the bonds. On the other hand, a similar effect has been proposed for the hydrogen bonds between water molecules in the hydrophobic solvation cages: they are destabilized as temperature increases, decreasing the enthalpic penalty of their dissociation. In addition, since the ordered water systems prevent intramolecular hydrophobic interactions in the polymer, their destabilization makes such interactions, and subsequent polymer collapse, more likely.[114] The system is complex and incompletely understood, and there is no single dominant theory describing the molecular origin of temperature dependant phase-transition.

One useful feature of the PNIPAAm system is that the LCST of the system is tunable, allowing for the phase separation behavior to be tailored to the requirements of an application. As described above, increased ionic strength can be used to lower the LCST of

the polymer. In addition, the LCST of the polymer can be altered via the inclusion of comonomers. NIPAAm copolymers with ionic or polar monomers incorporated have an elevated LCST, while copolymers incorporating hydrophobic monomers have a depressed LCST.[114] The stereochemical order of the polymer also has an impact: isotactic poly(diethylacrylamide) (PDEAm), a related temperature-sensitive smart polymer, has an LCST of 40°C, elevated from the 32°C LCST of heterotactic PDEAm (figure 1.6).[125]

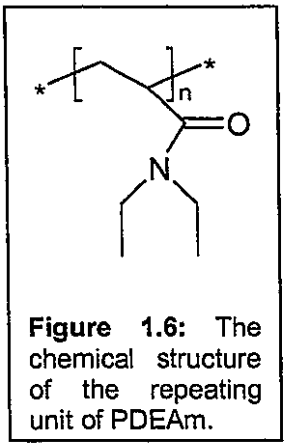

Figure 1.6: The chemical structure of the repeating unit of PDEAm.

1.3.2 PNIPAAM aggregation behavior

At temperatures above the LCST, hydrophobic PNIPAAm molecules aggregate; this aggregation is observable as the increase in turbidity of PNIPAAm solutions above the LCST. An understanding of the mechanism of PNIPAAm aggregation and the structure and properties of PNIPAAm aggregate particles is important for the work at hand, which relies on the aggregation of PNIPAAm-conjugated molecules and PNIPAAm-coated particles. PNIPAAm aggregation can roughly be described as a three-step process. Initially, PNIPAAm molecules collapse from a random coil configuration to a globular configuration. This collapse has been observed by static and dynamic light scattering experiments, which show a radical decrease in the radius of gyration and hydrodynamic radius of PNIPAAm in very dilute solutions upon elevation of the temperature above the LCST; further analysis of light scattering data reveals that this transition is accompanied by a change in the shape of the PNIPAAm molecules from random coils to hard spheres.[121] The coil-globule transition of PNIPAAm has also been observed via atomic force microscopy[126] and rheological

techniques[127]. Evidence that this initial transition is intramolecular (i.e., it results from the collapse of single hydrophobic molecules rather than the aggregation of many molecules) comes from microcalorimetric studies, which establish that the polymer collapses in domains of approximately 500 monomers each.[128] These studies of the phase transition of single PNIPAAm molecules must be performed either at very low polymer concentration or in the presence of surfactants in order to prevent higher-order aggregation events that would obscure the data.

Figure 1.7: Transmission electron micrograph of PNIPAAm mesoglobules, stained with tungstophosphoric acid. The scale bar corresponds to 500 nm. Reproduced from reference 130, © Copyright 1997, with permission from Elsevier.

The single-molecule globules formed by PNIPAAm above its LCST are not stable; molecular collapse is soon followed by the formation of "mesoglobules": extremely monodisperse spherical particles, with radii on the order of 100 nm, made up of many polymer molecules. Mesoglobules, which are stable for days at a time at low concentrations, have been observed via dynamic light scattering and transmission electron microscopy (Figure 1.7).[129-131] Hahn *et al.* have characterized the sedimentation behavior of PNIPAAm and NIPAAm copolymer mesoglobules; as the temperature of a PNIPAAm solution is increased above the LCST, the sedimentation coefficient of PNIPAAm molecules increases from ~3 S (comparable to a protein molecule) to ~800 S.[115] This sedimentation coefficient translates to a settling velocity of about 5×10^{-5} mm/min in the earth's gravitational field;

however, further PNIPAAm aggregation creates particles that sediment more quickly. At sufficiently high concentrations, a third aggregation step takes place: the formation of micrometer-scale aggregates. This step has not been studied in detail, but it most likely involves the association of mesoglobules into progressively larger aggregates in a flocculation process.

1.3.3 Smart polymer applications

Reviews of the current and potential applications of smart polymers to the biosciences have been published.[111,132] One key application of smart polymers has been to affinity precipitation systems: separation systems that rely on an interaction between a target molecule and an affinity ligand used to specifically precipitate the target from solution.[133-135] Smart polymers have made it possible to trigger the precipitation event with the polymer phase transition stimulus. In early smart polymer affinity precipitation work, PNIPAAm was conjugated to proteins to accomplish separation of antibodies[136] and antigens[137,138]. PNIPAAm has since been conjugated to a variety of ligands for affinity precipitation applications. These ligands include: dextran, for the separation of anti-dextran antibodies[139]; double-stranded DNA, for separation of DNA-binding proteins[140]; single-stranded DNA, for separation of oligonucleotide-labeled proteins[141]; lysozyme substrate analogs[142,143] and anti-lysozyme antibody fragments[144], for the separation of lysozyme; and iminobiotin, for separation of avidin[145]. Other temperature sensitive polymers are available for affinity precipitation: PDEAM has been conjugated to a protease substrate analog for the purification of subtilisin carlsberg[146]. Custom-designed copolymers, sensitive to both temperature and

pH, have been used in affinity precipitation schemes to purify proteins by metal-affinity interactions[147] and antibody-antigen interactions[148]. Finally, avidin has been separated using biotin-conjugated latex microbeads which aggregate in response to changes in ionic strength and pH.[149] Since standard bioconjugation techniques can be used to attach the many types of smart polymers to any of a wide variety of biomolecules, smart polymer based affinity precipitation allows for the design of highly specified bioseparation processes, with precisely engineered molecular characteristics. An example of such a design—in which protein engineering techniques are used to design a mutant protein/smart polymer affinity separation agent with highly specified properties—is described in detail in Chapter 2.

In addition to their widespread use in affinity precipitation, smart polymers have found applications in many other separation systems. PNIPAAm has been used as the basis of a capillary electrophoresis matrix that can be easily loaded into a capillary at low temperatures but that forms an effective DNA sieve above the polymer LCST.[150] Similarly, a temperature-sensitive polymer has served as the basis of a CE matrix with a mesh size that varies with temperature.[151] Smart polymers have also been used as control elements in chromatographic separations: temperature sensitive column packings have been developed for ionic[152,153], hydrophobic[154-157], size exclusion[158-161], and affinity[162-164] chromatography. In these chromatographic systems, the temperature responsiveness of the column allows either for different chromatographic resolution properties at different temperatures (thermally tunable columns) or for elution of a bound separation product in response to a temperature change.

Smart polymers have also seen a wide range of applications away from separation systems. Cross-linked hydrogels made from smart polymers have been shown to absorb and

deliver molecular payloads in a stimuli-responsive manner—a behavior with potential application to drug delivery.[165-167] Smart polymer hydrogels have also been used as valves in microfluidic devices: hydrogels are synthesized inside of microfluidic channels such that the channel is blocked when the gel is expanded but open when the gel is collapsed. Valves of this type have been implemented with both pH-[68,168-170] and temperature-responsive[69] smart polymers. Surfaces coated with thermoresponsive smart polymers have a variable, temperature-dependant hydrophobicity.[171] Such surfaces have been shown to allow eukaryotic cell attachment in a temperature-dependant manner: cells bind at high temperature, while the surface is hydrophobic, but they detach at lower temperatures, when the polymer on the surface transitions to its hydrophilic phase.[172,173] These applications rely on bulk properties of structures made from smart polymers; perhaps more exciting from a molecular engineering perspective are applications in which individual smart polymer molecules are conjugated to biomolecules in order to confer new properties to these biomolecules.[111] Conjugation of a temperature-sensitive smart polymer to the proteolytic enzyme trypsin makes it possible to control enzyme activity by allowing the enzyme to be removed from solution in response to thermal stimulus.[117,174-176] Control of enzyme activity has also been achieved via site-specific conjugation of a light-sensitive polymer to the enzyme endoglucanase 12A.[177] Conjugation of both light- and temperature-sensitive polymers to locations near the streptavidin binding site has been shown to impart stimuli-responsive biotin-binding behavior.[178-182] Finally, pH-sensitive polymers have been incorporated in biomolecular complexes to direct the intracellular delivery of therapeutic agents via pH-sensitive endosome disruption.[183-187]

An interesting application of smart polymers, and one that has a direct bearing on the work presented in this dissertation, is the synthesis of latex beads that incorporate PNIPAAm for the purpose of temperature-responsive flocculation. One example of such an application involves beads with surface coatings of both latex PNIPAAm and immobilized enzyme: the enzyme activity can be removed from solution by thermally flocculating the beads and returned to solution via reversal of the thermal stimulus.[188,189] Similar bead have been manufactured to bear antibodies on their surfaces, via both nonspecific adsorption and covalent attachment.[190] PNIPAAm chains conjugated to the surface of latex beads have been shown to control, in a temperature-responsive manner, the accessibility of soluble substrates to enzyme molecules also immobilized on the bead surfaces.[191] NIPAAm-containing latex beads have also been synthesized with a co-monomer that has RNA-binding properties; these beads can serve as an affinity precipitation system for RNA.[192] In the context of the work presented here, the key lesson of these PNIPAAm bead systems is that, immobilized on the surface of latex beads, the temperature-sensitive polymer confers its thermal sensitivity to the beads. PNIPAAm-coated beads aggregate in much the same manner as free PNIPAAm molecules do, apparently due to the impact of the PNIPAAm phase transition on the beads' surface properties. Chapters 4 and 5 describe work in which PNIPAAm-coated latex beads were used as a temperature-sensitive immobilization substrate in microfluidic channels.

1.4 The Biotin-Streptavidin System

1.4.1 Introduction

The streptavidin-biotin system plays a key role in many of the experiments described in this dissertation, either as a model system for affinity interactions (Chapters 2 and 4) or as a molecular linker in a bioassay system (Chapter 5). Streptavidin is a 53 kDa tetrameric protein produced in nature by the bacterium *Streptomyces avidinii*.[193-195] Each of the four streptavidin monomers binds one molecule of the vitamin biotin (Figure 1.8) with extraordinarily high affinity (Figure 1.9). Because of this high affinity, the capacity of streptavidin to bind multiple biotin molecules, and the ease with which a great variety of molecules can be biotinylated, the biotin-streptavidin system has become a key component of many processes in biotechnology and the biomedical sciences.[196,197] Streptavidin is named for its similarity to the avian protein avidin, which is another tetrameric biotin-binding protein, and which actually has a slightly higher biotin-binding

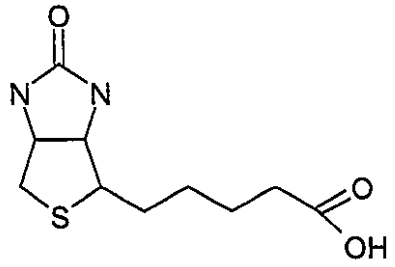

Figure 1.8: The chemical structure of biotin.

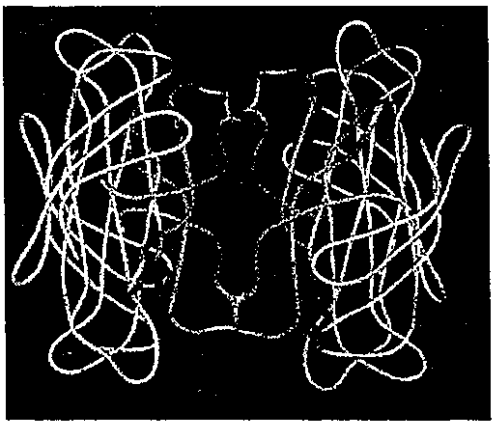

Figure 1.9: A ribbon diagram representation of the molecular structure of streptavidin. Bound biotin molecules are shown in red. The fourfold symmetry of the molecule is apparent, as is the orientation of the binding sites towards two binding faces on opposite sides of the molecule.

affinity than that of streptavidin.[195] Avidin, however, is a heterogeneously glycosylated protein with an exceptionally high pI; streptavidin's relative simplicity (including its bacterial origin, which make it more accessible to recombinant protein engineering) favors it for biotechnology applications.

The utility of the biotin-streptavidin system is limited, however, by the fact that, in practical terms, the biotin-streptavidin interaction is kinetically irreversible. The dissociation of bound biotin from streptavidin is a first-order process, described by a rate constant k_{off}. The dissociation rate constant of wild-type (WT) streptavidin from biotin at 25 °C is 5.6×10^{-6} s^{-1}, corresponding to a binding half-life of over 34 hours.[198,199] Since dissociation takes so long, biotinylated molecules that have been bound to streptavidin cannot reasonably be released and recovered in the laboratory. Fortunately, molecular engineering techniques have been applied to the biotin-streptavidin system, allowing for some fine-tuning of the interaction.

1.4.2 Molecular engineering of the biotin-streptavidin interaction

Work towards altering the characteristics of the biotin-streptavidin interaction has focused on recombinant protein engineering of streptavidin to yield mutants with relatively high biotin off-rates. Structural studies of the streptavidin-biotin complex have identified a number of important van der Waals and hydrogen bonding interactions at the biotin binding site.[200,201] Elimination of hydrophobic interactions via site-directed mutagenesis of various tryptophan residues resulted in between a one- and two-order-of-magnitude increase in the off-rate of biotin from streptavidin.[198,202] Mutagenic elimination of residues that form hydrogen bonds to the ureido group of biotin had a similar effect, increasing the rate of

dissociation by over 2 orders of magnitude relative to the wild-type protein.[203] These kinetic changes are accompanied by similar changes in the affinity binding constant.[198,203]

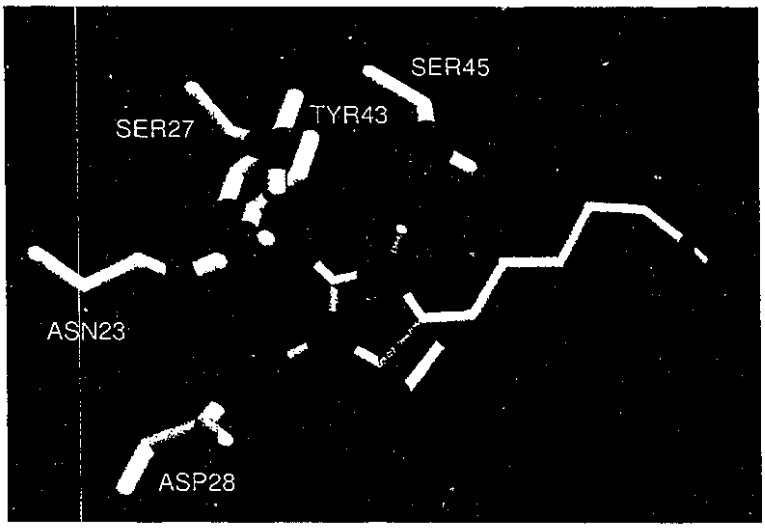

Figure 1.10: Key hydrogen bonds in the streptavidin binding pocket. In the S45A mutant, the hydrogen bond to residue Ser45 is eliminated. Image courtesy of D. Hyre.

In the work described in Chapter 2, a mutant streptavidin with an extraordinarily high biotin off-rate has been used to make the biotin-streptavidin system reversible, while retaining specificity and a high affinity. The mutant protein, in which residue 45 has been changed from serine to alanine (S45A) via recombinant techniques, has a biotin off-rate of 0.05 s^{-1} at 37°C, corresponding to a binding half-life of 14 seconds—over four orders of magnitude faster than dissociation from WT streptavidin (Figure 1.10).[204] Hence, when a complex of S45A streptavidin bound to a biotinylated macromolecule is treated with an excess of free biotin, the macromolecule should be completely displaced by the free biotin within minutes. In the work presented in the next chapter, this capacity for release has been investigated in the context of an affinity thermoprecipitation system, in which a conjugate of S45A streptavidin and thermoresponsive smart polymer serves as a bioseparation agent for a variety of biotinylated macromolecules.

Chapter 2: Affinity Thermoprecipitation and Recovery of Biotinylated Biomolecules via a Mutant Streptavidin-Smart Polymer Conjugate*

2.1 Summary

The first project described in this dissertation involves the development of an affinity precipitation system based on a conjugate of a smart polymer to a high off-rate streptavidin mutant. This work was originally undertaken as part of a long-term project seeking to adapt affinity precipitation technology to a microfluidic platform; however, the work described in this chapter stands independent of any of the work with microfluidics described in the subsequent chapters. The chapter begins with an introduction to bioseparation technologies, with a focus on affinity separation technologies. The design, implementation, and results of experiments with the new affinity precipitation system are then described.

2.2 Background: The Importance of Affinity Precipitation Among Bioseparation Technologies

2.2.1 Introduction to bioseparations

Separation is a key process in classical chemical engineering: purification of individual chemical species is necessary both for final products and for intermediates in

complex multi-operation processes. As the field of biotechnology has matured, the separation of specific biological molecules from complex mixtures has proven to be an equally important process. Efficient, specific bioseparation processes are necessary because of the stringent purity requirements in biological systems (both in pharmaceutics, where contamination with nonspecific biochemical agents poses a potential health risk, and in research applications, where such contamination can have an erratic effect on results). Efficiency is also important because of the limited availability of biological samples and the high cost of biochemical raw materials—little waste can be tolerated in a separation process. Beyond the requirements of efficiency and specificity, the field of bioseparations is complicated by the inapplicability of standard chemical separation processes to biomolecules. Biomolecules cannot be separated by distillation or, in general, solvent extraction; they are delicate and chemically similar to one another. Bioseparation processes must therefore be performed in gentle aqueous conditions and rely on subtle differences between biomolecular species. Fortunately, the differences between biomolecules, while subtle, are many, and a number of separation technologies have been developed to take advantage of these differences.

Though a thorough review of bioseparation technologies is beyond the scope of this dissertation, it is appropriate to briefly consider the breadth of the field. There are several comprehensive treatments of the field of bioseparations.[206-208] Though all categories of biomolecules have been the subject of separation processes, the bulk of work towards development of bioseparation technologies has focused on techniques for separating individual proteins and oligonucleotides. These technologies have traditionally separated molecules according to their physiochemical properties. Molecular weight is used to

separate molecules in ultrafiltration, dialysis, and gel perfusion chromatography; isoelectric point is used in salting-out precipitations and ion exchange chromatography; differential solubility is taken advantage of in various solvent-extraction and precipitation processes; and charge-to-mass ratio is the key to electrophoresis.

Though these technologies can be quite specific, and are capable of producing, under the proper conditions, products of high purity, they suffer from the reality that the physical properties of biomolecules lie on a continuous spectrum. The fact that there is overlap in, for example, the isoelectric points of proteins fundamentally limits such technologies. This limitation has led to great recent interest in affinity bioseparation systems—systems that rely on a specific biological interaction between a target biomolecule and an affinity ligand. Since affinity bioseparation systems rely on the biological properties of target molecules, they provide unparalleled specificity and resolution. Since this specificity is a property of the target molecule rather than the stringency and care with which the separation system is operated, affinity separation systems are relatively robust and easy to use.

2.2.2 The dominant technology: affinity chromatography

Affinity chromatography is the most commonly used affinity bioseparation technology. Campbell et al.[209] and Lerman[210] did early work on affinity chromatographic separations in the early 1950's; the technology was further developed by Cuartrecasas et al.[211] and Porath et al.[212]. Affinity chromatography relies on the attachment of an affinity ligand to an immobile matrix. A complex mixture containing the target biomolecule is passed over this matrix, and the target molecule binds to its affinity ligand, allowing the other components of the mixture to be washed away. The separated target molecule is then eluted

from the column, typically with a chemical eluent that weakens the affinity interaction. Affinity chromatography is very efficient and specific (delivering yields up to 90% and capable of increasing the relative concentration of a single species by a factor of 6000).[213] These strengths have made affinity chromatography a widely used technique.

A variety of affinity interactions have been employed in affinity chromatography systems. Primary among these are immunological (antibody/antigen) interactions and specific protein-protein interactions.[214] Similarly, enzymes have been purified by affinity to substrate analogs[215], and specific oligonucleotides have been purified by sequence complementarity[216]. Aside from these molecule-specific interactions, a number of techniques relying on affinity tags have been developed.[217] In these schemes, a target biomolecule is labeled, either chemically or via recombinant protein engineering, with a specific chemical moiety. The chromatographic matrix contains an affinity ligand with which this moiety associates. The most prominent example of this approach is metal affinity chromatography, in which target molecules are labeled with polyhistadine tags. These tags interact with divalent metal cations such as Ni^{2+}, Cu^{2+}, or Zn^{2+}, which are chelated to the matrix.[218] Another emerging technology involves tagging the target molecule with biotin and separating it by (strept)avidin affinity chromatography.[219,220]

The prominence of affinity chromatography has inspired the development of several microfluidic affinity chromatography separation systems: these are mentioned in Chapter 1, particularly sections 1.2.2 and 1.2.3. Chapter 4 describes the development of a new bioimmobilization platform for microfluidic affinity chromatography. Though the development of new affinity chromatography techniques remains a vibrant field, several new affinity separation technologies have recently emerged to offer alternatives that avoid some

of the drawbacks of affinity chromatography. Primary among these drawbacks is the need for an immobilized phase. The presence of an immobilized phase introduces diffusional limitations to the separation process: this issue is often addressed in real affinity chromatography systems by packing columns densely with beads, thereby maximizing the surface area to volume ratio of the columns. Unfortunately, as described in section 1.2.3.3, bead packing introduces its own problems, particularly on microfluidic platforms. In addition to issues related to diffusion and column packing, affinity chromatography systems often introduce problems in eluting the bound target molecule from the immobilized column phase. Often, harsh eluents are required to destabilize the interaction between target molecule and immobilized phase, and these eluents can damage the target molecules. The next two subsections (2.2.3-2.2.4) explore alternative technologies that seek to avoid the disadvantages of affinity chromatography.

2.2.3 Other affinity bioseparation technologies

Aqueous two-phase systems separate proteins by selective partitioning. Such systems rely on phase coexistence in aqueous systems containing water-soluble polymers. When such systems separate into polymer-rich and polymer-free phases, some proteins partition selectively into the polymer-rich phase. These proteins can then be purified by physical separation of the two phases.[221,222] The polymer in an aqueous two-phase system can be modified with an affinity ligand, improving the specificity of the separation.[221,223] While these systems eliminate the diffusional limitations present in affinity chromatography, their utility is limited by the difficulty of recovering the separation target.[213] Another promising affinity bioseparation technology is continuous annular affinity chromatography.[224,225] This

technology allows for continuous separations from a flowing stream, giving it an advantage over batch-based affinity chromatography; however, it requires specialized equipment with moving parts, making it difficult to adapt to a microfluidic system.

2.2.4 Affinity precipitation: A powerful approach

In affinity precipitation systems, affinity ligands are used to associate target biomolecules into high-specific-gravity aggregates, which are separated from bulk solution either by centrifugation or by sedimentation at 1 g. Several thorough reviews of the field are available[132-135]; this section provides a brief summary of recent work. There are two broad categories of approaches to affinity precipitation (Figure 2.1). In primary effect, or homogenous, affinity precipitation, multivalent affinity ligands are used to associate target molecules into networked complexes. In secondary effect, or heterogeneous, affinity precipitation, an affinity interaction is used to attach a target molecule to a second species which can be precipitated from solution in a controlled fashion. Examples of primary effect affinity precipitation include the precipitation of avidin by bis-biotin[194], the immunoprecipitation of antigens via antibody cross-linking[226], and the aggregation of charged biomolecules by polyelectrolytes[134]. Primary effect affinity precipitation strategies are notoriously nonuniform—the details of the protocol vary widely based on the nature of the target. Furthermore, precipitated product can be very difficult to recover.[134] This discussion, therefore, focuses on secondary effect affinity precipitation; the term "affinity precipitation" will henceforth refer to such strategies.

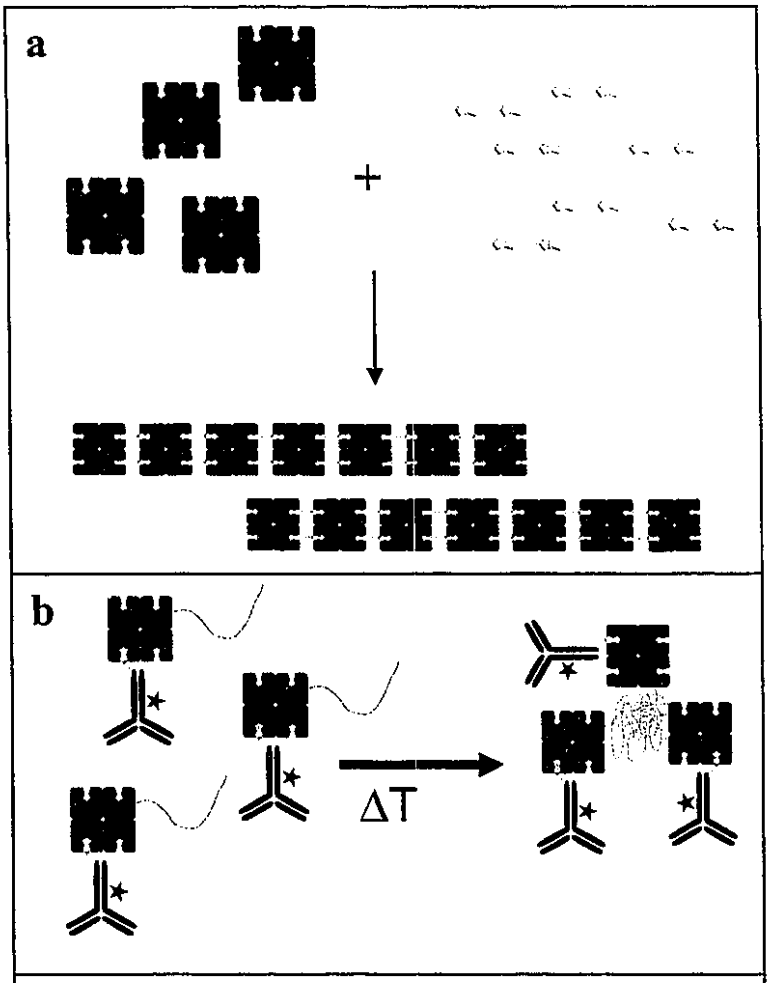

Figure 2.1: Affinity precipitation. (a) Primary effect affinity precipitation, in which the target molecule (dark blue) is aggregated by cross-linking via a multivalent affinity ligand (cyan). (b) Secondary effect affinity precipitation. The target molecule (magenta) is associated with an affinity macroligand. An environmental stimulus (temperature in this example), triggers aggregation of the macroligand, leading to precipitation of the target molecule.

The advantages of affinity precipitation are centered on the fact that the precipitation agent (the molecule to which the target molecule binds by affinity interaction, also referred to as an affinity macroligand, or AML) is present as a soluble species. This greatly reduces the diffusional and steric limitations on target-ligand binding present in affinity chromatography. Furthermore, the fact that the precipitation agent is soluble makes it easy to control and manipulate in a flow system. In addition, while chromatographic and electrophoretic separations must typically be performed in the direction of flow—making them batch processes—precipitation can be performed transverse to flow, allowing it to be run in a continuous mode.

Strategies for affinity precipitation have typically relied on stimuli-responsive polymers, which, as described in Chapter 1, undergo a reversible hydrophilic-hydrophobic phase transition in response to an environmental stimulus. This phase transition results in polymer aggregation; polymer aggregates can be separated from bulk solution by sedimentation, typically in a centrifugal field. In affinity precipitation systems, a stimuli-responsive polymer is chemically conjugated to an affinity ligand, creating an AML. This AML binds the target species in solution, and the target species is precipitated with the AML in response to the phase-separation stimulus. In this manner, the target species is separated from the other components of the bulk solution in response to an easily controlled environmental stimulus, and the AML-target molecule complex can be returned to a soluble state by reversal of this stimulus. The first paragraph of section 1.3.3 provides a brief survey of the breadth of applications of smart polymer-based affinity precipitation systems.

2.3 Experimental Objectives and Design Considerations

2.3.1 Objectives

The remainder of this chapter describes the development of a novel affinity thermoprecipitation system. This development was intended as a pilot study contributing to the eventual implementation of affinity precipitation in continuous flow microfluidic devices. Though this system was designed with an eye towards eventual incorporation in a microfluidic bioseparation system, initial characterization and optimization of the system was performed at the standard lab scale for the sake of simplicity. Therefore, the first goal of this project was to develop a system for separating biotinylated macromolecules from a bulk

solution via affinity with a streptavidin-smart polymer conjugate by centrifugation at an elevated temperature.

This goal was not novel—affinity precipitation via (strept)avidin conjugates has been demonstrated.[141,145] The second goal of this project, however, addressed a fundamental limit of the streptavidin-biotin system: this goal was to introduce reversibility to the association of biotinylated macromolecules with streptavidin. The incorporation of a high off-rate streptavidin mutant, as described in section 1.4.2, allowed for biotinylated macromolecules separated by this system to be recovered from the precipitation agent by treatment with excess free biotin. This work was completely novel, and it stands independently from the other projects described in this dissertation as a contribution to the field of affinity precipitation. As will be demonstrated by data presented in this chapter, it was important that the initial affinity precipitation system was designed with the final goal of reversibility in mind. The goals for this project can therefore be succinctly stated as follows:

1. Design a conjugate of a high off-rate streptavidin mutant with a thermoresponsive smart polymer for efficiently separating biotinylated biomolecules from bulk solution.
2. Demonstrate that separated biomolecules can be removed from this conjugate by treatment with excess free biotin.

2.3.2 Initial design considerations

In accomplishing the first goal, there were several important design choices to be made. Clearly, a streptavidin mutant and smart polymer had to be chosen. We chose the mutant S45A (described in section 1.4.2) by virtue of its high biotin off-rate, and the polymer

PNIPAAm, which has been used in many other thermoprecipitation schemes (see section 1.3.3). A more subtle option in this design process is the choice of a means of fabricating the protein-polymer conjugate. There are two possible approaches: direct covalent conjugation of the polymer to streptavidin and noncovalent attachment of a biotinylated polymer via biotin-streptavidin binding (streptavidin's tetrameric structure means that molecules conjugated to polymer in this manner still have binding sites available for binding the target molecules). Both of these options have been explored (Figure 2.2). Another design choice, important to both goals, was that of which target biomolecules to separate. The target molecules used in the work described below were biotinylated immunoglobin G (IgG) and a biotinylated single-stranded oligonucleotide. These molecules represent the two most important classes of bioseparation targets: proteins and oligonucleotides.

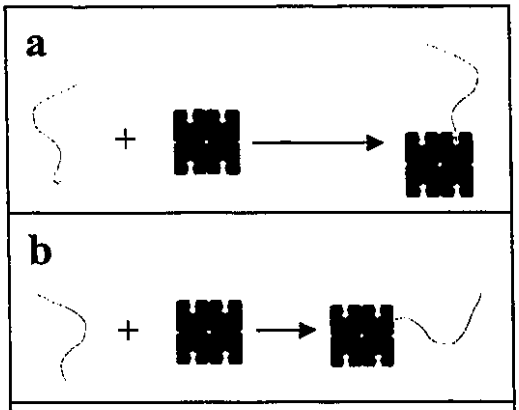

Figure 2.2: Creation of a precipitating streptavidin affinity macroligand. (a) Complexation of streptavidin with a biotinylated smart polymer. (b) Covalent conjugation of streptavidin to a smart polymer.

The final initial consideration was that of basic experimental design (figure 2.3). The biotinylated target molecule was tracked by labeling with a fluorophore. The target was incubated with the S45A-polymer conjugate (either covalent or noncovalent) and the solution was centrifuged at an elevated temperature, triggering aggregation and sedimentation of the conjugate. The supernatant was then removed and the pellet dissolved into fresh buffer at low temperature. The fluorescence of this redissolved pellet was measured to determine the fraction of target molecule separated by the thermoprecipitation. To test release of the target,

an excess of free biotin was added to the redissolved pellet and the thermoprecipitation step was repeated. This protocol was refined over time; the details of the final protocol are given below.

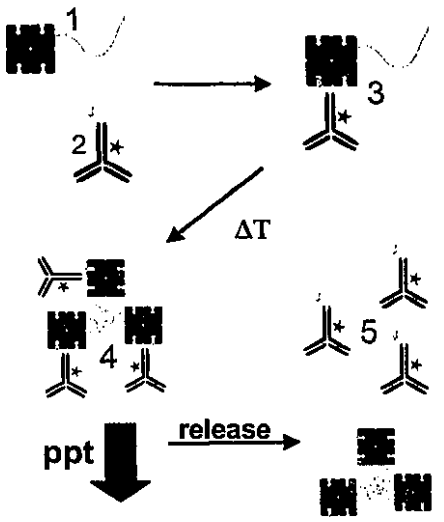

Figure 2.3: Diagrammatic representaion of the basic experimental protocol used in section 3.1. A streptavidin-polymer conjugate (1) is bound to a biotinylated macromolecule (2), forming a affinity complex (3). The temperature is raised, triggering the formation of smart polymer aggregates (4). These aggregates are precipitated (ppt) from solution via centrifugation. The separated aggregates are resolubilized and treated with excess free biotin, releasing the separated target molecule (5).

2.4 Experimental Materials and Methods

2.4.1 Preparation of PNIPAAm

Linear PNIPAAm containing a single terminal N-hydroxysuccinimidyl (NHS) ester group was synthesized by Zhongli Ding according to a previously published protocol.[117] The number-average molecular weight ($\overline{M}_n$) of this polymer was determined to be 11,000 by vapor pressure osmometry (VPO, device model OSV111, Knauer, Germany). The polymer LCST in pure water was determined to be 32°C. To generate free (unmodified) PNIPAAm matching the molecular weight distribution of this NHS-terminated polymer, the NHS-terminated polymer was dissolved in deionized water at 3.2 mg/ml and incubated at room temperature for 48 hours to allow for hydrolysis of the NHS group.

2.4.2 Preparation of S45A and WT streptavidin

The S45A streptavidin gene was constructed from the recombinant WT core streptavidin gene by PCR mutagenesis by Hyre et al.[204] Recombinant S45A and WT streptavidin were expressed and purified according to a previously published protocol.[202]

2.4.3 PNIPAAm-streptavidin conjugation

A solution of 20-30 mg/ml streptavidin (WT or S45A) in pH 7.6 phosphate buffered saline (PBS, 20mM phosphate, 5mM sodium chloride) was prepared. To this solution 50 µl of 140 mg/ml NHS-PNIPAAm solution in DMF was added. This reaction mixture was incubated, with rotation, at 4 °C overnight (figure 2.4). Following reaction, the PNIPAAm-containing species were thermoprecipitated. Thermoprecipitation proceeded as follows: the reaction mixture was centrifuged for ten minutes at 14,000 rpm (16,600 × g relative centrifugal force) in a microcentrifuge, which had been heated to 37 °C. The pellet was resolubilized by incubation in 150 µl pH 7.6 PBS (20mM phosphate, 5mM sodium chloride) at 4 °C for one hour followed by vortexing. The supernatant was subjected to centrifugation at 37 °C twice more, with resolubilization of each resultant pellet. The resolubilized pellets were pooled and the supernatant was reserved. The supernatant contained a high concentration of unreacted streptavidin—to this solution was added a fresh

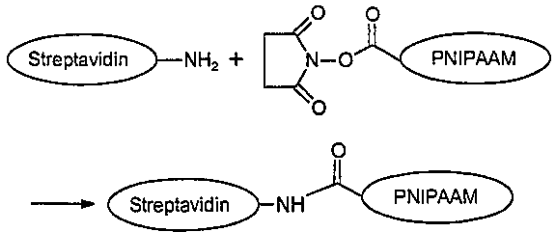

Figure 2.4: Reaction of streptavidin primary amine with NHS-PNIPAAm to form streptavidin-PNIPAAm conjugate.

volume of NHS-PNIPAAm solution, and the reaction and thermoprecipitation process was repeated. The reaction was repeated twice more, until most of the streptavidin in the supernatant had been reacted. The resolubilized pellets from each reaction were pooled and subjected to iminobiotin affinity chromatography[227], removing all unreacted polymer (iminobiotin-modified agarose beads were obtained from Pierce, Rockford, IL). Thermoprecipitation was repeated a final time with the resultant conjugate solution, in order to remove any unreacted streptavidin.

2.4.4 Biotinylation of PNIPAAm

A solution of 100 mg/ml NHS-PNIPAAm was prepared in DMF. 100 µl of this solution was added to a 4 mg/ml solution of biotin-PEO-amine (Pierce) in 1 ml pH 10 carbonate buffer and thoroughly mixed. This reaction mixture was incubated on ice for 2 hours. Polymer-containing species were then separated from the mixture by thermoprecipitation, as described above. Any remaining free biotin molecules were removed from the product solution by 48-hour dialysis across a 3500 Da molecular weight cut-off (MWCO) membrane into distilled water.

2.4.5 Biotinylated IgG and oligonucleotide preparation

Immunoglobulin G (IgG) was used as a model protein target molecule. It was biotinylated and fluorescently labeled in-house. Pooled bovine IgG was obtained from Sigma (St. Louis, MO) and dissolved at 15 mg/ml in pH 7.6 PBS (20 mM phosphate, 5 mM sodium chloride). To 800 µl of this solution was added 20 µl of 9 mg/ml NHS-LC-biotin (Pierce) in

DMF. Following incubation on ice for ten minutes, the reaction was quenched by the addition of 100 µl 100 mM pH 7.6 Tris buffer (the primary amines on the tris molecules provided an alternate target for the NHS groups on the modified biotin). The reaction mixture was then dialyzed overnight across a 10,000 molecular weight cut-off (MWCO) membrane into pH 7.6 PBS, with one buffer exchange. This biotinylated IgG was then fluorescently labeled with Texas Red C2 maleimide (Molecular Probes, Eugene OR), a thiol-reactive label. The IgG solution was concentrated to 400 µl and 40 µl of 20 mM tris(2-carboxythyl) phosphine hydrochloride (TCEP-HCL, Pierce) solution was added to reduce disufides. To this solution was added 40 µl of 30 mg/ml Texas Red C2 maleimide in DMSO. This reaction mixture was rotated at 4 °C for four hours and then dialyzed across a 10,000 MWCO membrane into pH 7.6 PBS for 48 hours, with two buffer exchanges.

Biotinylated, fluorescently labeled oligonucleotide was obtained directly from Integrated DNA Technologies (IDT, Coralville, IA). The single-stranded oligonucleotide had the sequence GGACTCAGGCTTATAGCTGT and contained a 5' fluorescein modification and a 3' biotin modification (with a tri-(ethylene glycol) spacer).

2.4.6 Analysis of conjugation products

The conjugation products were assayed spectrophotometrically, using a Hewlett-Packard model 8452A spectrophotometer (HP, Cupertino, CA). To determine the degree of biotinylation of the IgG-biotin conjugate, the 2-(4'-hydroxyazobenzene) benzoic acid (HABA) assay[228] was used. IgG concentration was monitored based on the optical density of the IgG solution at 280 nm, using an extinction coefficient of 210,000 $cm^{-1}M^{-1}$. The fluorophore-

labeling ratio for the IgG species was determined by measuring the optical density of the solution at 582 nm (the excitation maximum of Texas Red), using an extinction coefficient of 112,000 $cm^{-1}M^{-1}$. PNIPAAm-streptavidin conjugation yield was determined by monitoring the optical density of the product solution at 280 nm, based on a streptavidin extinction coefficient of 139,000 $cm^{-1}M^{-1}$ for the tetramer.

2.4.7 Separation and recovery with covalent conjugate, IgG target

Biotinylated, fluorescently labeled IgG (60 pmol) was incubated with 35× molar excess (based on tetramer concentration) of either S45A-PNIPAAm conjugate or WT-PNIPAAm conjugate in PBS. The separation experiments were performed in 500 µl pH 7.6 PBS with 20 mM phosphate and 5 mM sodium chloride. To these IgG/streptavidin-PNIPAAm solutions were added 20 µl 20 mg/ml bovine serum albumin (BSA, Sigma) to block non-specific interactions and 50 µl 3.2 mg/ml free PNIPAAm to aid thermoprecipitation. The initial fluorescence of each solution was measured, and thermoprecipitation was performed in triplicate at 37°C, as described above, with free PNIPAAm (3.2 mg/ml concentration, 50 µl) added to the supernatant after each centrifugation. The pellets were resolubilized and pooled in PBS such that the total volume of the pooled pellet solution was equal to the initial volume. An amount of BSA equal to the original amount of BSA was added to each pooled resolubilized pellet solution. The fluorescence of the pooled resolubilized pellet solution was measured and a 25× molar excess (relative to streptavidin binding sites) of free biotin (Sigma) was added. After incubating this solution for 20 minutes, the thermoprecipitation process was repeated, and the fluorescence

of the resulting pooled pellet solution was measured. To this resolubilized pellet solution was added a 25× molar excess of free biotin; the solution was then incubated overnight. Following this incubation, the thermoprecipitation process was repeated a final time and the fluorescence of the resulting pooled pellet solution was measured. Controls for this experiment included samples containing unconjugated streptavidin rather that streptavidin-PNIPAAm conjugate, samples containing free PNIPAAm but no streptavidin-PNIPAAm conjugate, samples containing neither streptavidin nor PNIPAAm, and samples to which no free biotin was added. All experiments were performed in triplicate. Fluorescence measurements were taken with a Hitachi F-4500 fluorescence spectrophotometer (Hitachi Instruments, Inc., Tokyo, Japan).

2.4.8 Noncovalent conjugate, IgG target

Separation experiments involving the noncovalent conjugate of S45A with biotin-PNIPAAm were performed in the same manner as the experiments involving the covalent conjugate, with the following exceptions. As a first step, a solution containing a 1:1 molar ratio of S45A streptavidin and biotin-PNIPAAm (4.2 μM in each) was prepared in 500 μM PBS (20 mM phosphate, 5 mM NaCl). To this solution was added biotinylated, fluorescently labeled IgG at 120 nM (a 35× molar deficiency relative to the streptavidin and biotin-PNIPAAm species). The thermoprecipitations and biotin additions otherwise proceeded as described above, with similar controls.

2.4.9 Covalent conjugate, oligonucleotide target

Experiments investigating the separation of the biotinylated oligonucleotide target via the covalent streptavidin-PNIPAAm conjugates were performed in the same manner as the experiments investigating the separation of IgG via these covalent conjugates, with the following exceptions. Initially, a solution containing 60 pmols of biotinylated, fluorescently labeled oligonucleotide was prepared in 250 µl pH 7.6 PBS with 20 mM phosphate and 100 mM sodium chloride. To this solution was added a 35× molar excess of WT- or S45A-PNIPAAm conjugate (according to streptavidin tetramer concentration). Ten µl 20 mg/ml BSA and 25 µl 3.2 mg/ml free PNIPAAm were then added. To samples that were to be thermoprecipitated at low temperature (28 °C), ammonium sulfate was added at 250 mM to decrease the LCST of the PNIPAAm. Thermoprecipitations were performed as described above, at either 37 °C or 28 °C. Biotin additions were as described above, maintaining a molar ratio of 25× excess free biotin relative to available biotin binding sites. Controls were similar to those described above. Fluorescence measurements for these experiments were performed on a Perkin Elmer LS50B fluorescence spectrophotomer (Perkin Elmer Instruments, Inc., Shelton, CT).

2.5 Results and Discussion

2.5.1 Results: Characterization of conjugation products

HABA assay of the IgG-biotin conjugate revealed an average of 1.5 biotin groups per IgG molecule; the ratio of IgG dye labeling was similar. HABA assay of the biotin-PNIPAAm

conjugation product showed that 20% of the polymer molecules had been biotinylated; in subsequent concentration calculations with this species, only the concentration of biotin moieties was considered. The low yield of this biotinylation reaction was most likely due to hydrolysis of the polymer NHS group during storage—NHS groups are highly labile to base-catalyzed hydrolysis even at very low concentrations of water. For the complete streptavidin-PNIPAAm conjugation procedure (four reaction cycles), the yield was about 20%. Similar results were observed for WT and S45A streptavidin. The low yield is likely due to the relative inaccessibility of primary amines on the surface of the streptavidin molecule, as well as hydrolysis of NHS groups during polymer storage.

2.5.2 Results: Separation of IgG with noncovalent biotin-PNIPAAm/S45A complex

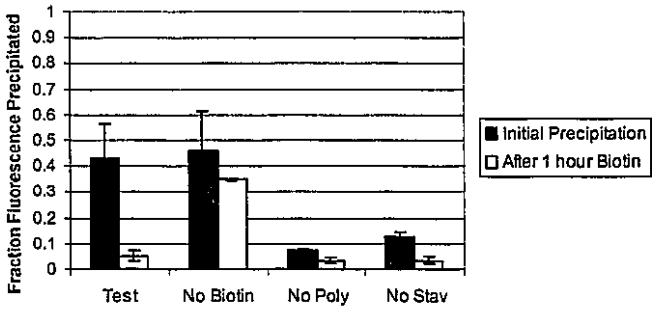

Figure 2.5: Data for separation of biotinylated IgG via noncovalent biotin-PNIPAAm / S45A complex. In each cluster of bars, data are given for biotinylated IgG precipitated initially and after 1 hour incubation with excess biotin. The cluster of bars on the far left describes the experiment; data for controls are in the clusters to the right.

Figure 2.5 shows the data for a set of thermo-precipitation experiments involving precipitation of biotinylated IgG by a noncovalent b-PNIPAAm/S45A complex. The bars show the normalized amount of fluorescence present in the resolublized pellet following each thermoprecipitation; they indicate the fraction of target molecule precipitated at each step. The test case and biotin-free control show significantly more IgG precipitation than the

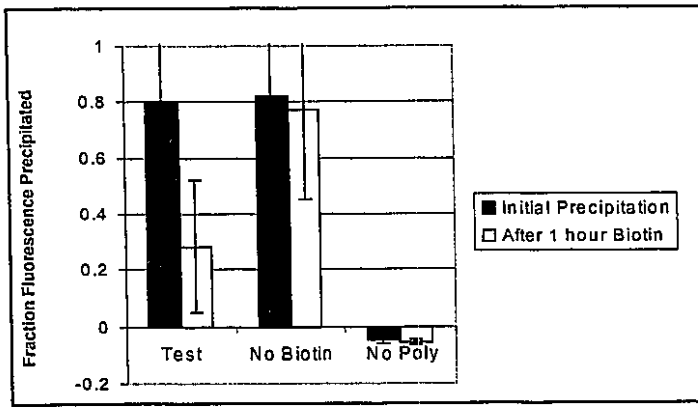

Figure 2.6: Data for precipitation and biotin treatment of fluorescently labeled S45A complexed with biotinylated PNIPAAm. Data are presented as described for figure 2.5. Total initial concentration of S45A is not precipitated, and release of precipitated S45A occurs.

negative controls. In addition, these data make clear that excess free biotin effects the release of streptavidin-bound biotinylated IgG. A significantly larger fraction of IgG remains associated with the precipitation complex in the biotin-free control than in the test sample.

The most outstanding feature of these data is that only a small fraction of target molecule was initially precipitated, despite the large molar excess of precipitating complex present. In order to assure that the streptavidin in these experiments was precipitated along with the biotinylated smart polymer, the experiments were repeated with fluorescently labeled streptavidin. Figure 2.6 shows the data for labeled streptavidin. It's clear from these data that the fraction of streptavidin precipitated during these experiments is far greater than that of the target proteins. Further, it is clear that the majority of this streptavidin is released from the b-PNIPAAm it is bound to by the addition of excess free biotin. This may be an undesirable feature in a system intended to isolate a biotinylated target protein.

2.5.3 Explaining incomplete thermoprecipitation in the noncovalent system

It is important to remember in working with high off-rate streptavidin mutants that these mutants come to equilibrium with biotinylated species in solution in a relatively short time frame. The kinetics of the wild-type streptavidin-biotin interaction are such that the molecules are kinetically locked together over the course of several hours. This is not so with high off-rate mutants. Let us therefore examine the equilibrium situation for a system of S45A streptavidin and biotinylated PNIPAAm. Due to the large size of the biotinylated polymer, only one polymer molecule can bind to each streptavidin binding face, allowing for up to two molecules to bind each streptavidin tetramer. The system is therefore described by two equilibria:

$$Stav + b - poly \xleftrightarrow{K_{eq}} Stav - b - poly$$
$$Stav - b - poly + b - poly \xleftrightarrow{K_{eq}} Stav - 2(b - poly)$$

We can write the following equations for these equilibria:

$$\frac{[Stav - b - poly]_{eq}}{[Stav]_{eq}[b - poly]_{eq}} = K_{eq}$$
$$\frac{[Stav - 2(b - poly)]_{eq}}{[Stav - b - poly]_{eq}[b - poly]_{eq}} = K_{eq}$$

where $[X]_{eq}$ represents the equilibrium concentration of species X and K_{eq} represents the thermodynamic equilibrium constant. Considering also the mass balances

$$[Stav]_{eq} + [Stav - b - poly]_{eq} + [Stav - 2(b - poly)]_{eq} = [Stav]_i$$
$$[b - poly]_{eq} + [Stav - b - poly]_{eq} + 2[Stav - 2(b - poly)]_{eq} = [b - poly]_i'$$

where $[X]_i$ is the initial concentration of the species X, we have four equations and four variables. If we redefine as:

$$[Stav-b-poly]_{eq} \equiv x_1, [Stav-2(b-poly)]_{eq} \equiv x_2, [Stav]_{eq} \equiv x_3, [b-poly]_{eq} \equiv x_4$$

and combine the equations, we have:

$$\frac{[Stav]_i K x_4}{K x_4 + K^2 x_4^2 + 1} + \frac{2[Stav]_i K^2 x_4^2}{K x_4 + K^2 x_4^2 + 1} + x_4 - [b-poly]_i = 0 .$$

Solving this equation numerically for a range of values of the ratio [b-poly]$_i$/[Stav]$_i$ yields the curves shown in figure 2.7. The species we're most interested in is Stav-b-poly, since it is the only species that contains a binding site for complexation with a biotinylated target molecule as well as the polymer necessary for precipitation. The concentration of this species is maximized when the ratio of initial concentrations is unity; even then, it makes up only a third of all streptavidin species.

The situation is more complex than this analysis shows, however. Upon addition of the biotinylated molecule, the system will re-equilibrate. This new equilibrium is described by:

$$Stav + b - poly \xleftrightarrow{K_{eq}} Stav - b - poly$$
$$Stav - b - poly + b - poly \xleftrightarrow{K_{eq}} Stav - 2(b - poly)$$
$$Stav + b - IgG \xleftrightarrow{K_{eq}} Stav - b - IgG$$
$$Stav - b - IgG + b - IgG \xleftrightarrow{K_{eq}} Stav - 2(b - IgG)$$
$$Stav + b - poly + b - IgG \xleftrightarrow{K_{eq}} Stav - b - poly - b - IgG$$
$$Stav - b - IgG + b - poly \xleftrightarrow{K_{eq}} Stav - b - poly - b - IgG$$

as well as the associated mass balances. This system is considerably more complex than the one considered above, so we will forgo a description of the full expansion of the equations. In the special case [Stav]$_i$=[b-poly]$_i$=2[b-IgG]$_i$, the ratio of the equilibrium concentration of the key species, Stav-b-poly-b-IgG, to the total concentration of all IgG species is 0.366. It seems that a system that uses biotinylated PNIPAAm is inherently limited to separating only a

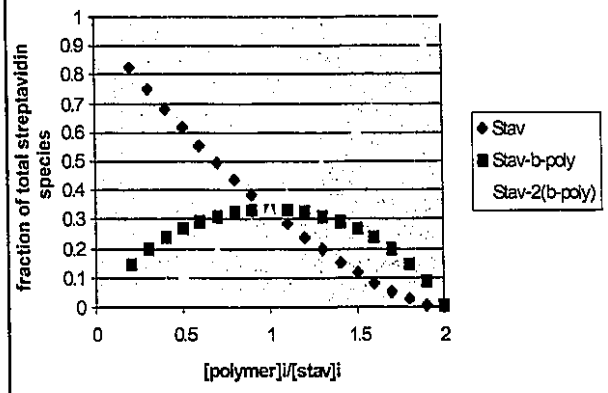

Figure 2.7: Equilibrium concentrations of streptavidin species in a solution containing streptavidin and biotinylated polymer. Possible species are unbound streptavidin, streptavidin bound to a single biotinylated polymer molecule, and streptavidin bound to two biotinylated polymer molecules. Equilibrium concentrations are shown over a range of initial polymer/streptavidin concentrations. The desired species, available for binding as an affinity macroligand, is the singly bound streptavidin molecule. The maximum possible concentration of this species, as a fraction of all streptavidin species, is only one third.

fraction of biotinylated target molecule from solution. The noncovalent separation system was therefore abandoned without further investigation.

2.5.4 Results: Separation of IgG with covalent streptavidin-PNIPAAm conjugates

Figure 2.8 shows the results of a separation/release experiment with biotinylated IgG and WT-PNIPAAm conjugate. The data shown are the fluorescent intensities of the resolubilized pellets at three points in the experiment—after an initial thermoprecipitation, after a thermoprecipitation which followed a 20 minute incubation with biotin, and after a thermoprecipitation which followed an overnight incubation with biotin—normalized to the initial fluorescent intensity. The three bars corresponding to the experiment described in section 2.4 are on the far left; also shown are data corresponding to the following controls: no

biotin added in the release steps, no polymer present (only unconjugated streptavidin present), no streptavidin present (only unconjugated polymer present), and neither polymer nor streptavidin present. Error bars are plus and minus one standard deviation over a series of three experiments. Except for a small co-precipitation effect evident with the unconjugated polymer, there was no nonspecific IgG thermoprecipitation observed in the control experiments. The WT-PNIPAAm conjugate was an effective thermoprecipitation agent, capable of separating all initially present biotinylated IgG. Release, however, was not effective. Even after overnight incubation with free biotin, only about 10-20% of the fluorescence was freed from the conjugate. This negligible release effect was comparable to the control in which free biotin has not been added.

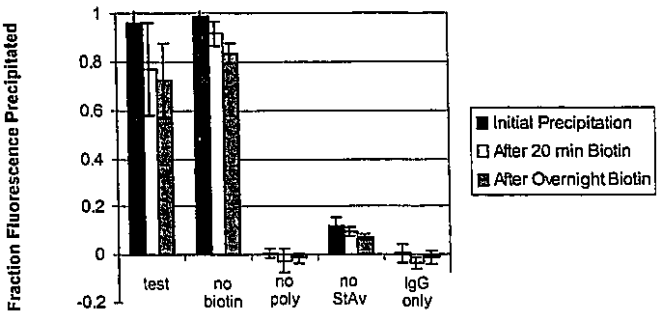

Figure 2.8: Data from separation and release of biotinylated IgG via WT-PNIPAAm conjugate. In each cluster of bars, data are given for biotinylated IgG precipitated initially, after 20 minutes incubation with excess biotin, and after overnight incubation with excess biotin. The cluster of bars on the far left describes the experiment; data for controls are in the clusters to the right.

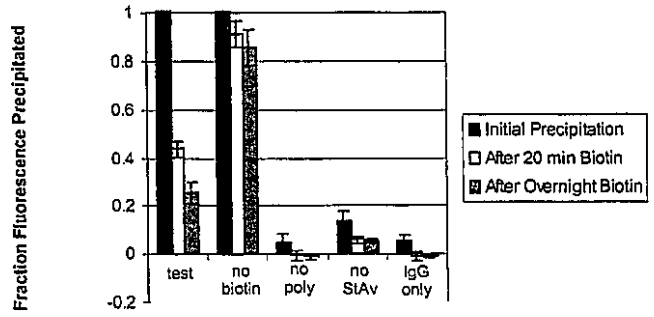

Figure 2.9: Data from separation and release of biotinylated IgG via S45A-PNIPAAm conjugate. Data are presented as in figure 2.8. Release of 70-80% of the target molecule is apparent.

Contrast the data for biotinylated IgG and the S45A-PNIPAAm conjugate, shown in Figure 2.9. All data presented in this figure are as in Figure 2.8. The S45A-PNIPAAm conjugate proved to be as effective a thermoprecipitation agent as the WT-PNIPAAm complex. However, it did release biotinylated IgG upon treatment with free biotin. 50-60% of the initially precipitated fluorescence was freed after 20 minutes' incubation with biotin and 70-80% of this fluorescence was freed after overnight incubation with biotin. This release effect was not seen in the biotin-free control.

2.5.5 Incomplete release of biotinylated IgG from S45A-PNIPAAm

Figure 2.10 shows a direct comparison of biotinylated IgG release from WT-PNIPAAm conjugate and S45A-PNIPAAm conjugate. Even after overnight incubation with free biotin, some biotinylated IgG remained bound to the S45A-PNIPAAm conjugate. This residually bound IgG might be explained by the fact that the IgG population contained some multiply biotinylated protein molecules. If multiple biotin moieties on a single IgG molecule bind to the same streptavidin molecule, a cooperative effect would be expected. In fact, it has been shown[229] that high off-rate streptavidin mutant molecules interacting with a biotinylated surface demonstrate a radically decreased apparent off-rate when allowed

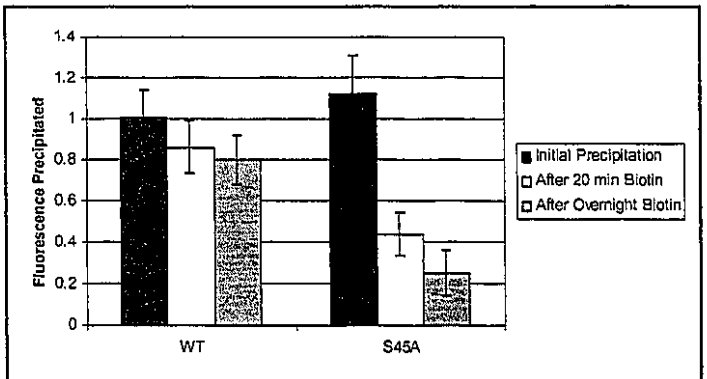

Figure 2.10: Direct comparison of separation and release of biotinylated IgG via WT-PNIPAAm conjugate and S45A-PNIPAAm conjugate. Bar order as described for figure 2.8.

to bind bivalently. In the context of these thermoprecipitation experiments, this decreased off-rate was observed as a population of multiply biotinylated IgG molecules that did not dissociate from the S45A-PNIPAAm complex in the same time frame as the majority of the biotinylated IgG. To control for this effect, separation and release was investigated for a molecule containing only a single biotin moiety—a biotinylated oligonucleotide.

2.5.6 Separation of oligonucleotide with covalent conjugates

The data for separation and release of the oligonucleotide target via the S45A-PNIPAAm conjugate at 37 °C are shown in figure 2.11. There are two important features apparent in these data: release of the biotinylated target after treatment with free biotin was rapid and nearly total; and a much smaller fraction of the initially present target molecule was precipitated than in the case of biotinylated IgG. The complete release demonstrates that a singly biotinylated molecule is not retained by the high off-rate conjugate in the presence of excess free biotin. The smaller fraction of initially precipitated oligonucleotide is indicative of a decrease in the equilibrium affinity of the S45A-PNIPAAm conjugate for biotinylated oligonucleotide relative to that for biotinylated IgG. This is further indicated by the data for

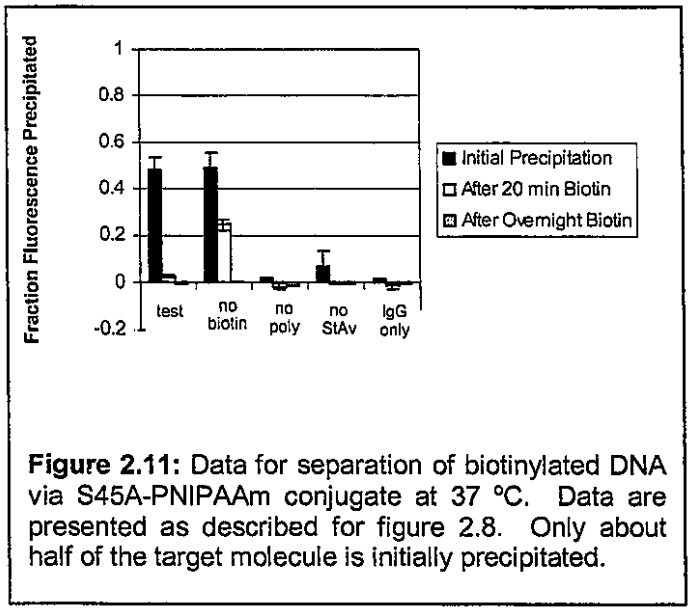

Figure 2.11: Data for separation of biotinylated DNA via S45A-PNIPAAm conjugate at 37 °C. Data are presented as described for figure 2.8. Only about half of the target molecule is initially precipitated.

the biotin-free control (second cluster of bars from the left, figure 2.11), which shows only a fraction of the initially precipitated oligonucleotide being captured in the second precipitation. This is consistent with a reequilibration of the streptavidin-biotin binding, at a lower-than-expected affinity, following the initial precipitation and removal of the unbound oligonucleotide in the supernatant.

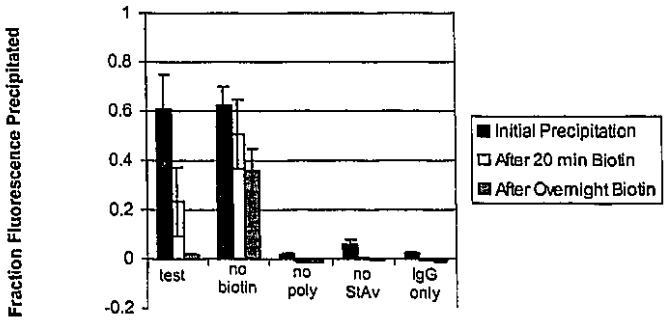

Figure 2.12: Data for separation of biotinylated DNA via S45A-PNIPAAm conjugate at 28°C. Data are presented as described in figure 2.8. Complete release of target molecule is apparent upon treatment with excess biotin.

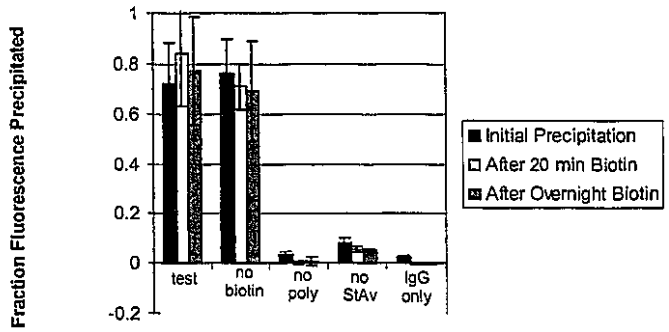

Figure 2.13: Data for separation of biotinylated DNA bia WT-PNPAAM conjugate at 28°C. Data are presented as described in figure 2.8. No release of target molecule is apparent, in contrast to data shown in figure 2.12 for S45A-PNIPAAm conjugate.

In order to improve the separation of biotinylated oligonucleotide, the separation experiments were repeated at a lower temperature (28 °C), in the presence of a moderate concentration of ammonium sulfate, which lowers the LCST of PNIPAAm. Figure 2.12 shows the data for thermoprecipitation and recovery of a biotinylated oligonucleotide 20-mer via S45A-PNIPAAm conjugate at 28 °C. The fraction of biotin-DNA initially precipitated is higher than at 37 °C, and the biotin-free sample remains bound to a much higher fraction of biotin-DNA throughout the experiment. This indicates that the increase in the biotin-S45A

affinity (and decrease in off rate) between 37 °C and 28 °C is large enough to significantly impact the utility of S45A as an affinity ligand. Compare the data for the S45A conjugate with those for the WT-PNIPAAm conjugate and biotinylated DNA (figure 2.13). These data are similar to those for the experiments with WT-PNIPAAm and biotinylated IgG, revealing complete and specific thermoprecipitation and no target recovery in response to treatment with free biotin.

The measured K_a for S45A streptavidin at 37 °C is 4.9×10^9 M^{-1}.[204] This means that, given the concentrations of streptavidin and biotinylated DNA used in these experiments, over 99.99% of the biotinylated oligonucleotide originally present in solution should be bound to streptavidin-PNIPAAm conjugate molecules at equilibrium. In order for the binding fraction to decrease to 50%, as observed at 37 °C, the K_a of the interaction must decrease by over four orders of magnitude. Similar decreases in the affinity of the biotin-streptavidin system have been observed for various chemical modifications to the biotin tail[230]; it is conceivable therefore that the conjugation of an oligonucleotide to biotin would decrease the affinity of the system. A four-orders-of-magnitude decrease in the affinity of WT streptavidin for biotinylated oligonucleotide would not be expected to be observable in these experiments, since the affinity of WT for unmodified biotin is nearly four orders of magnitude greater than that of S45A. The observed fraction of biotinylated oligonucleotide thermoprecipitated by the WT-PNIPAAm conjugate is therefore consistent with a general large decrease in the affinity of streptavidin for biotin conjugated to an oligonucleotide.

2.6 Conclusions

We have demonstrated an affinity precipitation system in which the replacement of WT streptavidin with a high off-rate streptavidin mutant allows for the triggered release of biotinylated macromolecules from the affinity precipitation agent. This release is a demonstration of the reversibility that high off-rate streptavidin mutants can impart to systems relying on the biotin-streptavidin interaction: a reversibility that is currently lacking in such systems. The system developed here also demonstrates some potential pitfalls of relying on high off-rate streptavidin mutants. Cooperative binding to multiply biotinylated molecules can partially eliminate the reversibility of the system, and unexpected decreases in the off-rate due to biotin modification can have drastic effects since the baseline off-rate is already unusually high. However, the techniques presented here open up a wide range of new possibilities for biotin-streptavidin technology, and demonstrate the power of coupling protein engineering and macromolecular conjugation technologies to develop novel conjugate molecules with highly specified properties. In the next chapter, the sedimentation properties of smart polymers in microfluidic channels are examined, in an assessment of the feasibility of adapting the system developed in this chapter to a microfluidic bioseparation.

Chapter 3: Smart Polymer Aggregation in Microfluidic Devices*

3.1 Summary

The work described in this chapter began as an extension of the work described in Chapter 2: an attempt to adapt an affinity precipitation system for bioseparations to a microfluidic platform. This scheme, as originally conceived, is described in Section 3.2. As pilot research towards this goal, the sedimentation behavior of smart polymer aggregates in microfluidic channels was characterized. This experimental work is described in Section 3.3, with results given and discussed in Section 3.4. Through these pilot studies, it was determined that sedimentation in microfluidic devices was an impractical means of separation. However, in the course these experiments, interesting properties were discovered in a new hybrid material. This material—latex nanobeads surface-modified with PNIPAAm—aggregates and adheres reversibly to the walls of a mylar microfluidic channel in response to a thermal stimulus. Experiments investigating this property are described in Section 3.3, with results given and discussed in Section 3.4. The temperature-triggered, reversible adhesion of PNIPAAm-coated nanobeads to the walls of microfluidic channels is a novel and potentially powerful means of biomolecular immobilization in microfluidic devices. The experiments described in this chapter establish the feasibility of such an immobilization system; applications are described in Chapters 4 and 5.

3.2 Motivation: Sedimentation of Smart Polymers in Microfluidic Devices

3.2.1 Fundamentals of sedimentation behavior

The work described in this chapter was undertaken as an evaluation of the feasibility of adapting an affinity precipitation system to a microfluidic platform. The design concept for such a system involved the separation of a stream containing a homogenous suspension of solid particles into two streams: one containing concentrated particles and the other cleared of particles (Figure 3.1). Smart polymer phase separation and aggregation could be used to trigger particle formation and to thereby control the separation process. In analyzing the feasibility of this concept, it was necessary to establish standards for the sedimentation behavior of smart polymer aggregate particles. These standards were based on the fundamentals of particle sedimentation.

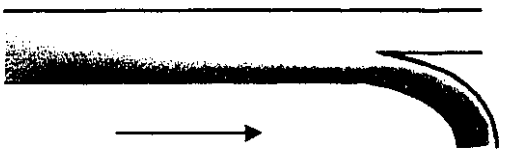

Figure 3.1: Separation of aggregate particles in a microfluidic device. A homogenous suspension of particles (gray) enters the device, flowing in the direction of the arrow. These particles settle into a zone that is split off from the rest of the flow. This produces two output streams: one enriched in particles, and one free of particles.

The details of particle sedimentation are covered in great depth by basic texts[232,233]; this section consists of a brief overview. Let us consider initially the sedimentation of a single particle. The terminal velocity of a spherical particle settling in a fluid at low Reynolds number is described by Stoke's law:

$$F = 6\pi\mu r v_s ,$$

where F represents the force on the particle, μ is the viscosity of the fluid, r is the radius of the particle, and v_s is the terminal settling velocity of the particle. For a solid spherical particle sedimenting under the force of gravity in a viscous flow, this equation has the analytical solution:

$$v_s = \frac{2r^2 g(\rho_p - \rho_f)}{9\mu},$$

where g is gravitational acceleration, ρ_p is the density of the particle, and ρ_f is the density of the fluid. For general particles, the value of the sedimentation velocity is given by:

$$v_s = sg ,$$

where s is the sedimentation coefficient of the particle, and is dependant on the size, shape, and density of the particle and the density and viscosity of the fluid. In a collection of settling particles at sufficiently low particle concentrations, each particle settles independently with this velocity. Systems at these concentrations are described as behaving in the "particulate settling" or "free settling" regime. Note that the velocity of sedimentation is independent of particle concentration in the particulate settling regime.

At higher concentrations, particles moving past one another begin to interact and interfere with each others' settling behavior; the system is then in the "hindered settling" regime. Due to the complexity of interparticle interactions, both direct and fluid-mediated, the description of sedimentation in the hindered settling regime is not analytically tractable; however, an empirical correlation has been developed by Richardson and Zaki[234]. Velocity of sedimentation in the hindered regime is related to free settling velocity by the relationship:

$$v_h = v_s \varepsilon^n ,$$

where v_h is the velocity of hindered sedimentation, ε is the volume fraction of fluid, and n is an empirical constant. The dependence on fluid volume fraction means that hindered sedimentation velocity does, in fact, depend on the concentration of particles. At particle concentrations above those in the hindered regime, the system enters the compression regime, in which particles are mechanically supported by one another, and little settling can be observed.

Consider now settling of particles from a homogenous suspension, beginning with the particle concentration in the particulate settling regime. As the particles at the top of the container settle out at a constant velocity, a zone of the fluid becomes cleared of particles, and a boundary is established between settled particles and cleared fluid (Figure 3.2). So long as the concentration of particles remains in the particulate settling regime, this boundary will move downward at a rate v_s. As

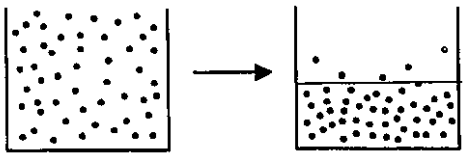

Figure 3.2: The establishment of a sedimentation boundary. Homogenously distributed particles settle into a zone of concentrated particles and a particle-free zone. The red line on the right represents an arbitrarily assigned sedimentation boundary.

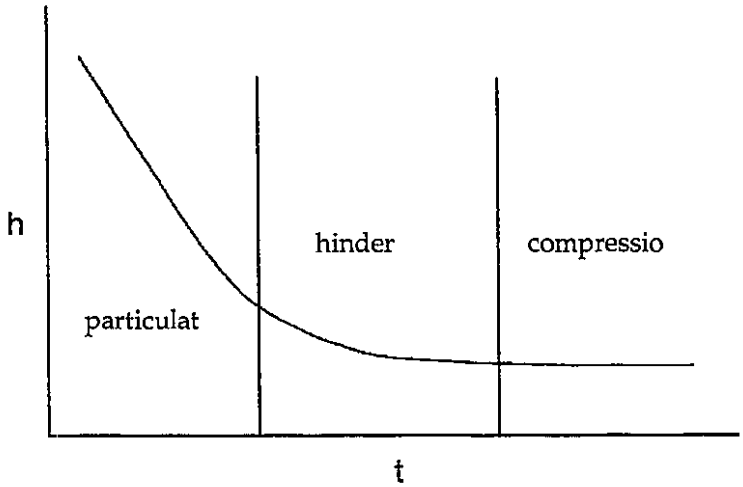

Figure 3.3: The change in the height of a sedimentation boundary (h) with time (t). The boundary initially moves with a constant velocity (particulate regime). As the concentration of particles increases, settling velocity becomes dependant upon concentration, and, therefore, boundary height (hindered regime). Finally, the system enters the compression regime, and little further settling can be observed.

the concentration increases and the system enters the hindered settling regime, the rate of movement of the boundary decreases, and it continues to decrease as the concentration increases. Finally, the system enters the compression regime, and no more settling is observed. This series of transitions is shown in Figure 3.3, which depicts the downward movement of a sedimentation boundary with time.

3.2.2 Research objectives and experimental design considerations

The sedimentation behavior described above poses a fundamental engineering optimization challenge: a separation system based on sedimentation should attempt to achieve the highest concentration possible of settled particles, but at high concentrations of settled particles, further sedimentation occurs relatively slowly. A high product stream concentration—and subsequently, a high quality separation—is at odds with a fast separation. This an especially important point for the system proposed in section 3.2.1: since sedimentation must take place within the residence time of the aggregated particles in the microfluidic channel, a fast sedimentation is necessary. In order, therefore, to determine whether such a system can feasibly perform efficient separations, it was necessary to investigate the rate of sedimentation of smart polymer aggregates in microfluidic channels. This investigation consisted of the straightforward microscopic observation of suspensions of aggregated smart polymers in a simple single-channel microfluidic device under static (no flow) conditions. Eliminating flow allowed for a baseline sedimentation rate to be determined; in evaluating the feasibility of adapting this system to a flow stream, this baseline served as a best-case scenario. Construction of the channel and details of the

observations are described in Section 3.3. Two temperature-responsive smart polymers—PNIPAAm and PDEAm—were examined, at a range of concentrations and polymer molecular weights, in order to determine if these parameters had any impact on sedimentation behavior. Sedimentation was performed at room temperature in the presence of high concentration of ammonium sulfate, which lowered the LCST of the polymers to below room temperature. This eliminated complications related to heating a microfluidic channel, including the complexities of heated channel construction and temperature-gradient-induced convective flow in the channel. The sedimentation rate for each system studied was determined simply by designating an arbitrary sedimentation boundary and recording the downward movement of that boundary over time.

In addition the behavior of smart polymer aggregates, a potential method for increasing the rate of smart-polymer triggered sedimentation was investigated. This method was based on the PNIPAAm latex-based flocculation systems described in Section 1.3.3.[188,189,192] PNIPAAm was covalently conjugated to the surface of latex nanobeads and these conjugate particles were observed in a heated microfluidic channel. However, rather than sedimenting, the PNIPAAm-coated beads aggregated and adhered to the walls of the channel in a reversible response to channel temperatures above the LCST of the polymer. This behavior was immediately apparent as a potential method for controllably and reversibly immobilizing biomolecules in microfluidic channels: a process the importance of which is described in Section 1.2.3. Consequently, the stability and reversibility of the observed adhesion behavior was studied in some detail.

3.3 Experimental Materials and Methods

3.3.1 Microfluidic device design and fabrication

Microfluidic devices were constructed from stacked sheets of poly(ethylene terephthalate) (PET). Two-dimensional features were cut into these sheets via ultraviolet (UV) laser ablation and the cut sheets were stacked and joined with adhesive to form three-dimensional features (see figure 3.4).[60] Adhesive-coated PET was obtained from Fralock, Inc. (San Carlos, CA). This substrate was machined with a computer-controlled CO_2 laser-cutting system (model M25, Universal Laser Systems, Scottsdale, AZ). The fluidic access ports in these devices were designed to be compatible with a standardized microfluidic manifold. The devices were held in the manifold by a screw-on pressure plate; PDMS gaskets sealed the external fluidic tubing on the manifold to the fluidic access ports machined in the device (Figure 3.5). This manifold served to connect the input and output ports of the

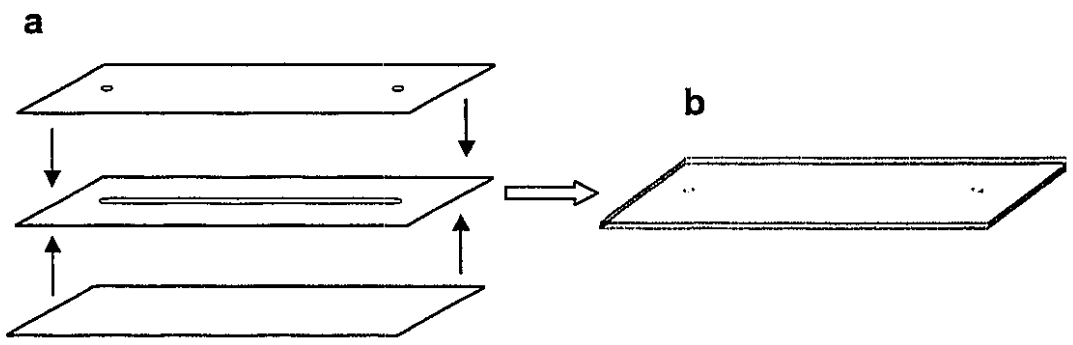

Figure 3.4: Device fabrication. Device features are cut into mylar sheets (a). These sheets are aligned and joined together with pressure sensitive adhesive, sealing off the features and forming a closed microfluidic device (b). This diagram shows a device made from three layers. The top layer contains fluidic access holes, the middle layer contains a channel, and the bottom layers seals off the channel.

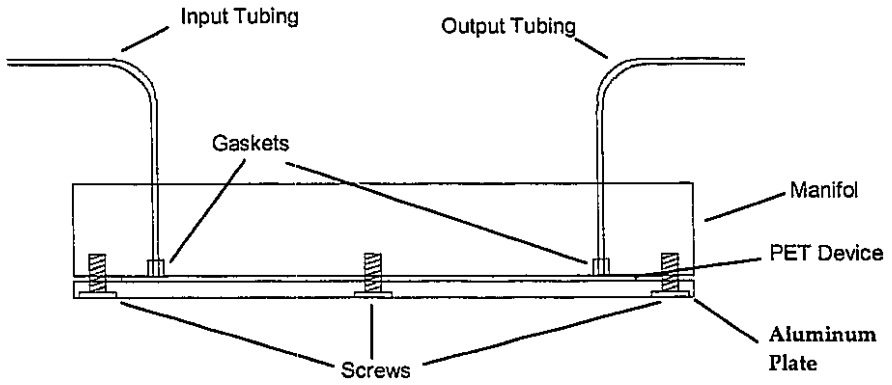

Figure 3.5: Fluidic manifold assembly for a stacked mylar device. Pressure on the device, delivered by the screws passing through an aluminum plate, secures the fluidic access points on the device to the gaskets in the manifold. Fluidic input and output tubing passes through these gaskets and are held against the access points on the device.

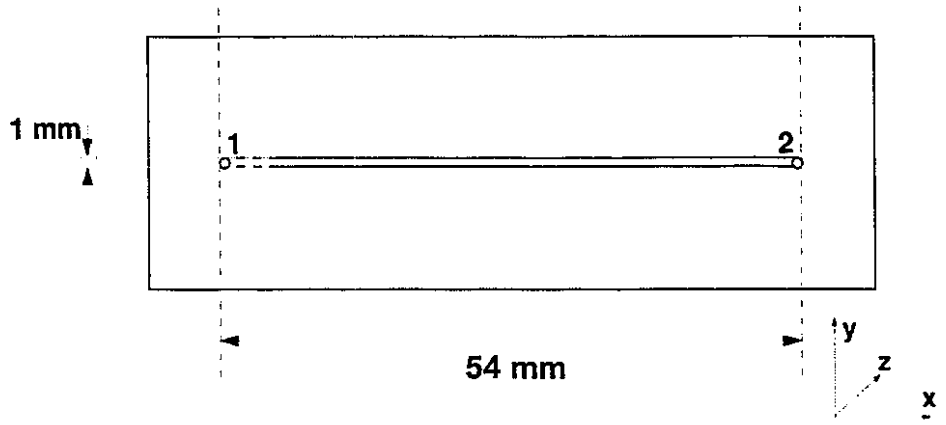

Figure 3.6: Top-view schematic of device used for polymer aggregate sedimentation experiments. The single channel had dimensions of 1 mm × 54 mm × 0.3 mm (in the z dimension). This diagram shows the channel input (1) and output (2) ports.

device to polyetheretherketone (PEEK) tubing. PEEK tubing had a 0.030 inch inner diameter (ID) and was obtained from Upchurch Scientific (Oak Harbor, WA). The device input and output were each connected by the manifold to about 6 cm of tubing.

A schematic of the device design used for the polymer sedimentation experiments is shown in Figure 3.6. This device contained a single channel with one input port and one output port, with dimensions of 54 mm × 1 mm × 300 μm. The channel was formed from a

sheet of 250 μm-thick PET, coated on each side with a 25 μm-thick layer of adhesive. The channel layer was sealed on each side by a 100 μm-thick sheet of PET; into one side the inlet and outlet ports were cut. The device used for PNIPAAm-coated nanobead experiments had a similar design, but it incorporated a thin film heater in a PET layer adjacent to the channel (Figure 3.7). The thin-film heater was obtained from Minco (Minneapolis, MN); this heater was operated using an electronic feedback controller (Minco) to maintain temperatures in the device channel between 40 and 45 °C. (A Therma-Clear™ model heater and HeaterStat™ model controller were used.) The heater was separated from the channel by two layers of PET. A 100 μm thick layer formed the wall of the channel and a 100 μm thick adhesive-coated layer joined the heater to the rest of the device. The heater itself was about 250 μm thick and was incorporated into a 250 μm thick PET layer. The heater was positioned so as to heat the entire length of the channel.

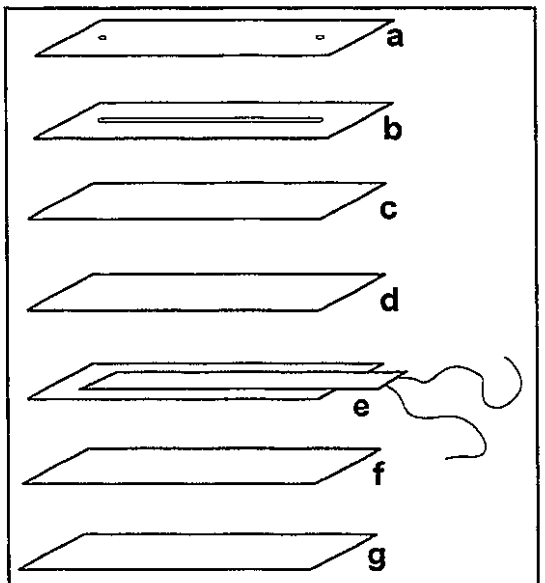

Figure 3.7: Exploded view of device with thin film heater incorporated. Layers shown are: (a) Device top with fluidic input and output holes. (b) Microfluidic channel. (c) Channel back wall. (d) Adhesive layer for attaching heater. (e) Heater layer (with wire leads of heater shown). (f) Adhesive layer. (g) Device bottom, sealing off adhesive.

3.3.2 Observations of smart polymer aggregate sedimentation

To monitor sedimentation of smart polymer aggregates in the microfluidic channel, the device was oriented as shown in Figure 3.8: with the y-axis parallel to the

gravitational field. The device was mounted on a translation stage, allowing for focus to various points on the z-axis and movement along the x-axis. A CCD camera (Optronics, Goleta, CA) was focused through a magnifying optical train along the z-axis of the device, which was illuminated from behind by a diffuse incandescent lamp. Images from the CCD camera were captured on a personal computer equipped with a Scion SG-9 video capture card (Scion Corp., Frederic, MD).

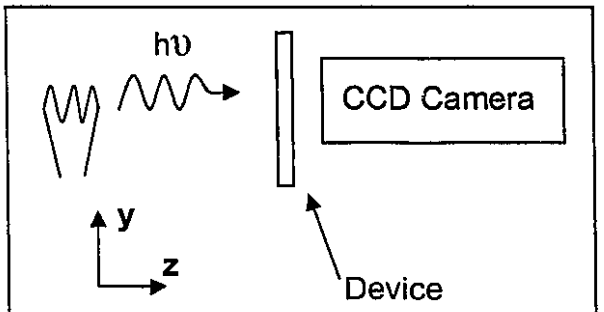

Figure 3.8: Observational apparatus for experiments involving sedimentation in a microfluidic channel. The y- and z-axes shown here correspond to those shown for the device design in figure 3.6. Light is shone through the thin axis of the device channel. Particles in the channel absorb and scatter light, and therefore appear dark in images captured by the CCD camera.

The polymers PNIPAAm and PDEAm were synthesized according to previously published protocols.[117,181] PNIPAAm molecular weight was determined by vapor pressure osmometry; PDEAm molecular weight was determined by gel permeation chromatography. Sedimentation experiments were performed for a number of molecular weights: PDEAm preparations of 6.7 kDa, 12.8 kDa, and 57.8 kDa; and PNIPAAm preparations of 5 kDa, 7 kDa, 11 kDa, and 21 kDa. In each sedimentation experiment, an aggregated polymer suspension consisting of a varying concentration of polymer, 600 mM ammonium sulfate, 20 mM phosphate, and 5 mM sodium chloride buffered at pH 7.6 was prepared. The addition of ammonium sulfate resulted in the immediate aggregation of the polymer at room temperature. For each polymer molecular weight, concentrations of 2 mg/mL, 3 mg/mL, and 4 mg/mL were prepared. PNIPAAm samples were also examined at 1 mg/mL. At the

beginning of each sedimentation experiment, the polymer aggregate suspension was injected into the microfluidic channel manually via a syringe connected by standard HPLC fittings (Upchurch, Oak Harbor, WA) to the manifold input PEEK tubing. After this initial loading, the channel was sealed off by an HPLC valve (Upchurch) and fluid in the channel was allowed to remain undisturbed by any flow field for the duration of the experiment. Once the aggregate suspension was loaded into the channel, images of the channel were captured by the CCD camera/ video capture card at a rate of once per minute for an hour. The channel was then rinsed by flowing through deionized water.

3.3.3 Analysis of sedimentation data

Images captured during the polymer aggregate sedimentation experiments were analyzed using in-house software built with the ImageMagick image-processing library (http://www.imagemagick.org). The image dimensions were 480 pixels along the device x-axis and 640 pixels along the device y-axis. Initially, the images were averaged along the x-axis, as shown in Figure 3.9. This process produced a set of average pixel intensities as a function of y-axis position (y-axis position is henceforth referred to as "height" or "channel height"). These functions were truncated

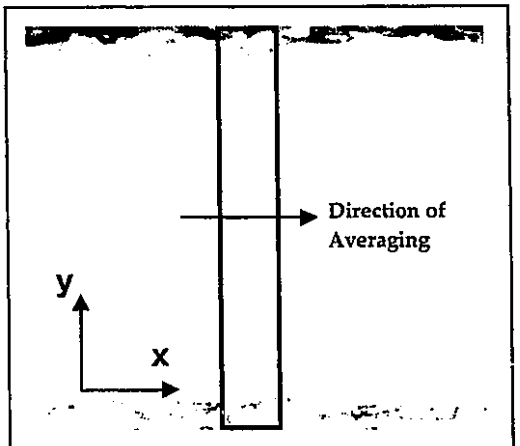

Figure 3.9: Channel immediately following introduction of polymer aggregate suspension. Axes as shown in Figure 3.6. The box shows the swath averaged along the x-axis for data analysis.

manually at each end to remove values corresponding to the top and bottom of the channel, seen at the top and the bottom of the image in Figure 3.9. The remaining average intensities reflected the concentration of aggregate particles at each point along the channel height; darker pixels corresponded to higher concentrations of aggregate particles. We attempted to establish an arbitrary sedimentation boundary for each "intensity vs. height" data set. Typically, this boundary could only be located in images taken at least 15 minutes into the sedimentation experiment, since it took this long for the aggregates to begin settling and form a sedimentation boundary. For each sedimentation experiment (corresponding to a time series of images), the initial image in which a sedimentation boundary could be established was identified, and the height of the sedimentation boundary was determined for each subsequent image in the series. This analysis yielded a data set of sedimentation boundary height vs. time for each experimental condition. A nominal sedimentation rate could be determined by making a linear regression to the linear region of each of these data sets.

Two approaches were taken to establish the location of the sedimentation boundary. The first method was based on the empirical observation that the concentration profile of a settling suspension is sigmoidal with height. Averaged pixel intensity was therefore fit to the Pearl-Reed sigmoidal curve as a function of channel height:

$$\bar{g} = \frac{1}{1 + ae^{-by}},$$

where $\bar{g}$ represents normalized grayscale pixel intensity, y is position in the channel, and a and b are arbitrary curve position and shape parameters. This equation was linearized by the transformation:

$$\overline{G} = \ln \frac{\overline{g}}{1-\overline{g}},$$

such that:

$$\overline{G} = \alpha + by, \text{ where } \alpha = -\ln a .$$

The data were fit to this function by linear regression to determine b and α. The Pearl-Reed curve is symmetric in the dependant variable, with the inflection point at $\overline{g} = 1/2$. This inflection point was used as the arbitrary sedimentation boundary.

For some images, however, it was difficult to fit the pixel intensity values to a sigmoidal curve: the data for these images, which typically involved relatively large aggregate particles, took the form of a step function. In these cases, a second method for determining the height of the sedimentation boundary was used. The arithmetic mean and standard deviation of the average pixel intensity was calculated for the five pixels closest to the top of the channel in the image. The sedimentation boundary was then assigned to the highest pixel in the image with an average intensity two standard deviations darker than this mean.

3.3.4 Preparation of PNIPAAm-coated latex beads

Primary amine-functionalized polystyrene latex beads were obtained from Polysciences (Warrington, PA). 100 nm diameter Polybead® Amino

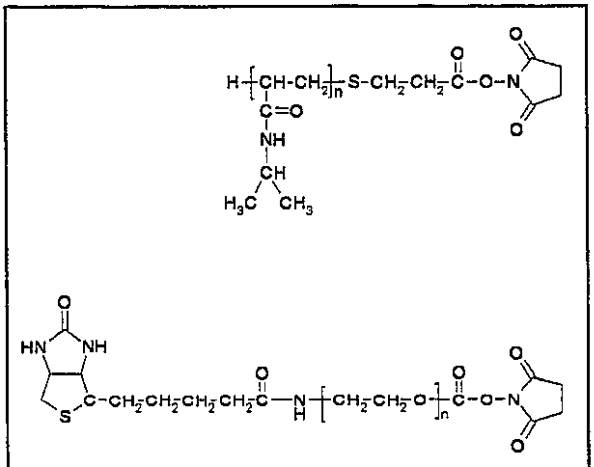

Figure 3.10: Chemicals used to modify latex beads. NHS-PNIPAAm (top) and NHS-PEG-b (bottom).

Microspheres were used in all experiments. The beads were covalently modified with 11 kDa PNIPAAm and 3.4 kDa poly(ethylene glycol)-biotin (PEG-b) via N-hydroxysuccinimide (NHS) ester conjugation chemistry. The PNIPAAm imparts temperature-responsive phase aggregation behavior to the beads, while the PEG-b allows the beads to be conjugated to a variety of biomolecules via the biotin-streptavidin interaction. The chemical structures of these modification agents are given in Figure 3.10. NHS-PEG-biotin was obtained from the Shearwater Corporation (Huntsville, AL). NHS-PNIPAAm was synthesized according to a previously published protocol[117], as in Chapter 2. The number-average molecular weight ($\overline{M}_n$) of this polymer was determined to be 11,000 by vapor pressure osmometry (VPO, device model OSV111, Knauer, Germany).

Beads were modified with NHS-PEG-biotin by reaction at a 1:10 molar ratio of surface amine groups to NHS-PEG-b at pH 9.0 and 4 °C overnight. Approximately 40% of the available amine groups on the bead surfaces were modified. Beads were separated from unreacted NHS-PEG-b by threefold centrifugation and resuspension. PEG-b modified beads were then reacted with NHS-PNIPAAm. The reaction was performed at a 10-fold molar excess of NHS-PNIPAAm relative to unmodified surface amine groups at pH 9.0 and 4 °C overnight. Beads were separated from unreacted NHS-PNIPAAm by threefold centrifugation and resuspension at 4 °C to avoid the phase transition and aggregation of unreacted NHS-PNIPAAm. In addition to the doubly modified PEG-b/PNIPAAm beads, singly modified PNIPAAm beads were prepared. All centrifugations were performed at a relative centrifugal force of 16,600 × g.

3.3.5 Analysis of conjugation reaction products

The concentrations of beads in bead suspensions were determined by measuring the optical density at 600 nm (OD_{600}) of these suspensions. This method of analysis was calibrated by measuring the OD_{600} of five serial dilutions of beads from 0.15 to 1.5 wt% and fitting these measurements by linear regression, resulting in the relationship

$$[bead]_{wt\%} = 0.0683 \cdot OD_{600} - 0.000522 .$$

The correlation coefficient for this regression was 1.000. Serial dilutions were made from unmodified Polybead® Amino Microspheres, and concentrations of all types of beads were determined from the derived relationship.

To determine the degree of conjugation of modification chemicals to nanobeads, two colorimetric assays were used. For biotinylated beads, a modified version of the (4'-hydroxyazobenzene) benzoic acid (HABA) assay was used.[228] This assay is based on the fact that HABA undergoes an increase in absorption at 500 nm upon binding to the biotin binding site of streptavidin. However, the association between HABA and streptavidin is weak, and HABA bound to streptavidin is promptly competed off by any free biotin in solution. Hence, the change in OD_{500} of a solution of streptavidin and HABA upon addition of a sample can be used to report on the concentration of biotin present in that sample. This change is typically calibrated via titration of the HABA/streptavidin solution with known concentrations of biotin. For the sample at hand, however, this straightforward assay is complicated by the fact that the beads scatter strongly at 500 nm. To take this effect into account, a non-traditional calibration approach was taken. Two solutions of beads were prepared—one solution containing the modified PNIPAAm/PEG-b bead sample, the other containing

unmodified beads. These solutions contained the same concentration of beads, as confirmed by absorbance at 600 nm. To calibrate the assay, a 10 μL aliquot of the unmodified bead solution was added to a solution of HABA/streptavidin. A series of aliquots of standard biotin solution was then added to this unmodified bead/HABA solution in order to generate a standard curve of OD_{500} vs. biotin concentration in the presence of beads. The biotin-modified bead sample was analyzed by adding a 10 μL aliquot of the modified bead suspension to a solution of HABA/streptavidin, identical to the HABA solution used to generate the standard curve. The OD_{500} of the combined solution was compared to the calibration curve to determine the biotin concentration.

The degree of modification of the PNIPAAm modified beads was determined using the 2,4,6-trinitrobenzene sulfonic acid (TNBSA) assay[235]; this assay had to be modified in a similar manner. TNBSA reacts with primary amines to produce a derivative with absorbance at 335 nm. Unfortunately, the latex beads used in this work also absorb strongly at this wavelength. To take this effect into account, bead samples to be reacted with TNBSA were divided into two aliquots: to one aliquot the TNBSA solution was added, to the other only buffer was added. The OD_{335} of the unreacted sample was subtracted from that of the reacted sample to isolate the TNBSA signal from the bead signal. This TNBSA signal was then divided by bead concentration, determined as described above, to produce a number proportional to the amount of free amine per bead.

3.3.6 Observations of bead aggregation, adhesion, and stability

Observations of bead aggregation and adhesion were made in the heated device described in the section "microfluidic device design and fabrication" above. This device was mounted and observed as described above in the section "observations of smart polymer aggregate sedimentation" (Figure 3.8). The bead suspension injected into the microfluidic channel consisted of 0.3 wt% doubly modified b-PEG/PNIPAAm beads, 0.3 wt% singly modified PNIPAAm beads, and 2.5 mg/mL free PNIPAAm in pH 7.6 PBS (20 mM phosphate, 5 mM NaCl). The singly modified beads and free PNIPAAm were added to decrease the concentration of doubly modified beads required to form a continuous adherent network on the channel walls. The suspension was degassed by agitation under vacuum for approximately five minutes immediately prior to use. Bead suspension was injected into the channel from a syringe directly connected to the manifold tubing. Upon activation of the device heater, images were captured at a rate of 3 per minute to obtain a visual record of bead aggregate formation and adhesion. To observe dissolution, the heater was deactivated at a nominal zero time point and images were subsequently captured at a rate of 3 per minute. Images were processed and analyzed using in-house software based on the ImageMagick library.

Further experiments were undertaken to explore the stability of bead adhesion. The device was mounted in the manifold and 300 μL of bead matrix suspension were injected into the primary fluid input port of the channel from a syringe directly connected to the manifold tubing. The manifold tubing was then connected to a 1.5 mL sample loop filled with degassed pH 7.6 PBS. This sample loop was connected to a computer-controlled syringe

pump system (Kloehn Co., Ltd., Las Vegas, NV) fitted with 100 μL syringes. After activating the heater, matrix formation was allowed to proceed in the absence of flow for 10 minutes. The pumps were then activated, pushing buffer through the system at a rate of 10 μL/min. Fluid flowing through the device was captured at the exit of the manifold output tubing in 50 μL aliquots. After 70 minutes, the heater was deactivated while the flow was maintained at a constant rate. Aliquots continued to be collected for an additional 40 minutes as the matrix dissolved. The output aliquots were then diluted to 500 μL in deionized water and the OD_{600} of each aliquot was measured to obtain a bead concentration, as described above. This experiment was performed in triplicate.

3.4 Results and Discussion

3.4.1 Results: Smart polymer aggregate sedimentation

Figure 3.11 shows a series of images from a PDEAm sedimentation experiment. The downward movement of the sedimentation boundary as the experiment proceeds is apparent. Figure 3.12 shows a typical fit of intensity profile data from one of these images to a Pearl-Reed sigmoidal curve. The inflection point of this curve, which was arbitrarily designated as the sedimentation boundary, is highlighted. All PDEAm data taken after the formation of sedimentation boundaries could be successfully fit to Pearl-Reed sigmoidal curves. Figure 3.13 shows the sedimentation boundary height over the course of an experiment, with a linear regression to the part of the curve corresponding to the particulate settling regime shown. Similar linear regressions were performed for each sedimentation

experiment: Figure 3.14 shows the corresponding sedimentation rates plotted as a function of polymer molecular weight and concentration. Attempts were made to study PDEAm concentrations lower than 2 mg/mL; however, polymer aggregate suspensions at these concentrations were insufficiently dense to absorb the light necessary to produce quality sedimentation images. Concentrations greater than 4 mg/mL displayed no appreciable sedimentation in the time frames studied.

A series of images demonstrating PNIPAAm aggregate sedimentation is shown in Figure 3.15. PNIPAAm aggregate particles were larger than PDEAm aggregate particles. As a result, the image grayscale profiles from PNIPAAm sedimentation experiments had a step functional form; they could not be easily fit to sigmoidal curves. The second method of sedimentation boundary determination described in section 3.3 was therefore used for data from these experiments. The determined

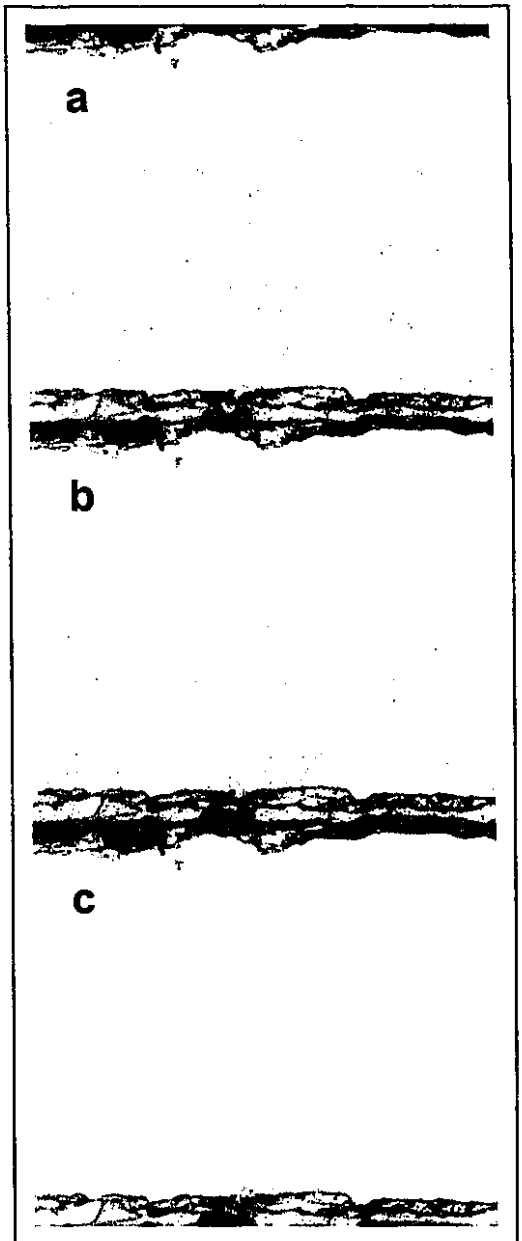

Figure 3.11: A series of images taken during the sedimentation of PDEAm aggregates. Channel orientation as in figure 3.9. (a) 10 minutes after injection of aggregate suspension. (b) 20 minutes. (c) 30 minutes. Downward movement of the sedimentation boundary is apparent.

sedimentation rates over the set of PNIPAAm sedimentation experiments are given in Figure 3.16.

3.4.2 Lessons from polymer aggregate sedimentation data

The PDEAm data reveal a clear trend relating polymer concentration and sedimentation rate. As concentration increases, sedimentation rate decreases. This is expected from the theory described in Section 3.2.1: as particle concentration increases, the suspension becomes increasingly crowded, and the particles begin to hinder one another. Though it is unclear from these data whether the differences between the 2 mg/mL and 3 mg/mL samples are sufficiently significant to indicate a transition from the particulate to

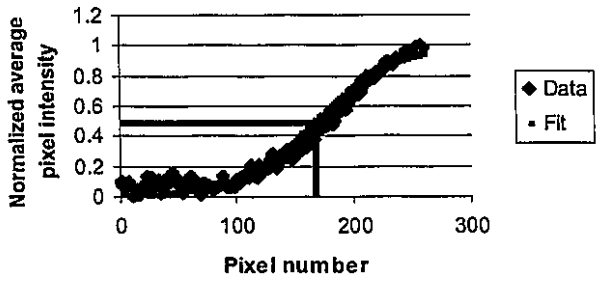

Figure 3.12: A typical fit of grayscale data from a PDEAm aggregate sedimentation experiment to a Pearl-Reed curve. The inflection point is indicated on both axes by the red lines. These data are from an experiment with 12.8 kDa polymer at 4 mg/mL.

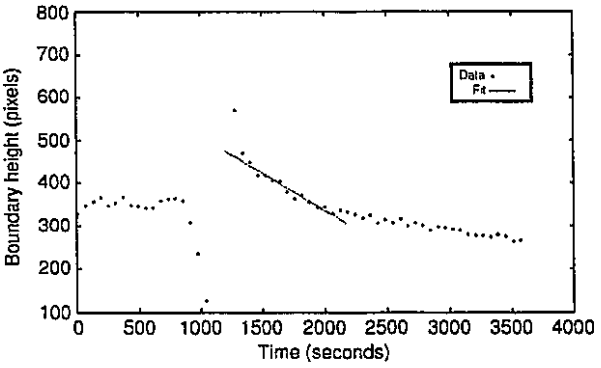

Figure 3.13: Sedimentation boundary height in a PDEAm sedimentation experiment as a function of time. Each data point corresponds to the boundary height in a single image. A linear regression fit to the initial linear portion of the sedimentation curve is also shown. Points prior to the beginning of this fit (about 1400 s) are artifacts produced when the image analysis routine is applied to images in which no clear sedimentation boundary is apparent.

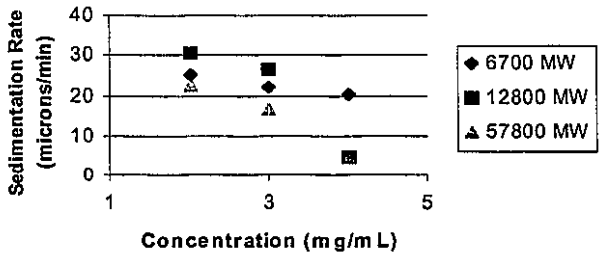

Figure 3.14: PDEAm sedimentation rate as a function of polymer concentration and molecular weight.

hindered settling regime, the radically decreased rates of sedimentation observed at 4 mg/mL indicate that these samples, at least, show signs of hindered sedimentation. No conclusions on a relationship between sedimentation rate and polymer molecular weight can be drawn from the PDEAm data. While PNIPAAm particles showed, in general, faster sedimentation than PDEAm particles, their was significantly more scatter in the PNIPAAm data, and no trends can be observed in these data.

From an engineering point of view, these questions of trends in the sedimentation data are less important than the fundamental question of whether the observed sedimentation rates are sufficient to facilitate a sedimentation-based separation process in a flowing fluid stream. A sedimentation-based separation device would operate by splitting off a flow stream from which particles have been cleared by sedimentation. The distance over which

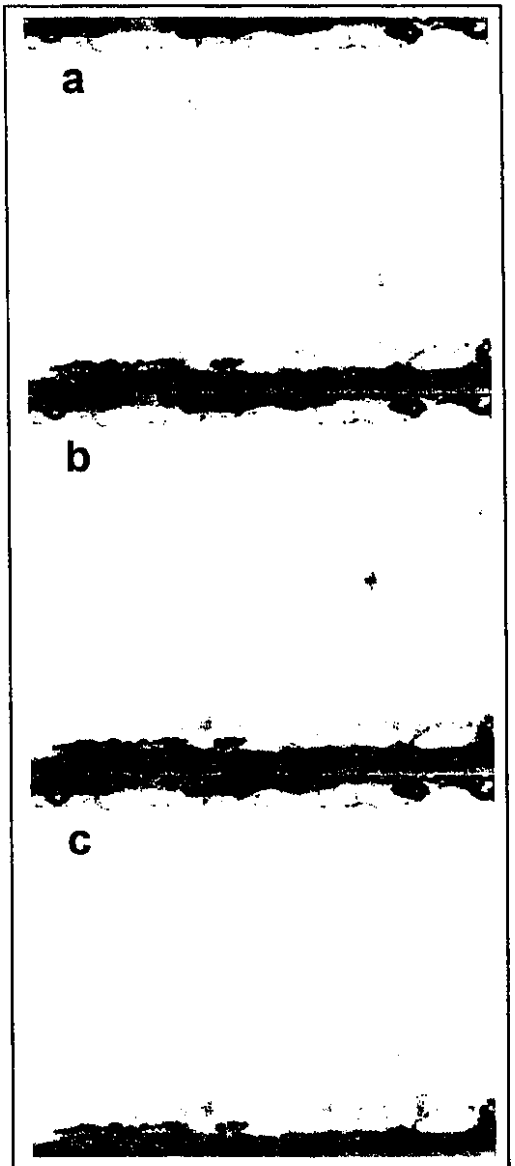

Figure 3.15: A series of images taken during the sedimentation of PNIPAAm aggregates. Channel orientation as in Figure 3.9. (a) Immediately following injection of polymer aggregate suspension. (b) 2.5 minutes after initial injection; settling of particles is evident. (c) 6.5 minutes after initial injection; most particles have settled to the bottom of the channel. These images are from an experiment involving 21 kDa PNIPAAm at a concentration of 4 mg/mL.

such particles must sediment in order for such a separation to be effective would therefore be determined by the size of the channel through which the particle-cleared fluid flows. With the laser-ablation fabrication technology used to make the devices in which these experiments were performed, the minimum possible channel width is about 300 μm. For the fastest PNIPAAm particle sedimentation rate observed, 140 μm/min, this distance would require a channel residence time of 2.1 minutes. For PNIPAAm sedimentation rates closer to the median observed rate, the required residence time begins to approach 5 minutes. For the most rapidly sedimenting PDEAm particle, the residence time necessary to effect a separation increases to 10 minutes. Based on average linear flow rates, these residence times translate to volumetric flow rates of between 1.6 and 7.7 μL/min in the device constructed for these experiments. While these are achievable flow rates for a microfluidic system, they are quite slow, and they represent an absolute best-case scenario. In a real flow system, the fluid at the center of the channel will be moving at a rate considerably faster than the average linear flow rate, and will therefore have a shorter residence time. Furthermore, there is no guarantee that polymer aggregate particles sedimenting in a flowing stream will settle at the same rate as in a stagnant fluid. To compensate for such complicating factors, it was deemed desirable to find a more rapidly sedimenting smart polymer separation agent before sedimentation-in-flow experiments were considered. PNIPAAm-coated latex beads were investigated as such as system.

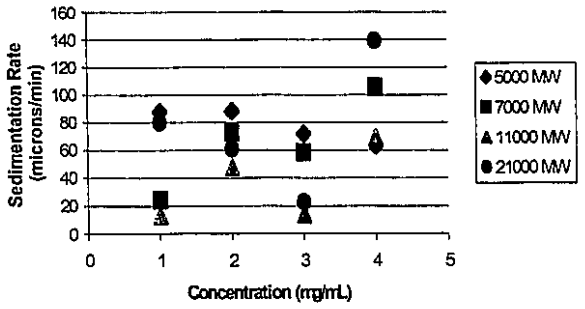

Figure 3.16: PNIPAAm aggregate sedimentation rate as a function of polymer concentration and molecular weight.

3.4.3 Characterization of latex bead modification products

To determine the degree of biotinylation on PNIPAAm/PEG-b modified latex beads, a HABA assay was performed. Based on the concentration of amine groups on the beads reported by the bead manufacturer, 40% of available primary amine groups had reacted with NHS-PEG-biotin. Approximately 60% of the reactive amine moieties originally on the beads were therefore available for modification by NHS-PNIPAAm in the subsequent reaction. Unfortunately, a TNBSA assay to quantify the extent of total modification of these beads failed to produce sensible results. However, the beads displayed aggregation behavior at temperatures above the LCST of PNIPAAm, demonstrating sufficient polymer conjugation for function. A TNBSA assay of beads modified only with PNIPAAm did produce sensible results: these beads had 66% as many free primary amines as unmodified beads, indicating that ~34% of the available primary amines were modified with NHS-PNIPAAm. These beads demonstrated temperature-sensitive aggregation behavior as well.

3.4.4 Characterization of bead aggregation and adhesion in microfluidic channels

The initial intention in modifying latex beads with PNIPAAm was to take advantage of their flocculation properties to accelerate sedimentation. However, initial observations of the behavior of these beads in a heated microfluidic channel revealed that while they did, in fact, aggregate in response to a thermal stimulus, the aggregates did not sediment. Rather,

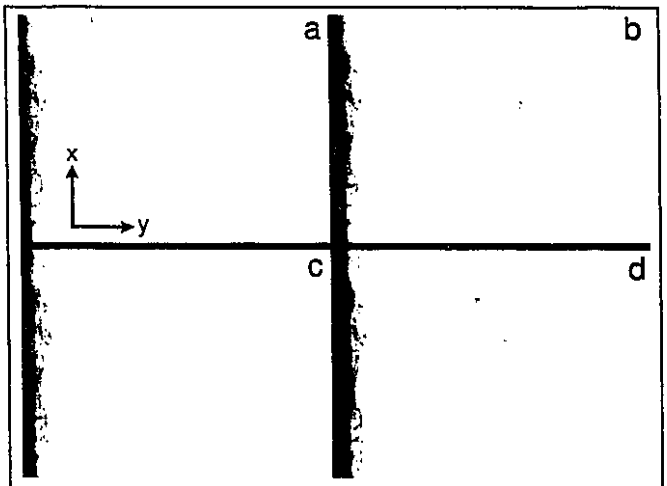

Figure 3.17: A series of images showing matrix formation and dissolution, taken in a type A channel under static (no flow) conditions. X- and y-axes on this figure correspond to those shown in Figure 3.6 and the edge of the channel can be seen at the left side of each image. (a) Matrix suspension at room temperature. (b) After approximately 30 seconds of heating, aggregates of beads can be seen. (c) After approximately 2 minutes of heating, aggregates have formed large structures that are adhering to the channel wall. (d) Approximately one minute after heater deactivation, bead structures can be seen dissolving. Each panel in this figure is approximately 1 mm wide (in the y dimension).

they formed extended fibrous structures that adhered to the walls of the channel. Figure 3.17 shows a series of images demonstrating the formation and dissolution of these structures in response to temperature changes. In Figure 3.17a, the channel is filled with the bead matrix suspension at room temperature; 3.17b shows the channel approximately 30 seconds after the heater has been activated—aggregate formation is apparent; in 3.17c, the aggregates have coalesced into large aggregated networks which have adhered to the side of the channel after about 2 minutes of heating; finally, 3.17d shows the network dissolving about 1 minute after the heater was deactivated. Once network dissolution was complete, the channel appeared as it does in Figure 3.17a. In order to assign a numerical index to the process of adherence and network formation, images like those in Figure 3.17 were analyzed by taking simple averages of the grayscale values of the image pixels. Though the average grayscale was the same in images before (Figure 3.17a) and after (Figure 3.17c) adhesion, the standard deviation from the mean was significantly greater in images containing aggregated beads than in those containing free bead suspension.

Figure 3.18 shows a plot of standard deviation versus time for two series of images: one taken from an aggregate formation and adhesion experiment, the other from an aggregate dissolution experiment. Both of these experiments took place in a temperature-controlled channel in the absence of flow. It is clear from Figure 3.18 that adhesion and dissolution take place on similar time scales, about 3-6 minutes for the bead, heater, and device combination used in this experiment.

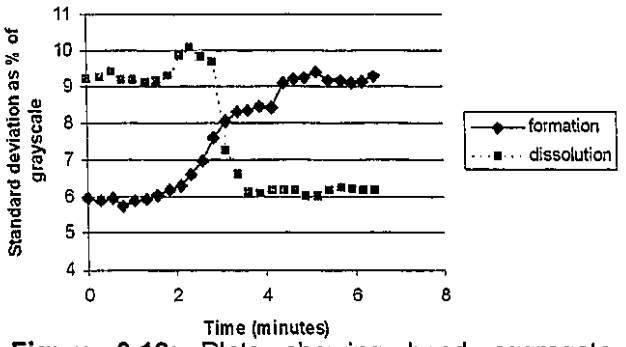

Figure 3.18: Plots showing bead aggregate network formation and dissolution, derived from images like those in Figure 3.17. These plots give the standard deviation from the mean grayscale in sequential images captured after heater activation (the zero time point for the "formation" plot) or heater deactivation (the zero time point for the "dissolution" plot). Standard deviation is plotted on the y-axis, while time since heater activation or deactivation is plotted on the x-axis. The structure formation that can be seen in Figures 3.17b and c results in an increased standard deviation that is reflected in these plots. These plots reveal that for the system used in the present experiments, matrix formation and dissolution take place on a similar time scale, about 3 to 6 minutes. Prior to averaging, a strip of 100 × 480 pixels containing the channel edge seen to the left of the images in Figure 3.17 was excised from each image. Image statistics were taken on a pixel-by-pixel basis over the remaining 540 × 480 pixels.

Of course, the behavior of PNIPAAm beads in a microfluidic channel is of minimal practical interest in the absence of a flowing fluid stream. Continuously pumping an aqueous suspension of the beads into a heated channel resulted in aggregate formation, but no adhesion to the channel wall. However, when aggregated and adhered beads were subjected to flowing fluid, they remained adhered, so long as the temperature of the channel was maintained above the PNIPAAm LCST. Figure 3.19 shows a plot of the concentration of beads in the output of a channel over time under a 10 μL/min flow. The output was collected in 50 μL aliquots, such that each point represents the previous five minutes' worth of flow

through the system. The x-axis is labeled according to the total volume that has been pumped through the system at each point. Beads were initially adhered to the channel walls under static conditions, with no flow through the channel. The peak apparent in the first 100 μL leaving the system represents beads that did not adhere to the side of the channel during this initial formation step. After this initial flowthrough peak, no beads are present in the next 700 μL leaving this system. The heater was deactivated at 70 minutes into the experiment (corresponding to the 700 μL point in Figure 3.19). It took another 10 minutes (100 μL) for the bead matrix to dissolve and pass through the manifold output tubing. The peak at the 800 μL point represents these released matrix beads. The two peaks in this plot have similar areas, indicating that about 50% of the initially injected bead suspension adhered to the channel walls until the elution step, while another 50% was non-adherent and was washed out of the channel immediately. These data demonstrate that the matrix is stable under flow conditions

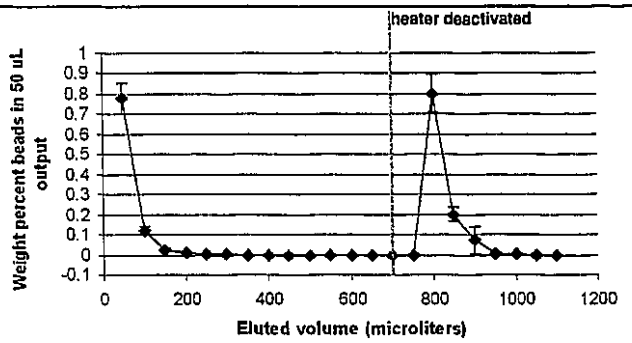

Figure 3.19: Concentration of beads in samples collected from the manifold output line over the course of a flow experiment. Bead adhesion formation was performed in the absence of flow; 10 μL/min flow was initiated at the zero volume point of this plot. Each point represents 5 minutes of flow through the system, corresponding to a 50 μL sample. The y-axis gives the concentration of beads in the samples, determined spectrophotometrically as described in the experimental section. The x-axis gives the total volume that has flowed through the system at the time of collection of each sample. The heater was activated prior to the initiation of flow, and it remained on until the indicated point at 700 μL, at which point it was deactivated. The initial peak, at about 50 μL, corresponds to beads that did not adhere to the channel during the initial adhesion step. The peak at 800 μL corresponds to beads entering the flow stream from the dissolved matrix. The lack of beads in the output stream between these points indicates that the adhered beads remained stable and intact in the presence of flow. Displayed points represent the arithmetic means of data from three experiments; error bars are ± one standard deviation.

for long periods of time and that it maintains reversibility after being exposed to prolonged flow conditions.

3.5 Conclusions

Smart polymer sedimentation has been investigated as a means of controlled separation in microfluidic devices. Experiments were performed to determine the rates of sedimentation of aggregates of the temperature-responsive polymers PNIPAAm and PDEAm in stagnant fluid in a microfluidic channel. These rates proved to be insufficient to facilitate an effective separation in a microfluidic device in a reasonable time frame. In an attempt to increase the rate of sedimentation of the temperature-sensitive particles, PNIPAAm was conjugated to the surface of polystyrene latex beads. Rather than sedimenting in response to a thermal stimulus, however, these beads aggregated and adhered to the walls of the microfluidic channel.

Fortunately, this controllable adhesive property is also potentially valuable in microfluidic devices: it can be used as a means of controlled immobilization of biomolecules. Experiments described in this chapter have demonstrated that adhered beads are stable in the presence of flow through the channel, and that the adhesion is reversible upon reversal of the thermal stimulus, even after prolonged adhesion. In future chapters, PNIPAAm-coated beads are demonstrated to be controllable, reversible immobilization substrates for bioanalytical systems, including an affinity chromatography system and an immunoassay. The application of smart polymer aggregate sedimentation to separation in microfluidic devices is not studied further in experiments described in this dissertation; however,

experiments in this chapter have demonstrated that such an application may be an intriguing, if challenging, possibility.

Chapter 4: A Smart Microfluidic Affinity Chromatography Matrix Composed of Poly(*N*-isopropylacrylamide)-Coated Beads*

4.1 Summary

The experiments described in Chapter 3 have established that PNIPAAm-coated polystyrene latex beads aggregate and adhere reversibly to the walls of PET microfluidic channels in response to a thermal stimulus. Furthermore, these experiments have established that this adhesion is stable in the presence of flow for over an hour, so long as the thermal stimulus is maintained. These properties—controlled, reversible, stable adhesion—make PNIPAAm-coated latex beads a potentially ideal platform for biomolecular immobilization in microfluidic devices. In order to demonstrate this potential, PNIPAAm-coated beads co-modified with biotin were deployed as a reversibly immobilized affinity chromatography matrix to separate streptavidin from a microfluidic flow stream. Affinity chromatography was chosen as a demonstration technology because, as described in Section 2.2, it is a bioseparation technology of central importance in modern biochemistry and molecular biology laboratories. Furthermore, affinity chromatography is an appropriate initial demonstration because it is a relatively straightforward technology to implement: to serve as an affinity chromatography substrate, the beads only need by modified with a small molecule affinity moiety, rather than with a relatively large, complex protein. This chapter

describes the implementation and investigation of a "smart bead"-based affinity chromatography system. Section 4.2 describes the design options considered in the process of this implementation, including options for attaching an affinity moiety to the beads, for loading the beads into the microfluidic device, and for introducing the appropriate solutions to the microfluidic flow stream. Section 4.3 describes in detail the experimental protocols employed; results of these experiments are given and discussed in Section 4.4. This chapter concludes with a brief overview of the implications of these results.

4.2 Objectives and Experimental Design Considerations

The objective of the work described in this chapter is simple: to demonstrate the feasibility of an affinity chromatography system based on thermally immobilized PNIPAAm-coated beads. For this proof-of-principle system, little work was done to optimize the performance of the chromatography or to compare the system's performance to the state-of-the-art in microfluidic affinity chromatography. Furthermore, a simple biomolecular affinity model system was chosen to provide the interaction by which the affinity separation was effected. This was the biotin-streptavidin system, described in detail in Section 1.4. The high affinity, fast on-rate, and practically irreversible binding of this system make it an appealing option. PNIPAAm beads were therefore co-modified with biotin and streptavidin was injected into the microfluidic channel as a separation target molecule.

Two options were explored in attaching biotin to the beads. Biotin groups were conjugated to beads either through a short linker consisting of a five-carbon-long alkane chain, or through a 3.4 kDa PEG linker. This variable allowed the importance of the distance

of the biotin group from the bead surface to be explored: an important parameter given the potential of the PNIPAAm molecules bound to the bead surface to interfere sterically with streptavidin binding. Successfully demonstrating smart bead affinity chromatography also involved an exploration of some options for microfluidic device geometry. Two devices geometries were investigated. The first type of device involved a single, straight, homogenously heated channel. A second design attempted to eliminate some limitations encountered in using the first type of device. This new design involved multiple channels for injection of a variety of reagents, a geometry designed to maximize surface area and minimize bubble formation, and a heater configuration designed to eliminate clogging of the channel input and output ports with aggregated beads.

The final parameter that was optimized in designing chromatography experiments was the methodology for injecting a variety of flow stream components into the device. Affinity chromatography protocols necessarily involve flowing a sequence of different reagents—corresponding to the steps of sample binding, washing, and elution—through the column. For the purposes of this work, microfluidic approaches to controlling the order in which solutions were delivered to the column were avoided. This simplified the experimental results by focusing the experiments on the chromatographic performance of the device rather than on the performance of any microfluidic flow control elements. Two approaches to delivering various solutions to the device were explored. In the first approach, a sequence of solutions was pre-loaded into a sample loop and delivered to the device via the syringe pump system. In the second approach, solutions were loaded into two separate sample loops and the solution to be delivered to the device was selected manually by operation of a flow injection valve.

4.3 Materials and Methods

4.3.1 Preparation of PNIPAAm and bead modification

Primary amine-functionalized polystyrene latex beads were obtained from Polysciences (Warrington, PA). 100 nm diameter Polybead® Amino Microspheres were used in all experiments. The beads were covalently modified with 11 kDa PNIPAAm and one of two types of biotin reagents via N-hydroxysuccinimide (NHS) ester conjugation chemistry. NHS-PNIPAAm (Figure 3.10) was synthesized according to a previously published protocol.[117] The number-average molecular weight ($\overline{M}_n$) of this polymer was determined to be 11,000 by vapor pressure osmometry (VPO, device model OSV111, Knauer, Germany). The two biotin reagents used were NHS-LC-biotin (Pierce; LC stands for "long chain"), which consists of a biotin group separated from an NHS ester by an alkane chain (Figure 4.1), and NHS-PEG-biotin (NHS-PEG-b, obtained from Shearwater Corp., Huntsville, AL), which consists of a biotin group separated from an NHS-ester by a 3.4 kDa PEG molecule (Figure 3.10).

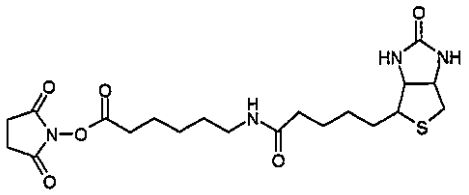

Figure 4.1: NHS-LC-biotin; a reagent used to biotinylate amine-coated latex beads.

Beads co-modified with PNIPAAm and PEG-b were prepared exactly as described in Section 3.3 of the previous chapter. Beads were modified with NHS-LC-biotin by reaction at a 1:5 molar ratio of surface amine groups to NHS-PEG-b at pH 9.0 and 4 °C overnight.

Approximately 50% of the available amine groups on the bead surfaces were modified. Beads were separated from unreacted NHS-LC-biotin by threefold centrifugation and resuspension. LC-biotin modified beads were then reacted with NHS-PNIPAAm. The reaction was performed at a 10-fold molar excess of NHS-PNIPAAm relative to unmodified surface amine groups at pH 9.0 and 4 °C overnight. Beads were separated from unreacted NHS-PNIPAAm by threefold centrifugation and resuspension at 4 °C to avoid the phase transition and aggregation of unreacted NHS-PNIPAAm. In addition to the two types of doubly modified biotin/PNIPAAm beads, singly modified PNIPAAm beads were prepared. All centrifugations were performed at a relative centrifugal force of 16,600 × g.

4.3.2 Preparation of chromatographic bead suspension

The bead suspension injected into the microfluidic channel consisted of 0.3 wt% doubly modified biotin/PNIPAAm beads (either PEG-b/PNIPAAm or LC-biotin/PNIPAAm beads, depending on the experiment), 0.3 wt% singly modified PNIPAAm beads, and 1.67 mg/mL free PNIPAAm in pH 7.6 phosphate buffered saline (PBS, 50 mM phosphate, 5 mM NaCl). The singly modified beads and free PNIPAAm were added to decrease the concentration of beads required to form a continuous adherent network on the channel walls. The suspension was degassed by agitation under vacuum for approximately five minutes immediately prior to use.

4.3.3 Streptavidin preparation and labeling

Wild-type streptavidin was expressed and purified according to a previously published protocol.[202] Streptavidin was labeled with a succinimidyl ester of AlexaFluor® 488 carboxylic acid (Molecular Probes, Eugene, OR), an amine-reactive fluorescent dye with an absorbance maximum at 494 nm and emission maximum at 518 nm. The conjugation reaction was performed at an eightfold excess of AlexaFluor® relative to streptavidin tetramers, in aqueous conditions, at pH 9.0 and 4 °C. The reaction was allowed to proceed overnight, and unreacted dye was separated from labeled streptavidin by 72-hour dialysis across an 11,000 Da molecular weight cut-off (MWCO) membrane into pH 7.6 PBS.

4.3.4 Analysis of modification products

The conjugation products were assayed spectrophotometrically, using a Hewlett-Packard (Cupertino, CA) model 8452A spectrophotometer. To determine the degree of biotinylation of biotinylated beads, the HABA assay[228] was used, as described in Section 3.3. To quantify unreacted primary amines on singly modified PNIPAAm beads, the TNBSA assay[235] was used, also as described in Section 3.3. Streptavidin concentration was monitored based on the optical density of streptavidin solutions at 280 nm, using an extinction coefficient 139,000 $cm^{-1}M^{-1}$ for the tetramer. The fluorophore-labeling ratio for the streptavidin was determined by measuring the optical density of the solution at 494 nm (the excitation maximum of AlexaFluor® 488), using an extinction coefficient of 71,000 $cm^{-1}M^{-1}$.

The concentration of beads in bead suspensions was determined by measuring the optical density at 600 nm (OD_{600}) of these suspensions, as described in Section 3.3.

4.3.5 Microfluidic devices

Two types of microfluidic devices were used. Initial experiments were performed with the heated device described in the previous chapter (Section 3.3, Figures 3.6 and 3.7). For the purposes of this chapter, this single channel, uniformly heated device will be referred to as a "type A" device. A second ("type B") device design was utilized in later chromatography experiments. This device was, like the type A device, manufactured from layers of laser-ablated PET; a diagram of the type B design is shown in Figure 4.2. Chromatography was performed in a primary channel with ports for fluidic input and output, with

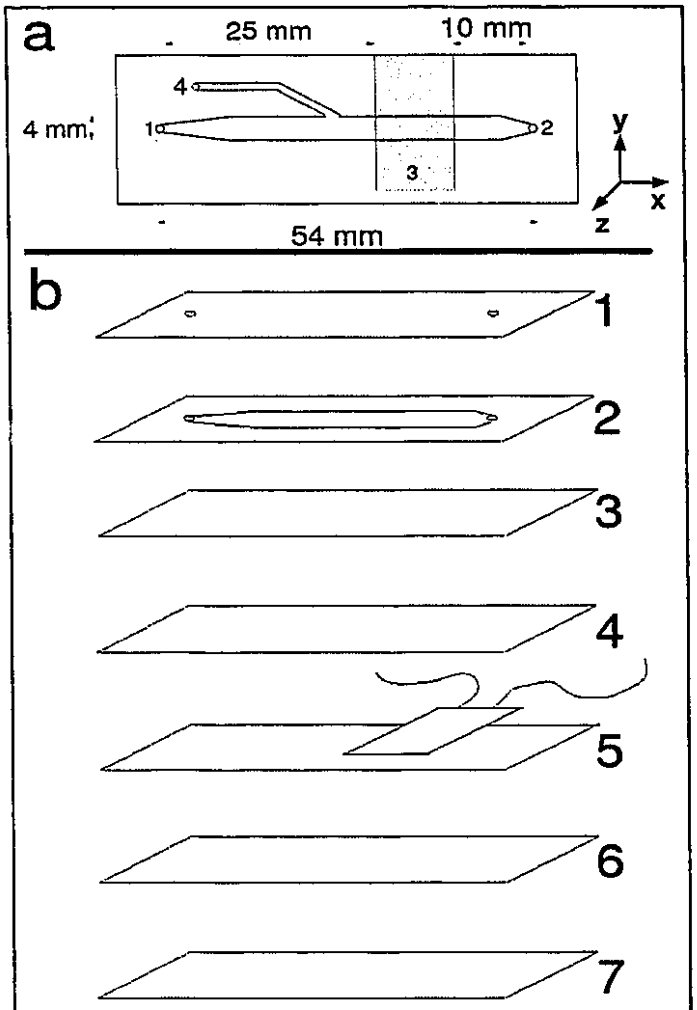

Figure 4.2: Diagrams of the type B device used in chromatography experiments. a: A top view of the device, showing the main channel with dimensions 54 mm × 4 mm × 0.3 mm (perpendicular to the plane of this diagram). Also shown are input (1) and outlet (2) ports, the heated region (3), and the small auxiliary channel used to inject smart bead suspension (4). b: An exploded view of the device, showing each of the machined PET layers from which the device was assembled. These layers were: 0.1 mm thick, with inlet and outlet ports (1); 0.250 mm thick, with the channel cut into it and coated on each side with 0.025 mm adhesive (2); 0.1 mm thick (3); 0.05 mm thick, coated on each side with 0.025 mm adhesive (4); 0.25 mm thick, with a rectangle cut out for placement of the 0.25 mm thick heater, shown here with two wire leads (5); 0.05 mm thick, coated on each side with 0.025 mm adhesive (6); and 0.1 mm thick (7).

dimensions of 54 mm × 4 mm (at the widest point in the channel) × 300 μm. The channel was formed from a sheet of 250 μm-thick PET, coated on each side with a 25 μm-thick layer of adhesive. The channel layer was sealed on each side by a 100 μm-thick sheet of PET; into one side the inlet and outlet ports were cut. In addition to the main input and output ports to the fluidic channel, a small injection channel for introducing bead suspension into the primary channel was incorporated into the device; this channel was cut into the same PET layer as the primary channel and was fed by an inlet cut into the same layer as the primary input/output ports. A thin-film heater obtained from Minco (Minneapolis, MN) was incorporated into the device; this heater was operated using an electronic feedback controller (Minco) to maintain temperatures in the device channel between 33 and 37 °C. (A Therma-Clear™ model heater and HeaterStat™ model controller were used.) The heater was separated from the channel by two layers of PET. A 100 μm layer formed the wall of the channel and a 100 μm adhesive-coated layer joined the heater to the rest of the device. The heater itself was about 250 μm thick and was incorporated into a 250 μm-thick PET layer. The heater was aligned to heat only a portion of the channel and adherent bead network formation occurred only in the heated region. The heated region was 19 mm wide, beginning 25 mm after the channel inlet and ending 10 mm before the channel outlet.

Assembled devices were mounted in a microfluidic manifold incorporating an aluminum pressure plate and polydimethylsiloxane (PDMS) gaskets to seal the input and output ports of the device to polyetheretherketone (PEEK) tubing, as described in the previous chapter. PEEK tubing had a 0.030 inch inner diameter (ID) and was obtained from Upchurch Scientific (Oak Harbor, WA). The device input and output were each connected by the manifold to about 6 cm of tubing. Additional tubing was connected to this fixed tubing

using standard HPLC fittings, also obtained from Upchurch. The sample loop and all pump lines were also constructed from 0.030 inch ID PEEK tubing. Flow was directed by computer-controlled syringe pumps (Kloehn Co., Ltd., Las Vegas, NV) fitted with 100 μL syringes. All fluids were pushed through the system with deionized water from the syringes, such that there was never any sample in contact with the syringes themselves. Two pumps were operated in a continuous handshake mode, with one syringe filling while the other dispensed, to provide a continuous buffer flow over long periods of time. In experiments involving a flow injection valve and a second sample loop, a third pump was operated independently to inject the streptavidin sample.

4.3.6 Chromatography

Two techniques were explored in performing chromatography experiments. In the first technique, a sample loop was loaded sequentially with a series of solutions and the contents of the sample loop were pumped through the chromatography device. In the second technique, one sample loop was loaded with buffer, while a second sample loop was loaded with the streptavidin-containing sample. A flow injection valve was used to select between the buffer (for washing and elution steps) and the sample (for the sample loading step). Type A device were used exclusively for the single-sample-loop experiments, whereas type B devices were used exclusively for the valve-selected, double-sample-loop experiments. In both experimental techniques, bead suspension was injected into the channel, heated, and allowed to adhere in the absence of flow before any fluid was pumped through the device.

Chromatography in type A devices proceeded as follows. Three hundred microliters of the bead suspension were injected into a type B channel from a syringe directly connected to the manifold input tubing. The 1.5 ml sample loop, disconnected from the device input line and pump line, was then filled with the following sequence of solutions: 100 μL PBS, to serve as a column wash; 150 μL fluorescently-labeled streptavidin solution at a concentration of 2.5 μM; and 1250 μL PBS, to wash through excess streptavidin and to serve as the elution buffer. All solutions had been previously degassed. The sample loop was then connected between the manifold input and the pump system. After activating the heater, bead aggregation and adhesion was allowed to proceed in the absence of flow for 10 minutes. The pumps were then activated, pushing buffer through the system at a rate of 10 μl/min. Fluid flowing through the device was captured at the exit of the manifold output tubing in 50 μl aliquots. After 70 minutes, the heater was deactivated while the flow was maintained at a constant rate. Aliquots continued to be collected for an additional 40 minutes as the matrix dissolved. In some experiments, the heater was deactivated after only 50 minutes, prior to collection of additional elution samples. The output aliquots were then diluted to 500 μl in deionized water and the fluorescence of each sample was measured on a Perkin Elmer LS50B fluorescence spectrophotomer (Perkin Elmer Instruments, Inc., Shelton, CT), with excitation at 492 nm and emission at 518 nm. For negative controls, a biotin-free bead suspension—consisting of 0.6 wt% singly modified PNIPAAm beads and 1.67 mg/mL free PNIPAAm in pH 7.6 phosphate buffered saline—was utilized. Experiments were performed in triplicate.

Chromatography in type B devices proceeded as follows. Two hundred microliters of the bead suspension were injected into a type B channel manually via a small bead injection channel, connected by the manifold to a short length of PEEK tubing. After bead injection,

this tubing was closed off by a standard HPLC tubing valve, preventing flow through the injection channel. The input port of the device was connected to the output of a flow injection valve that allowed to operator to select between two flow sources: a 0.3 mL sample loop and a 1.5 mL sample loop. The 1.5 mL sample loop was filled with degassed PBS. The 0.3 mL sample loop contained fluorescently labeled streptavidin in degassed PBS at a concentration of 2.5 μM. After the bead suspension had been injected into the primary channel, the heater was activated and bead aggregation and adhesion was allowed to proceed in the absence of flow for 10 minutes. The pumps were then activated, pushing buffer from the 1.5 mL sample loop through the system at a rate of 20 μL/min. Fluid flowing through the device was captured at the exit of the manifold output tubing in 50 μL aliquots. After 2.5 minutes of buffer wash, the injection valve was switched to the 0.3 mL sample loop, allowing the streptavidin sample to flow into the device. The valve was switched back to the buffer-containing sample loop after 15 seconds, making the volume of the injected streptavidin sample 5 μL. After allowing the sample to bind and excess to be washed out (25 minutes after the initiation of flow), the heater was deactivated while the flow was maintained at a constant rate. Aliquots continued to be collected for an additional 15 minutes as the adhered beads dissolved. The output aliquots were then diluted to 500 μL in deionized water and the fluorescence of each sample was measured on a Perkin Elmer LS50B fluorescence spectrophotomer (Perkin Elmer Instruments, Inc., Shelton, CT), with excitation at 492 nm and emission at 518 nm. The OD_{600} of each sample was also measured, using a Hewlett-Packard model 8452A spectrophotometer (HP, Cupertino, CA). For negative controls, free biotin was added to the streptavidin sample at a concentration of 50 μM. This excess of free biotin would be expected to occupy all available streptavidin binding pockets,

eliminating any interaction between the sample and the beads in the channel. Experiments were performed in triplicate.

4.3.7 Subtraction of bead background signal from fluorescence measurements

The presence of beads in the output samples introduced a scattering signal in the fluorescence measurements for samples containing beads. This signal made the measured fluorescence higher than it would be in a sample containing no beads. To correct for this effect, a set of samples containing a range of bead concentrations (determined by the OD_{600} of the samples) without streptavidin were analyzed in the fluorescence spectrophotometer. This analysis yielded a linear relationship between bead concentration (as determined by OD_{600}) and scattered fluorescent signal. For each chromatographic sample, the OD_{600} was measured and this linear relationship was used to determine what scattering signal to subtract from the measured fluorescence signal. Subtraction was performed only for results of experiments in type B channels; in the discussion below, data for which background subtraction has been performed are clearly identified.

4.4 Results and Discussion

4.4.1 Conjugation of PNIPAAm to beads and fluorescence labeling of streptavidin

To determine the degree of biotinylation of biotin-modified latex beads, HABA assays were performed. Based on the concentration of amine groups on the beads reported by the bead manufacturer, 40% of available primary amine groups had been biotinylated in the PEG-b/PNIPAAm beads, whereas 50% had been modified in the LC-biotin/PNIPAAm beads. Approximately 50-60% of the reactive amine moieties originally on the beads were thus available for modification by NHS-PNIPAAm. Unfortunately, a TNBSA assay to quantify the extent of total modification of these beads failed to produce sensible results. However, the beads displayed aggregation behavior at temperatures above the LCST of PNIPAAm, demonstrating sufficient polymer conjugation for function. A TNBSA assay of beads modified only with PNIPAAm did produce sensible results: these beads had 66% as many free primary amines as unmodified beads, indicating that ~34% of the available primary amines were modified with NHS-PNIPAAm. These beads demonstrated temperature-sensitive aggregation behavior as well. The degree of labeling of 3.1 AlexaFluor® groups per streptavidin tetramer was determined spectrophotometrically, using known extinction coefficients for streptavidin at a wavelength of 280 nm and for the fluorophore at 494 nm.

4.4.2 Microfluidic device fabrication and operation

The evolution of device designs evident in this chapter was driven by practical problems encountered in performing chromatography in a type A device. The narrow channel of the type A device restricted the maximum possible flow rate: at above about 10 μL/min, shear forces would pull adhered beads from the channel walls. In the wider type B channel, on the other hand, beads would remain adhered at flow rates above even the 20 μL/min operating rate. In a type B device, the primary flow channel, fed at its input port by the pump system, widened between the input and output ports to provide an expanded surface to which PNIPAAm-coated beads could adhere. The slowly tapered geometry at the primary flow channel input allowed for efficient and complete wetting-out of the relatively hydrophobic PET; more sudden channel width changes were found to lead to bubble formation when fluid was first introduced into the channel. The type B flow channel was heated only in a limited region, starting about 25 μm from the input port and ending 10 μm from the output port. Bead aggregation and adhesion was limited to this heated region. Restriction of the size of the heated region was found to be necessary to keep bead aggregates from clogging the input and output ports; a problem often encountered in operating type A devices.

Loading the bead suspension into type A channels proved to be another source of difficulty. In experiments with type A channels, the fluidic manifold input tubing was disconnected from the pump line and a syringe was used to manually inject bead suspension directly through this input tubing. However, this process required the pump line to then be reconnected to the manifold input tubing, a procedure that occasionally introduced air

bubbles into the tubing, ruining the experiment. This problem was solved in type B devices via the addition of a narrow bead injection channel, which had a separate input port. The bead injection channel intersected with the primary flow channel between the primary input port and the beginning of the heated region. The injection channel allowed for bead suspension to be injected manually into the device without disconnecting the pump lines from the primary input port. During experiments, there was no flow through the bead injection channel: it was used only to introduce bead suspension into the channel prior to experiments.

4.4.3 Chromatography results: LC-biotin/PNIPAAm beads in a type A device

Figure 4.3 shows a schematic of the protocol used in the chromatography experiments described in this chapter. Figure 4.4 shows the results of such an experiment using a chromatographic matrix based on thermally immobilized LC-biotin/PNIPAAm-coated beads. This experiment was performed in a type A

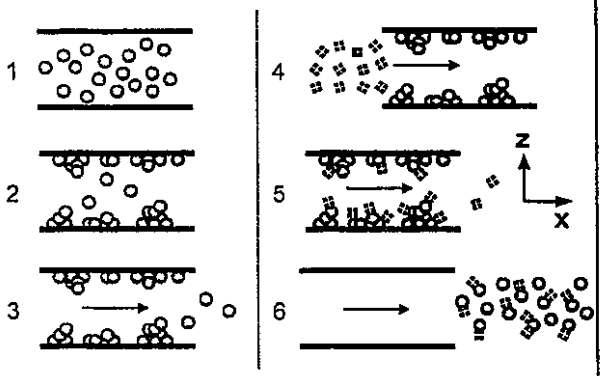

Figure 4.3: A schematic of the experimental protocol for streptavidin affinity chromatography. The channel is initially filled at room temperature with a suspension of biotinylated, PNIPAAm-coated beads (1). The temperature in the channel is then raised to 45 °C and the beads aggregate and adhere to the channel walls (2). Buffer is then pumped through the channel (the presence of flow is indicated in this schematic by an arrow), washing out any unbound beads (3). A fluorescently labeled streptavidin sample is then introduced into the flow stream (4). Streptavidin binds the beads, and any unbound streptavidin is washed out of the channel (5). Finally, the temperature is reduced to room temperature, leading to the break up of the bead aggregates. Beads, bound to labeled streptavidin, elute from the channel (6). X- and z-axes in this figure correspond to those shown in Figure 4.2.

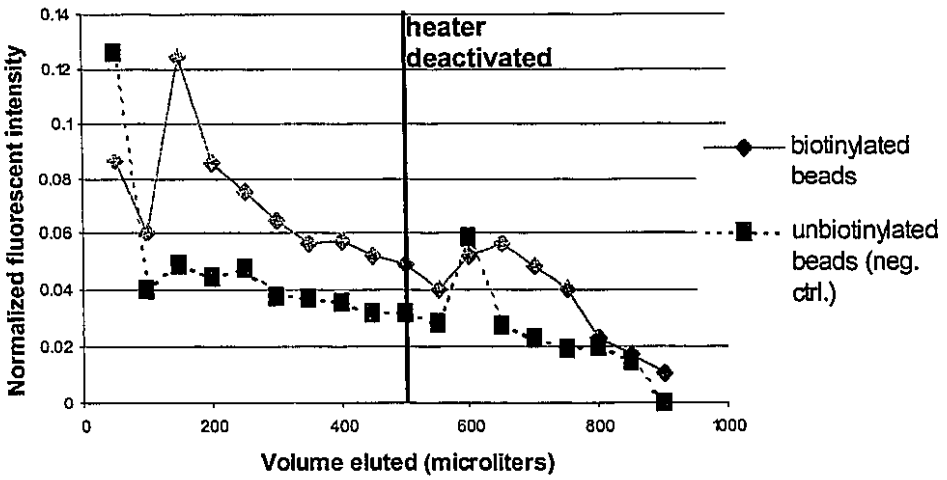

Figure 4.4: Results of streptavidin affinity chromatography via LC-biotin/PNIPAAm-coated beads in a type A device. The negative control data are for the same experiment performed with beads that had been coated with PNIPAAm, but not biotinylated. Matrix formation took place prior to the introduction of flow; a 10 μL/min buffer flow was introduced at the zero volume point of this plot. Each point represents 5 minutes of flow through the system, corresponding to a 50 μL sample. The y-axis gives the fluorescence in the samples, normalized to the total fluorescence captured at the output. The x-axis gives the total volume that has flowed through the system at the time of collection of each sample. The heater was activated prior to the initiation of flow, and it remained on until the indicated point at 500 μL, at which point it was deactivated. In both the experiment and the negative control, a 150 μL bolus of fluorescently labeled streptavidin entered the channel at the 100 μL point. These data reflect the dispersion of samples encountered in the operation of the type A device: peaks are broad and indistinct. It is possible to pick out a peak corresponding to unbound streptavidin passing through the system in the "biotinylated beads" trace, and both traces contain elution peaks corresponding to adhered beads dissociating from the channel walls and leaving the system. However, it is impossible to see any significant difference between the two traces, and to therefore observe any specific streptavidin-biotin binding. Each trace in this plot represents the results of a single experiment.

device. The plot represents the fluorescence from labeled streptavidin present in the system output under continuous 10 μL/min flow. The fluorescence measurements reported on the y-axis are normalized by the total fluorescence captured in the output throughout the experiment. Adhesion of the bead matrix was initiated by activating the heater in a bead-suspension-filled channel ten minutes prior to the initiation of flow. The zero point on the x-axis of Figure 4.4 represents the initiation of flow (with heat maintained). The sample loop connected between the pumps and the channel was filled sequentially with 100 μL PBS, to

serve as a column wash; 150 μL fluorescently labeled streptavidin solution; and 1250 μL PBS, to wash through excess streptavidin and to serve as the elution buffer. A peak corresponding to labeled streptavidin that failed to bind the immobilized bead can be seen clearly starting at the 150 μL point of the "biotinylated beads" sample. This peak has a long tail, spread out considerably from the 150 μL volume of streptavidin initially injected in the sample loop. This spreading is explained by laminar Taylor dispersion of the injected bolus of streptavidin during sample loading and pumping.[236] There is no similarly sharp peak in the trace for the negative control, though there is a similar tail evident in this trace.

At 50 minutes (500 μL) into the experiment, the heater was deactivated, triggering matrix dissolution. At the 600 μL point of the both traces in Figure 4.4, elution peaks can be seen, corresponding to labeled streptavidin bound to the beads that made up the matrix. It's impossible to determine, based on these data, whether the biotinylated-coated beads bound more streptavidin than the unbiotinylated beads. In an attempt to improve the binding of biotin-coated beads, the spacer with which biotin was attached to the beads was lengthened. It was hoped that by attaching biotin to the beads via a 3.4 kDa PEG tether, steric hindrance of streptavidin-biotin binding would be reduced. This would be consistent with the work of Yasui et al., who demonstrated that PNIPAAm molecules conjugated to the surface of latex beads can block the access of small molecules to enzymes also on the surface of the beads.[191]

4.4.4 Chromatography results: PEG-b/PNIPAAm beads in a type A device

Figure 4.5 shows the results of an experiment using a chromatographic matrix based on thermally immobilized PEG-b/PNIPAAm-coated beads. As with the experiment with LC-biotin/PNIPAAm beads, this experiment was performed in a type A device. Other

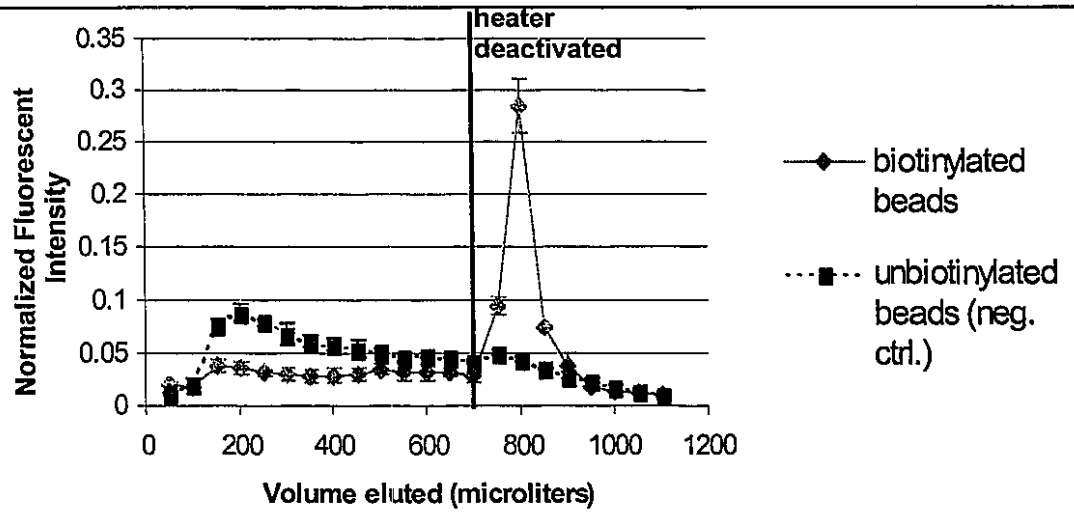

Figure 4.5: Results of streptavidin affinity chromatography via PEG-b/PNIPAAm-coated beads in a type A channel. The negative control data are for the same experiment performed with beads that had been coated with PNIPAAm, but not biotinylated. Matrix formation took place prior to the introduction of flow; a 10 μL/min buffer flow was introduced at the zero volume point of this plot. Each point represents 5 minutes of flow through the system, corresponding to a 50 μL sample. The y-axis gives the fluorescence in the samples, normalized to the total fluorescence captured at the output. The x-axis gives the total volume that has flowed through the system at the time of collection of each sample. The heater was activated prior to the initiation of flow, and it remained on until the indicated point at 700 μL, at which point it was deactivated. In both the experiment and the negative control, a 150 μL bolus of fluorescently labeled streptavidin was introduced at the 100 μL point. Peaks corresponding to unbound streptavidin passing through the channel at this point can be seen in both traces. The peak for the negative control is higher, indicating the less streptavidin bound the immobilized beads in the negative control. The "biotinylated beads" trace also contains a clear elution peak, corresponding to streptavidin bound to beads eluting from the channel in response to decreasing channel temperature. These observations are indications of specific streptavidin binding to the beads. Each trace in this plot represents the results of three experiments, with error bars indicating ± one standard deviation.

experimental details were also similar: beads were allowed to adhere to the channel walls in the absence of flow, flow was initiated, a streptavidin sample was injected into the device channel via sequential loading in the sample loop, and the heater was deactivated. The main protocol difference between this experiment and that presented above was the amount of time between injection of the streptavidin sample and the deactivation of the heater. This amount of time was increased for this experiment in order to allow any unbound

streptavidin to wash through the channel, thereby allowing the chromatographic trace to return to a baseline before the elution step.

Starting at the 150 μL point, a peak corresponding to unbound streptavidin can be seen in both the experimental ("biotinylated beads") and negative control traces. This peak is larger in the negative control trace, indicating that less streptavidin bound the beads when they were not biotinylated. At 70 minutes (700 μL) into the experiment, the heater was deactivated, triggering dissolution of the adhered bead aggregates. At the 750 μL point of the experimental trace in Figure 4.5, an elution peak begins, corresponding to labeled streptavidin bound to the eluting beads. The negative control trace contains no similar elution peak, indicating negligible streptavidin association with the biotin-free matrix. The biotinylated smart-polymer beads, adhered in a temperature-sensitive manner to the channel wall, thus act as an effective affinity chromatography matrix to specifically separate streptavidin from the flowing input stream.

While this experiment does demonstrate successful affinity chromatography via smart polymer-coated beads, the broad unbound streptavidin peak is of some concern. This peak is so much broader than the elution peak because of the method of introducing the streptavidin sample into the system. The streptavidin sample was loaded sequentially into a 1.5 mL sample loop, along with wash and elution buffer. During the process of sample loading and pumping, the streptavidin in the sample loop was dispersed a volume far greater than the original 150 μL. This dispersion broadens the unbound peak, and makes it difficult to judge the relative amount of streptavidin in this peak for the experiment versus the negative control.

4.4.5 Chromatography results: PEG-b/PNIPAAm beads in a type B device

In order to generate a sharper unbound streptavidin peak, injection of the streptavidin sample was performed with a flow injection valve. This valve allowed the source of the fluid being pumped into the channel to be selected from one of two sample loops. One sample loop contained buffer, the other contained streptavidin solution. Since the valve was located immediately upstream of the microfluidic device, dispersion of the streptavidin sample in the flow stream was minimized. The use of a flow injection valve also allowed the volume of the injected bolus of streptavidin to be minimized: while experiments based on a single sequentially packed sample loop required at least a 150 μL sample of streptavidin for proper sample loading, the valve could be used to inject as little as 5 μL. The experiments described in this section were also performed in a type B microfluidic device, the advantages of which are described in Section 4.4.2. The negative control used for the experiment described in this section also differed from previous negative controls. Channels used in negative controls were loaded with the same bead suspension used in the experiment, rather than with a suspension made up exclusively of unbiotinylated beads. However, the sample used in the negative control contained an excess of free biotin, which bound the binding pockets of the labeled streptavidin, making it unable to bind the biotinylated beads.

Figure 4.6 shows the results of a streptavidin affinity chromatography experiment and the corresponding negative control. The plot corresponds to an experiment similar to those described above. Adherence of the bead matrix was initiated by activating the heater in a bead-suspension-filled channel in the absence of flow. The zero point on the x-axis of Figure 4.6 represents the initiation of flow (with heat maintained). A 5 μL volume of

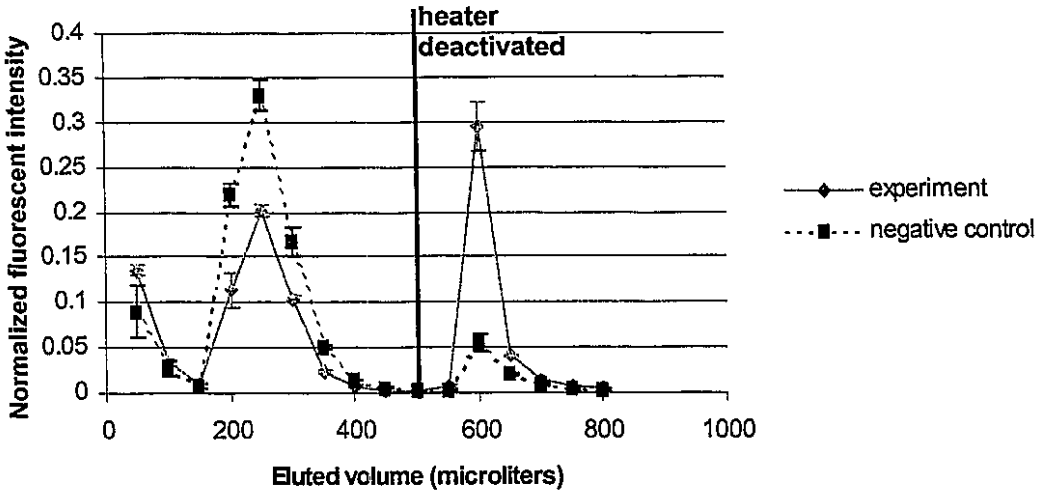

Figure 4.6: Results of streptavidin affinity chromatography via PEG-b/PNIPAAm-coated beads in a type B device, using a flow injection valve to introduce the streptavidin sample. As with the experiments described above, matrix formation took place prior to the introduction of flow; a 20 μL/min buffer flow was introduced at the zero volume point of this plot. Each point represents 2.5 minutes of flow through the system, corresponding to a 50 μL sample. X- and y-axes are as described for Figures 4.4 and 4.5. The heater was activated prior to the initiation of flow, and it remained on until the indicated point at 500 μL, at which point it was deactivated. In both the experiment and the negative control, a 5 μL bolus of fluorescently labeled streptavidin was introduced at the 50 μL point. In the negative control, this streptavidin sample contained an excess of free biotin, making it incapable of binding the biotinylated beads. The remainder of the fluid pumped through the system was buffer. A broad peak, corresponding to unbound streptavidin, can be seen at the 200 μL point of both traces. This peak is significantly broadened from 5 μL due to dispersion of the streptavidin bolus during sample injection. Significantly less streptavidin passes through the system at the beginning of the experimental trace, indicating that the immobilized beads bind streptavidin. The peak starting at 600 μL on this trace corresponds to this bound streptavidin eluting with beads, since bead aggregates dissolved and dissociated from the channel walls as the channel temperature decreased. Displayed points represent the arithmetic means of data from three experiments; error bars are ± one standard deviation.

fluorescent streptavidin was injected 2.5 minutes into the experiment. The peak corresponding to this streptavidin, at the 200 μL point, is spread out considerably from this volume due to dispersion. This dispersion, however, is not nearly as drastic as that encountered using earlier sample loading techniques, and both experimental and control traces return to baseline at only 400 μL into the experiment. Note that the peak starting at the 200 μL point of the experimental trace (diamonds) is smaller than that for the negative

control (squares). This indicates that rather than passing through the channel, some labeled streptavidin in the sample was bound by the biotin groups in the chromatographic matrix.

At 25 minutes (500 μL) into the experiment, the heater was deactivated, triggering dissolution of the adhered bead aggregates. At the 600 μL point of the experimental trace in Figure 4.6, an elution peak can be seen, corresponding to labeled streptavidin bound to the no-longer-adhered beads. The negative control trace contains a much smaller peak at this point; the significance of this residual peak is explored in the next section. These data are a clear indication that streptavidin in the sample specifically binds the biotinylated immobilized beads in the channel, and that the bound streptavidin can be eluted from the channel in a temperature-responsive manner.

4.4.6 Bead fluorescence background correction

As described in the Section 4.3, the presence of beads in chromatographic samples introduced an extraneous fluorescent signal in those samples. All fluorescent signals reported earlier in this chapter therefore reflect not only the concentration of streptavidin in

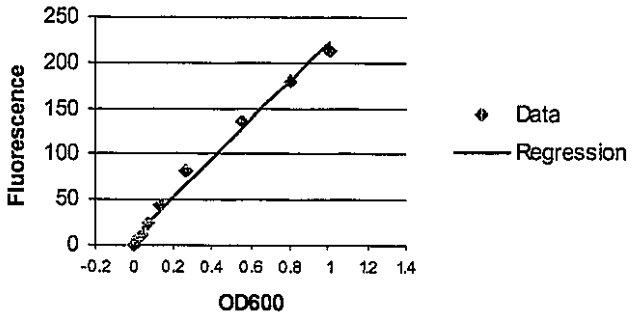

Figure 4.7: The relationship between OD_{600} and fluorescent intensity for serial dilutions of the bead suspension used in chromatography experiments. These OD_{600} vs. fluorescence data points were fit to a linear regression, which took the form:

$$fluorescence = 210.50 \cdot OD_{600} + 9.875 .$$

The correlation coefficient (R^2) for this regression was 0.988. This correlation was used to determine the fluorescence contribution of beads in chromatographic samples, based on the measured OD_{600} of these samples. This contribution could then be subtracted from the total fluorescent signal.

each sample, but a combined signal contributed to by both the labeled streptavidin and by any beads in the sample. This is an issue at two points in each chromatographic experiment: the first few samples from each experiment contain the beads that failed to initially adhere to the channel walls, and the samples from the elution peak contain the beads eluting from the channel walls. The fact that there are beads in these samples means that the fluorescent intensities reported for these samples in the experiments above are higher than they would be if only labeled streptavidin contributed to the fluorescent signal. To correct for this factor, the expected fluorescent signal from the beads was calculated and subtracted from the total fluorescent signal. The data used to calculate the contribution from beads are shown in Figure 4.7. Serial dilutions of the chromatographic bead suspension were prepared; the fluorescent intensity of each of these dilutions was measured under the same instrument conditions used to measure the fluorescence of the chromatography samples. In addition, the OD_{600} of each dilution was measured. A linear regression to these data was then performed, allowing an empirical relationship between bead OD_{600} and fluorescence contribution to be derived. Since the OD_{600} for each sample for the experiment described in Section 4.4.5 had been measured, and the streptavidin-labeling fluorophore had no absorbance at 600 nm, this relationship could be used to derive an expected bead contribution to the sample fluorescence. This contribution was then subtracted from each fluorescence data point, resulting in the plot shown in Figure 4.8.

This plot shows the same data as that shown in Figure 4.6, with the fluorescent signal arising from the presence of beads in samples subtracted prior to data normalization and averaging. The subtraction process has no significant impact on the overall interpretation of the data. The experimental trace continues to show a prominent elution peak and a smaller

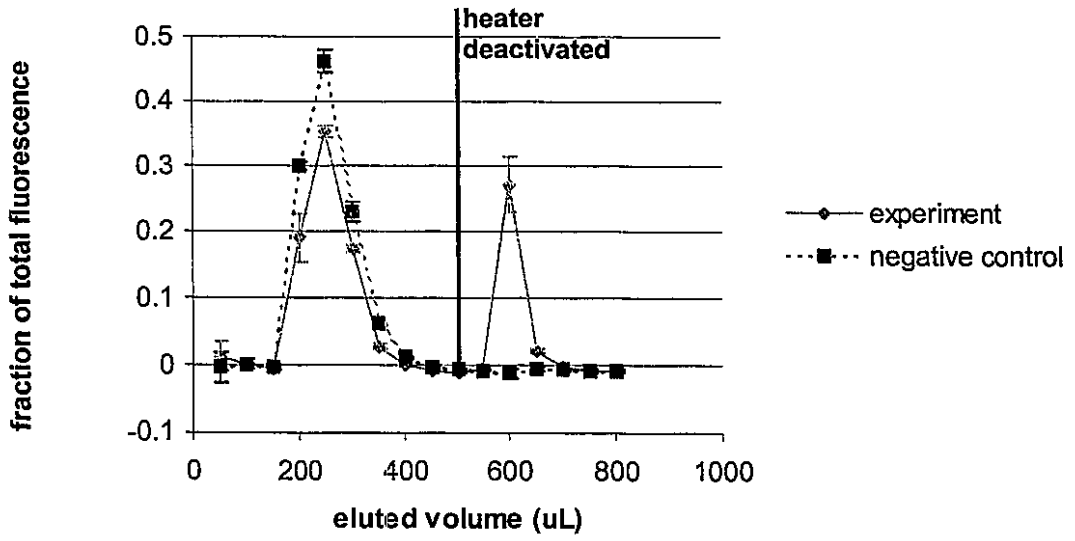

Figure 4.8: Results of streptavidin affinity chromatography via PEG-b/PNIPAAm-coated beads in a type B device, using a flow injection valve to introduce the streptavidin sample. These data are exactly as described for Figure 4.6. In fact, they are the same data for the same experiment, with subtraction for the bead fluorescent signal, as determined via the relationship shown in Figure 4.7, performed. Eliminating the bead signal greatly reduces the intensity at the first two points in the trace, which arises entirely from the unbound beads initially washed from the channel. The height of the elution peak in the experimental trace is also reduced, and the elution peak in the negative control trace is eliminated completely.

unbound streptavidin peak than the negative control. The background subtraction process has affected the data most at those points where the fluorescent signal of the sample was a result entirely of the presence of beads. For example, in the first two points of both traces in Figure 4.6, the elevated fluorescence values are due to beads that have failed to adhere to the channel walls being washed through the system. There is no similar elevation apparent in Figure 4.8, as the signal arising from the beads has been eliminated. A similar effect can be seen in the elution peak of the negative control. The fact that a small peak can be seen at the 600 μL point of Figure 4.6, but that this peak is gone in Figure 4.8, indicates that the peak is due entirely to the presence of beads in elution samples in the negative control. In other words, no nonspecific streptavidin binding to immobilized beads can be observed in the negative control. The data in Figure 4.8 also represents quantitative binding more accurately

than that in Figure 4.6. The fluorescent values in the unbound streptavidin peak of the negative control trace in Figure 4.8 add up to about 1.0, consistent with the observation that no streptavidin bound the immobilized beads. On the other hand, the unbound peak of the experimental trace in this figure represents about 75% of the entire streptavidin sample, while the other 25% is fully accounted for by the elution peak. It is likely that much of the 75% of the streptavidin sample not captured by the beads in this experiment was flowing through a region of the channel too distant from the walls to allow diffusion to the adhered beads within the channel residence time. It is, on the other hand, not likely that the amount of streptavidin injected into the channel exceeded the total binding capacity of the immobilized beads; experiments with type A channels (Section 4.4.4) demonstrate binding of significantly more streptavidin when larger volumes of streptavidin solution are injected. The issue of incomplete sample binding may in the future be addressed through the use of narrower channels that place more of the fluid closer to the channel walls. However, the capacity demonstrated in the experiment at hand (about 3 pmol streptavidin captured and eluted), is already within range of practical microfluidic applications.

4.5 Conclusions

The work described in this chapter shows how PNIPAAm-coated beads, which were previously established to adhere stably and reversibly to the walls of microfluidic channels in response to a thermal stimulus, can be used as a stationary phase in protein affinity chromatography. In the process of refining this chromatographic system, several conclusions were drawn regarding performance optimization. For example, it was found that

streptavidin binding to PNIPAAm-coated, biotinylated beads was maximized when the biotin was attached by an extended (3.4 kDa, in this case) linker. This is a sensible conclusion, given that the surface-bound PNIPAAm molecules would be expected to sterically hinder binding of macromolecules to groups close to the bead surface. In addition, it was found that, since the adhesion of the immobilized beads became unstable in response to shear forces above certain linear flow rates, increasing the volumetric flow rate (and, therefore, the speed with which samples could be processed) required increasing the channel volume. This could be accomplished, however, by increasing the breadth of the channel in the y-dimension (see Figure 4.2), which avoids increasing the distance through which target molecules must diffuse to reach the immobilized beads while increasing the channel surface area to which beads can adhere. Finally, the protocol and equipment used to handle the sample fluid were found to be critical factors in obtaining a high-quality chromatogram. There is much room for improvement in these factors, especially via on-chip integration of sample-handling channels and valves. This integration, however, is beyond the scope of this chapter, which seeks only to demonstrate the feasibility of an isolated microfluidic separation operation.

The approach described in this chapter has several advantages over current techniques of immobilization for microfluidic chromatography. For example, the reversible immobilization of PNIPAAm-coated beads allows for the packing of microfluidic affinity chromatography columns at the time of use. A single device can therefore be used to separate any number of target species, depending on how it is packed. The ability to easily remove the immobilized beads allows for straightforward renewal of a microfluidic chromatography column, improving the reusability and flexibility of devices. The responsiveness and

reversibility of the matrix might also allow a device user to control the exact location and timing of a separation by controlling the location and timing of temperature changes on the device. Finally, reversible matrix formation simplifies the elution process: separated biomolecules can be eluted by lowering the channel temperature, eliminating the need for harsh chemical eluents.

The basic technology of biomolecular immobilization by smart polymer-modified beads is not limited to applications in affinity chromatography. Chapter 5 explores the application of this immobilization platform to an immunoassay, and a variety of other applications are proposed in Chapter 6.

Chapter 5: Smart poly(N-isopropylacrylamide)-coated beads as a controlled immobilization substrate for a solid-phase microfluidic immunoassay

5.1 Summary

The adaptation of immunoassay technology to microfluidic formats is an important prerequisite to the widespread adaptation of microfluidic approaches to sample analysis. In this chapter, the PNIPAAm-coated beads described in previous chapters are used as a controllable, reversible immobilization substrate for a competitive solid-phase immunoassay. This application calls for the attachment of antibodies to the PNIPAAm-coated beads; it therefore demonstrates that PNIPAAm-coated beads are an appropriate immobilization substrate for active macromolecules.

5.2 Objectives and Experimental Design Considerations

Immunoassays—methods for detecting and quantifying biomolecules via the binding of these molecules to antibodies—have become essential tools in both clinical and research laboratories. The applications and fundamental science of immunoassay technology are dealt with in great detail in basic texts.[237,238] Because of the central importance of immunoassays to modern biochemical analysis, the adaptation of immunoassay techniques

to microfluidic platforms is a prerequisite to the widespread acceptance of microfluidic analytical technologies. Several microfluidic immunoassays have been developed.[52,74-78] In fact, any microfluidic technology capable of detecting binding between two molecular species is eligible for adaptation to an immunoassay. This chapter describes the adaptation of the PNIPAAm-coated bead immobilization platform to a solid-phase competitive immunoassay. This work involved attaching active antibodies to the beads. This is in stark contrast to the work described in the previous chapter, which required only functionalization of the beads with a small molecule moiety. The fact that PNIPAA-coated beads can successfully bear active antibodies not only demonstrates the applicability of this system to an important class of molecules, but it also bodes well for the potential of smart bead-mediated immobilization of arbitrary macromolecules, since antibodies are especially large and fragile proteins. As with the chromatographic system demonstrated in Chapter 4, the immunoassay demonstrated in this chapter is not intended to be as sensitive or accurate as state-of-the-art immunoassays, but merely to establish that PNIPAAm-coated beads are a viable immobilization substrate for a solid-phase antibody binding assay.

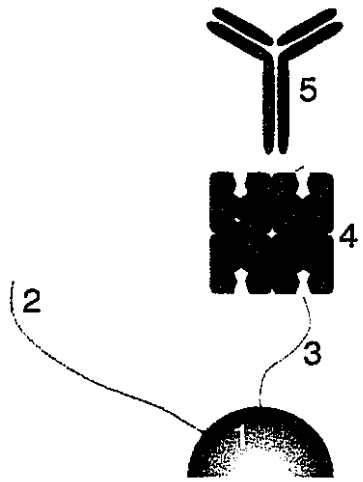

Figure 5.1: A diagrammatic representation of the smart bead construct used for the digoxin immunoassay. A 100 nm diameter latex nanobead (1) is surface-conjugated with PNIPAAm (2) and PEG-biotin (3). Streptavidin (4) is bound to the exposed biotin, providing a binding site for the biotinylated anti-digoxin IgG (5).

The target molecule for this assay was digoxin, a commonly prescribed drug used to treat symptoms of heart failure and certain arrhythmias. Monoclonal

antibodies to digoxin are readily available, and several digoxin immunoassays have been developed.[239-242] An antibody-bearing bead construct was built up from the co-modified PNIPAAm/PEG-b beads described in previous chapters. As shown in Figure 5.1, this construct was built by binding streptavidin to the biotinylated beads, and then binding biotinylated anti-digoxin immunoglobulin G (IgG) to the free biotin binding pockets on this bound streptavidin. These antibody-bearing beads were thermally immobilized to the walls of a microfluidic channel to serve a substrate for an immunoassay.

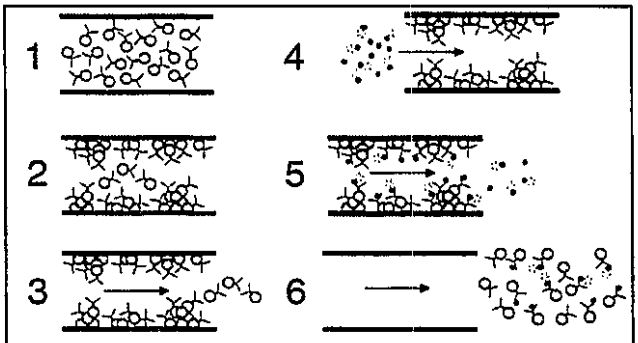

Figure 5.2: A schematic of the immunoassay protocol. Suspended smart beads are loaded into the PET microfluidic channel (1). The temperature in the channel was then increased from room temperature to 37 °C, resulting in aggregation and adsorption of the beads to the channel wall (2). Flow was initiated (the presence and direction of flow is indicated by an arrow in this diagram), washing unadsorbed beads out of the channel (3). A mixture of fluorescently labeled digoxigenin (at a fixed concentration) and digoxin (at varying concentrations) was flowed into the channel (4); components of this mixture that fail to bind the immobilized antibodies were washed through (5). Since digoxin and labeled digoxigenin compete for antibody binding, the higher the concentration of digoxin, the more labeled digoxigenin will flow through at this step. Finally, the temperature in the channel is reduced, and the aggregation/adsorption process reversed: antigen-bound beads leave the channel with the flow stream (6).

A schematic of the immunoassay protocol is shown in Figure 5.2. Digoxin was assayed in a competitive format. The samples introduced into the channel in which the beads were immobilized contained a fixed concentration of fluorescently labeled digoxigenin, a molecule for which anti-digoxin IgG has strong cross-reactivity. These samples also contained varying concentrations of digoxin: the molecule to be assayed. Binding of digoxin to the immobilized antibodies competed with the binding of

fluorescent digoxigenin such that as the concentration of digoxin in samples increased, the amount of fluorescent species bound to the beads decreased. Fluorescence arising from the labeled digoxigenin could be measured either as unbound digoxigenin flowed through the channel early in the experiment or as digoxigenin eluted bound to antibody-coated beads later.

The equilibrium-binding configuration for a competitive immunoassay can be treated analytically. Consider the binding of two analytes, one labeled and one unlabeled, to a set of surface binding sites. These binding reactions are described by the chemical equations:

$$A + S \underset{k_2}{\overset{k_1}{\leftrightarrow}} AS \quad (5.1)$$

$$A^* + S \underset{k^*_2}{\overset{k^*_1}{\leftrightarrow}} A^*S \quad (5.2)$$

A: Unlabeled analyte
A*: Labeled analyte
S: Binding site on an antibody

where A represents the unlabeled analyte, A^* represents the labeled analyte, and S represents a binding site. This situation is described by the equilibrium equations:

$$K = \frac{[AS]}{[A]([S]_0 - [AS] - [A^*S])} \quad (5.3)$$

$$K^* = \frac{[A^*S]}{[A^*]([S]_0 - [AS] - [A^*S])} \quad (5.4)$$

where [X]represents the concentration of species X, $[S]_0$ represents the initial concentration of binding sites, and K^* and K are the equilibrium binding coefficients for the labeled and unlabeled analytes, respectively. Solving equation 5.3 for $[S]_0$:

$$[S]_0 = \frac{[AS]}{K[A]} + [AS] + [A^*S] \quad (5.5)$$

If we define T as the total concentration of unlabeled analyte and T^* as the total concentration of labeled analyte:

$$T \equiv [AS] + [A]$$
$$T^* \equiv [A^*S] + [A^*] \quad (5.6),$$

and R as the ratio of bound unlabeled analyte concentration to total unlabeled analyte concentration:

$$R \equiv [AS]/T \quad (5.7),$$

then $[S]_0$ can be expressed as:

$$[S]_0 = R\left[\frac{1}{K(1-R)} + T + T^*\right] \quad (5.8).$$

Solving for T:

$$T = \frac{[S]_0}{R} - \frac{1}{K(1-R)} - T^* \quad (5.9).$$

If it is assumed that binding of the labeled analyte has the same equilibrium constant as binding of the unlabeled analyte, the right sides of equations 5.3 and 5.4 can be set equal to yield the following relationship:

$$\frac{[A^*S]}{T^*} = \frac{[AS]}{T} \quad (5.10).$$

In other words, the R in equation 5.9 represents the ratio of bound labeled analyte concentration to total labeled analyte concentration. Since the total concentration

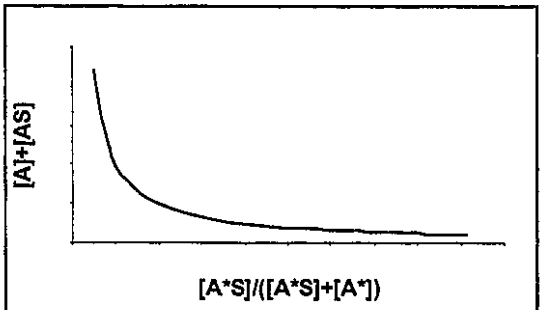

Figure 5.3: The relationship described by equation 5.9. The x-axis corresponds to the ratio of bound labeled analyte concentration to total labeled analyte concentration; the y-axis corresponds to the total concentration of unlabeled analyte. A competitive immunoassay seeks to find the y-axis value of a sample by measuring the x-axis value.

of labeled analyte in a competitive immunoassay is known and fixed, equation 5.9 gives the total concentration of unlabeled analyte as a function of the concentration of bound labeled analyte, which is a measurable quantity. Figure 5.3 shows the relationship described by equation 5.9—the relationship between total unlabeled analyte and fraction of bound labeled analyte—for typical values for K, $[S]_0$, and T^*.

5.3 Materials and Methods

5.3.1 Materials

Digoxin was obtained from Sigma (St. Louis, MO), as was biotinylated, monoclonal murine anti-digoxin IgG (clone DI-22). BODIPY® FL digoxigenin was obtained from Molecular Probes (Eugene, OR). Structures for both chemical are given in Figure 5.4. Wild-type streptavidin was expressed and purified according to a previously published protocol.[202] An *N*-hydroxysuccinimidyl ester of PNIPAAm (NHS-PNIPAAm) was synthesized according to a previously published protocol.[117] The number-

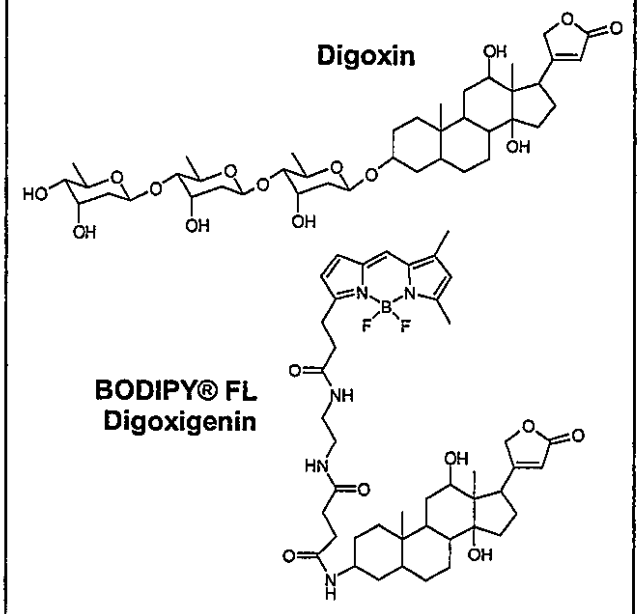

Figure 5.4: Analyte and labeled analyte analog used in immunoassay experiments.

average molecular weight ($\overline{M}_n$) of this polymer was determined to be 11,000 by vapor pressure osmometry (VPO, device model OSV111, Knauer, Germany). Primary amine-functionalized polystyrene latex beads were obtained from Polysciences (Warrington, PA). 100 nm diameter Polybead® Amino Microspheres were used in all experiments. Beads were co-modified with PNIPAAm and 3.4 kDa poly(ethylene glycol)-biotin (PEG-b) via N-hydroxysuccinimide (NHS) ester conjugation chemistry. NHS-PEG-biotin was obtained from the Shearwater Corporation (Huntsville, AL). In addition to the doubly modified PEG-b/PNIPAAm beads, singly modified PNIPAAm beads were prepared. The preparation and characterization of both types of beads were as described in Chapter 4.

5.3.2 Loading of beads with anti-digoxin IgG and preparation of bead suspension

Doubly modified beads were incubated with wild-type streptavidin in phosphate buffered saline (PBS, 50 mM phosphate, 5 mM NaCl), with equimolar amounts of streptavidin tetramers and available biotin moieties, for 15 minutes, saturating the beads with streptavidin. To remove any unbound streptavidin, these beads were centrifuged at a relative centrifugal force of 16,600 × g and a temperature of 4 ºC for 15 minutes. The supernatant was removed and the beads were resuspended in pH 7.6 PBS. This suspension was vortexed and agitated at 4 ºC for 2 hours to assure that no bead aggregates remained. Bioinylated anti-digoxin IgG was then loaded onto the beads by adding it to the streptavidin-coated bead suspension at a 20 × molar excess of streptavidin (assuming streptavidin

tetramers bound at a 1:1 stoichiometry to biotin moieties in the first step). To prepare beads for a negative control, this final step of adding antibody was omitted.

The bead suspension injected into the microfluidic channel consisted of 0.10 wt% doubly modified b-PEG/PNIPAAm beads loaded with streptavidin and anti-digoxin IgG, 0.40 wt% singly modified PNIPAAm beads, and 2.5 mg/mL free PNIPAAm in pH 7.6 PBS. The singly modified beads and free PNIPAAm were added to decrease the concentration of doubly modified beads required to form a continuous adherent network on the channel walls, and to thereby conserve protein reagents. The suspension was degassed by agitation under vacuum for approximately five minutes immediately prior to use.

5.3.3 Microfluidic devices

Experiments were performed in a type B device, as described in Chapter 4. All device mounting and plumbing details were as described for experiments with a type B device in Chapter 4.

5.3.4 Digoxin immunoassay experiments

Digoxin immunoassay experiments proceeded as follows. Two hundred microliters of bead suspension (described above, in the section entitled "loading of beads with anti-digoxin IgG and preparation of bead suspension") were injected into the primary device channel manually via a small matrix injection channel, connected by the manifold to a short length of PEEK tubing. After bead injection, this tubing was closed off with a standard HPLC tubing valve, preventing flow through the injection channel. The input port of the

device was connected to the output of a flow injection valve that allowed to operator to select between two flow sources: a 0.3 mL sample loop and a 1.5 mL sample loop. The 1.5 mL sample loop was filled with degassed PBS. The 0.3 mL sample loop contained BODIPY® FL digoxigenin in degassed PBS at a concentration of 2.5 μM. This sample loop also contained digoxin in concentrations varying from 0 to 12.8 μM (concentrations of 0, 1.28, 2.56, and 12.8 μM were investigated). After the matrix suspension had been injected into the primary channel, the heater was activated and matrix formation was allowed to proceed in the absence of flow for 10 minutes. The pumps were then activated, pushing buffer from the 1.5 mL sample loop through the system at a rate of 20 μL/min. Fluid flowing through the device was captured at the exit of the manifold output tubing in 50 μL aliquots. After 2.5 minutes of buffer wash, the injection valve was switched to the 0.3 mL sample loop, allowing the labeled digoxigenin/digoxin sample to flow into the device. The valve was switched back to the buffer-containing sample loop after 1.25 minutes, making the volume of the digoxigenin/digoxin sample 25 μL. After allowing the sample to bind and excess to be washed out (25 minutes after the initiation of flow), the heater was deactivated while the flow was maintained at a constant rate. Aliquots continued to be collected for an additional 15 minutes as the matrix dissolved. The output aliquots were then diluted to 500 μL in deionized water and the fluorescence of each sample was measured on a Perkin Elmer LS50B fluorescence spectrophotomer (Perkin Elmer Instruments, Inc., Shelton, CT), with excitation at 492 nm and emission at 511 nm. The OD_{600} of each sample was also measured, using a Hewlett-Packard model 8452A spectrophotometer (HP, Cupertino, CA). Experiments were performed in triplicate for each concentration investigated. Fluorescence arising from beads present in samples was corrected by background subtraction as described in Chapter 4.

5.4 Results and Discussion

Figure 5.5 shows a record of the fluorescent signal measured at the device output throughout digoxin immunoassay experiments at four digoxin concentrations. The y-axis

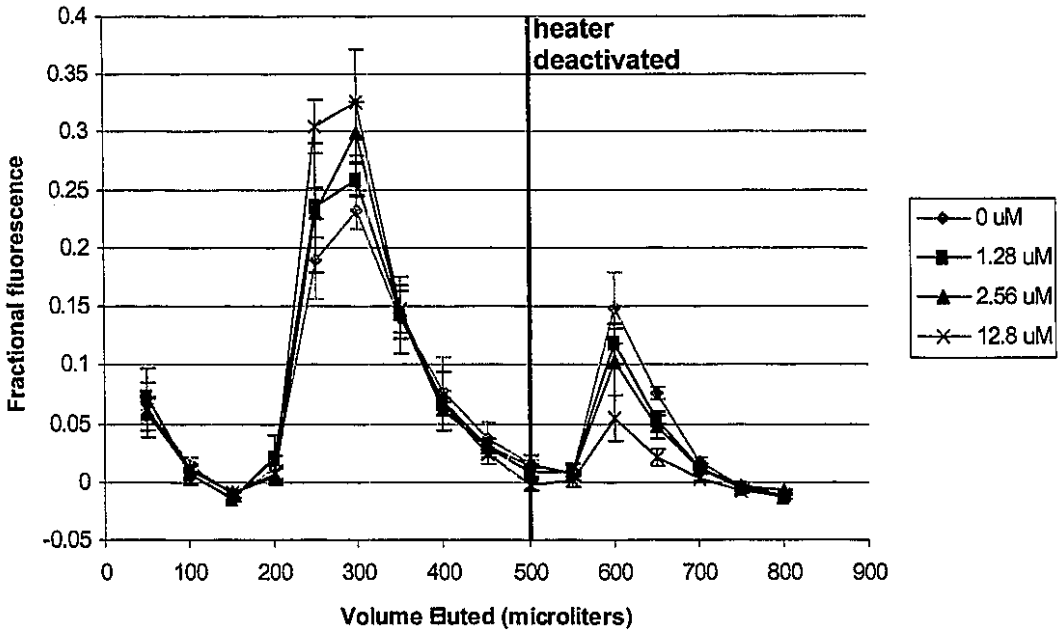

Figure 5.5: The fluorescent intensity of the device output throughout the digoxin immunoassay experiments. The x-axis corresponds to the total volume of fluid that has flowed through the device at each point; each point represents a 50 μL sample. The y-axis corresponds to the fluorescent intensity measured in each of these samples, normalized to the total fluorescence observed throughout the duration of the experiment. The data traces correspond to immunoassays with varying concentrations of digoxin: 0 μM (orange diamonds), 1.28 μM (dark blue squares), 2.56 μM (light blue triangles), and 12.8 μM (magenta x's). Flow was initiated with the heater activated; the heater was deactivated at the 500 μL point, as shown. In each of the data traces, two peaks can be seen. The first peak, beginning at the 250 μL point, corresponds to unbound labeled digoxigenin flowing past the immobilized antibodies and out of the channel. As digoxin concentration increases, less digoxigenin can bind the antibodies, and the size of this peak increases. The second peak, beginning at the 600 μL peak, corresponds to bound labeled digoxigenin eluting with the no-longer-immobilized beads. As digoxin concentrations increase, less digoxigenin is bound to the beads, and the size of this peak decreases. Error bars are ± one standard deviation over three experiments.

values on this plot correspond to the fluorescent intensities of 50 μL volumes of output, each normalized to the total output fluorescence throughout the experiment. The x-axis values correspond to the total volume pumped through the system at each output collection point. The zero point on the x-axis corresponds to the initiation of pump-driven flow, after bead aggregation and adhesion had been allowed to take place in the heated channel for ten minutes. The initially elevated fluorescence values at the 50 and 100 μL points are due to non-adherent beads being washed out of the channel. The peaks that begin at 250 μL represent unbound BODIPY® FL digoxigenin flowing past the immobilized antibodies and out of the channel. At the 500 μL point, the heater was deactivated, lowering the temperature in the channel and resulting in the dissolution of the adherent bead matrix. The beads were washed out of the channel, along with bound streptavidin, antibodies, and bound digoxin and fluorescent digoxigenin. The fluorescent signal from this bound digoxigenin is observed as the peak beginning at the 600 μL point. Compare the plot in Figure 5.5 to that in Figure 5.6, which shows the data for a negative control in which the beads were loaded with streptavidin but no antibody was bound to this streptavidin. Minimal binding is apparent in this

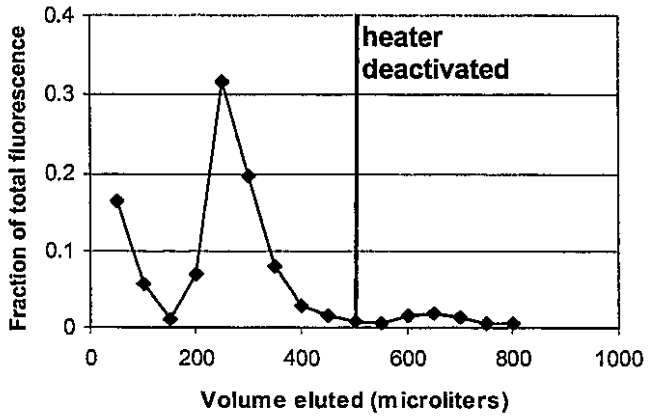

Figure 5.6: Negative control for the immunoassay experiments. Beads were loaded with streptavidin, but with no anti-digoxin IgG. Data are as described for Figure 5.4. Note that there is no significant elution peak, indicating a minimal non-specific interaction between the digoxin/digoxigenin species and the immobilized beads in the absence of antibody.

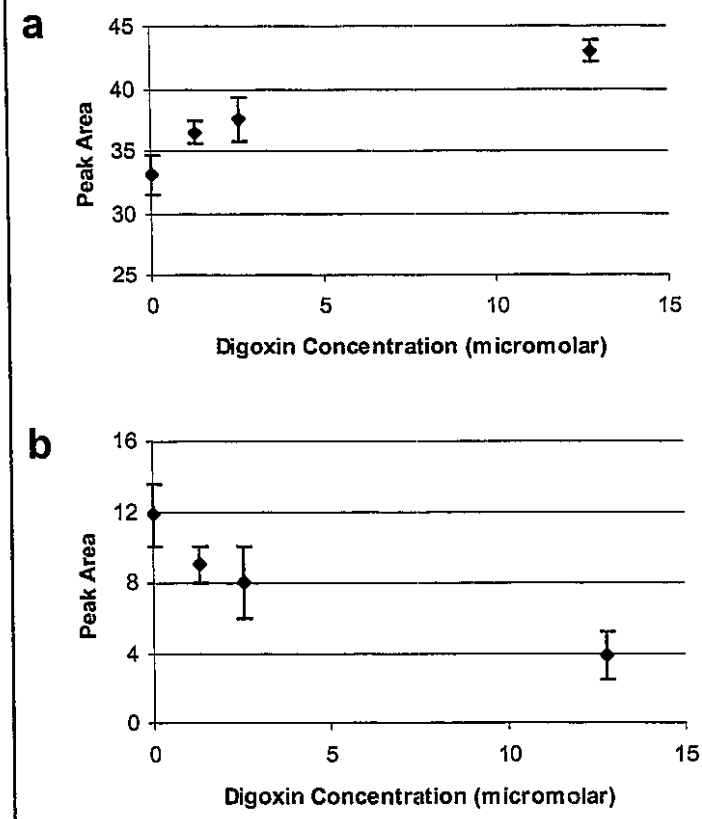

Figure 5.7: Integrated flowthrough and elution peak area as a function of digoxin concentration. a: Integrated area of the flowthrough (250 μL) peaks from figure 5.4 as a function of digoxin concentration. As digoxin concentration increases, so does competition for antibody binding, and the amount of labeled digoxigenin bound to the immobilized antibodies decreases. The amount of digoxigenin flowing directly through the system therefore increases, increasing the size of this peak. b: Integrated area of the elution (600 μL) peaks as a function of digoxin concentration. Increasing concentrations of digoxin decrease the amount of labeled digoxigenin bound to the eluting beads, thereby decreasing the size of this peak. All error bars are ± one standard deviation over three experiments.

negative control; the binding observed in the immunoassay experiments is therefore clearly a result of specific binding of digoxin or digoxigenin to the immobilized antibodies.

Looking again at Figure 5.5: as digoxin concentration increases, the flowthrough peak at 250 μL becomes larger while the elution peak at 600 μL becomes smaller. This change is due to digoxin competition with fluorescent digoxigenin for binding to the immobilized antibodies. As less labeled digoxigenin binds the beads, more passes through the channel with the flowthrough peak, and less flows out with the beads in the elution peak. Unfortunately, as is clear from the error bars in Figure 5.5 (± one standard deviation over three experiments), it is difficult to distinguish between different digoxin concentrations based simply on the peak heights. While the height of the 0 μM peak

is statistically distinguishable from that of the 12.8 μM peak, the error bars for any two adjacent peaks overlap, indicating that the difference in the heights of these peaks is not statistically significant. To some extent, this relative lack of precision is to be expected for this system: the process of bead adhesion to the channel wall is imprecise, and the amount of immobilized antibody therefore varies slightly with each trial.

Nevertheless, the data from these experiments are sufficiently rich to produce a precise calibration curve for a digoxin immunoassay. Figure 5.7 shows two plots of peak area as a function of digoxin concentration; Figure 5.7a corresponds to the flowthrough peak, while Figure 5.7b corresponds to the elution peak. Peak areas were obtained simply by integrating the peaks shown in Figure 5.5 after drawing straight lines between the data points. The flowthrough peak was integrated from the 200 μL point to the 450 μL point while the elution peak was integrated from the 550 μL point to the 700 μL point. In both Figures 5.7a and 5.7b, while the 1.28 and 2.56 μM points remain statistically indistinguishable, the 0 and 12.8 μM points are now distinguishable from all other points. This indicates that by analyzing peak area data, the immunoassay presented here is capable of detecting concentrations of digoxin as low as 1.28 μM and distinguishing varying concentrations of digoxin over an order of magnitude. In fact, the flowthrough peak data is

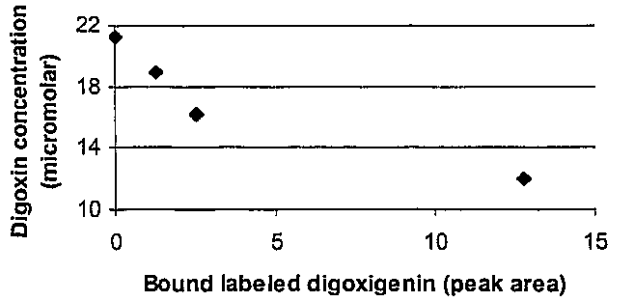

Figure 5.8: Digoxin concentration in immunoassay samples as a function of elution peak area. These are the same data as shown in Figure 5.6b, with the axes inverted. Compare to the theoretical competitive immunoassay curve in Figure 5.3.

sufficient to provide the full calibration curve throughout this range: this peak is completely collected after 22.5 minutes, meaning that the assay can be performed in under half an hour.

Figure 5.8 shows the data depicted in Figure 5.7b with the axes inverted. The axes now match those in Figure 5.3: the y-axis corresponds to the total amount of unlabeled digoxin in the sample, while the x-axis corresponds to the amount of labeled digoxigenin bound to the immobilized antibody (differing from the x-axis of Figure 5.3 by only a scale factor of total labeled analyte concentration). In broad terms, based on a comparison between the shape of the theoretical curve and the form of the experimental data, the immunoassay described in this chapter performed as expected from theory. Beyond this general assessment, it is difficult to make any concrete conclusions regarding the quality of the fit of these data to theory. The model described in Section 5.2, while sufficient to describe the general shape of expected data, makes many assumptions that are not necessarily valid for the experiments described here. Further modeling was not attempted, as the conclusions to be drawn from this work are not dependant on any strict theoretical construct.

5.5 Conclusions

The digoxin immunoassay demonstrated in this chapter is a powerful proof-of-principle for immobilization via PNIPAAm-coated smart beads. It was possible to generate a calibration curve for the assay over an order of magnitude of digoxin concentrations, with sensitivity to concentrations as low as 1.28 μM. More importantly, the immobilization technique used to generate this curve—temperature-dependant immobilization of IgG- and PNIPAAm-coated beads to the walls of the microfluidic channel—allowed for all

experiments to be performed in a single device over a period of several weeks with a fresh immobilized antibody reagent for each new experiment. Loading this reagent took only ten minutes, and not once during this series of experiments was it necessary to remove the device from the fluidic manifold connecting it to the sample delivery system. This platform is completely general: any molecule that can biotinylated or otherwise bound to the surface of a latex bead can be immobilized in microfluidic channels via this technology. Finally, the precise and reversible temperature-responsive nature of the smart polymer gives engineers a novel means of control for microfluidic processes, since the spatial distribution of immobilized molecules in a microfluidic device can be controlled merely by controlling the temperature at various locations in the device.

Chapter 6: Conclusions and Outlook

Microfluidic technology has the potential to transform modern clinical and research laboratory biochemical analysis. It is, however, a young field, and only a small fraction of available molecular engineering technologies have been explored in terms of their applicability to the solution of microfluidic problems. This dissertation has described attempts to bring the advantages of one such technology—stimuli-responsive polymer conjugate engineering—to bear on issues involving the control of bioseparations and biomolecular immobilization in microfluidic devices. Smart polymers seem like a natural fit for microfluidic devices: they allow macroscopic environmental controls to be transduced into micro- and nano-scale signals. Since the environmental stimuli to which smart polymers are sensitive are easily accessible in microfluidic devices, these polymers seem like ideal tools with which to execute control on the microfluidic scale. In the early work described in this dissertation, this control element was pursued in the context of a familiar smart polymer application: separation via stimulus-triggered sedimentation. Chapter 2 describes a pilot study in which a smart polymer conjugate-based separation system was developed, and Chapter 3 describes the analysis of this system's fitness to application in microfluidic devices. Unfortunately, this work revealed that smart polymer-mediated sedimentation is not a particularly practical separation process in a microfluidic context. However, it simultaneously revealed another facet of microfluidic systems where smart polymer-mediated control can be useful: immobilization of biomolecules. PNIPAAm-coated latex beads were found to adhere in a temperature sensitive, reversible, stable manner to the walls of PET microfluidic channels. Chapter 4 describes how these beads, co-modified with biotin,

can serve as a temperature-controlled microfluidic affinity chromatography matrix for separation of streptavidin. Chapter 5 describes the modification of the beads with an antibody to serve as a substrate for a solid-phase microfluidic immunoassay.

While the work described in Chapters 2 and 3 was not expanded into a working microfluidic separation system, some valuable conclusions can be drawn from it. The system described in Chapter 2 is especially important in the context of applications of the biotin-streptavidin system. Biotin-streptavidin binding is typically perceived as an irreversible process—the dissociation kinetics of the binding interaction are so slow that biotinylated macromolecules cannot be separated from a streptavidin substrate in a reasonable laboratory time frame. However, the work in Chapter 2 demonstrates that, through the use of high off-rate streptavidin mutants, reversibility can be introduced in the biotin-streptavidin system while high affinity and specificity is maintained. The results described in Chapter 2 also highlight some potential pitfalls of working with high off-rate streptavidin mutants, including decreased off-rate resulting from cooperative binding and reduced affinity to certain biotinylated species. As for Chapter 3, while the work described there failed to produce a viable microfluidic smart polymer affinity precipitation system, it did establish that smart polymer aggregate sedimentation can be observed in microfluidic channels, and described some of the bounds of this sedimentation behavior. This information may be valuable to future microfluidic sedimentation projects.

Nevertheless, the most promising and innovative work described in this document is the development of a smart bead system for immobilizing biomolecules in microfluidic channels in a temperature-sensitive manner. There are a number of straightforward experiments that can be performed to expand upon this work. The most obvious of these are

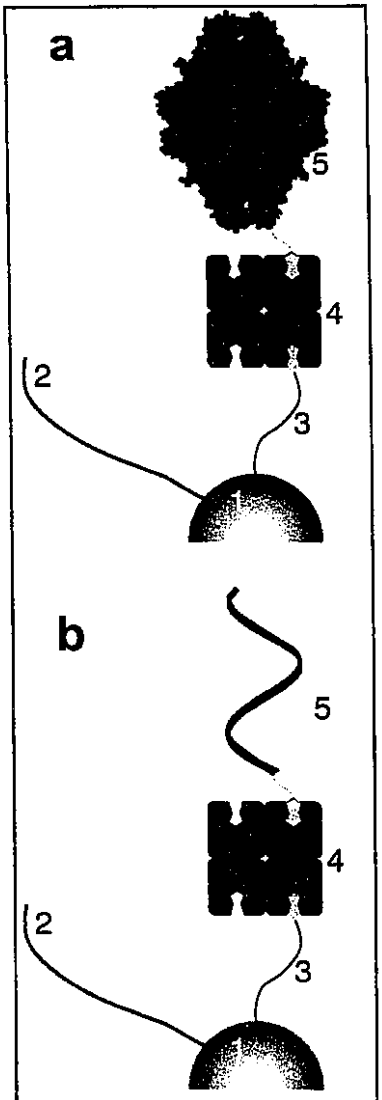

Figure 6.1: Proposed smart bead constructs for biomolecular immobilization. In both a and b, a bead (1) is shown co-modified with PNIPAAm (2) and PEG-biotin (3). Biotin groups in both constructs bind streptavidin molecules (4). This streptavidin, in turn, is bound to biotinylated β-galactosidase (5) in a and a biotinylated single-stranded oligonucleotide (5) in b.

further demonstrations of the generality of smart beads as an immobilization system. Figure 6.1 shows diagrams of proposed smart bead/biomolecule constructs, like that shown in Figure 5.1. Figure 6.1a shows a biotinylated enzyme attached to the beads. Such a construct could be used as the basis for a microfluidic bioreactor; such bioreactors have potential research application in high-throughput screening of enzyme inhibition, which is important to the screening of combinatorial molecular libraries during drug design. Active enzyme immobilization on smart beads could also serve as the basis for developing an enzyme-linked immunoassay, which would be more sensitive than the assay presented in Chapter 5. Figure 6.1b show a single-stranded oligonucleotide as part of a smart bead construct. Such a construct could be immobilized in a microfluidic channel to serve as an affinity separation substrate for complimentary oligonucleotides, either as means of detecting their presence or in preparation for further processing. In addition to serving as an immobilization substrate for biomolecules, smart beads might be useful for immobilizing cells. Beads modified with cell adhesion molecules could be thermally

immobilized in a microfluidic channel and cells cultured on the channel walls. Once in place in a microfluidic channel, various molecules could be delivered to the cells in a controlled fashion, and the cells could be observed microscopically of via the analysis of any cell metabolism products in the downstream flow. A platform like this one could be a valuable step towards the development of automated, high-throughput cell culture technologies, as well as a tool for affinity isolation of specific cell types, such as stem cells.

In addition to being a versatile means of biomolecular immobilization, smart beads are promising as a microfluidic control element. Figure 6.2 shows a prospective application of temperature-sensitive immobilization in a separation process. In two separate temperature-controlled regions of a microfluidic channel, beads are immobilized such that the beads in each region bear different affinity moieties. A mixed solution containing several biomolecules of interest is passed through the channel. Each region of immobilized beads specifically binds a different biomolecular species from this mixed solution. The temperatures in the heated regions are then lowered sequentially, releasing the beads—along with their distinct bound affinity cargos—at separate times. Downstream flow control elements can segregate the two types of beads into separate flow streams. In this manner, a single channel can be used to separate multiple species from a single flow stream simultaneously. This concept can be scaled up to separate an arbitrarily large number of species in a single affinity column. This mode of separation highlights a key feature of the smart beads: they enable the connection of a single control element to a discreet biochemical functionality. The user of a microfluidic device is given precise control over the distribution of the biomolecules immobilized within the device. This level of biochemical control can be further enhanced by the development of immobilization substrates based on a variety of

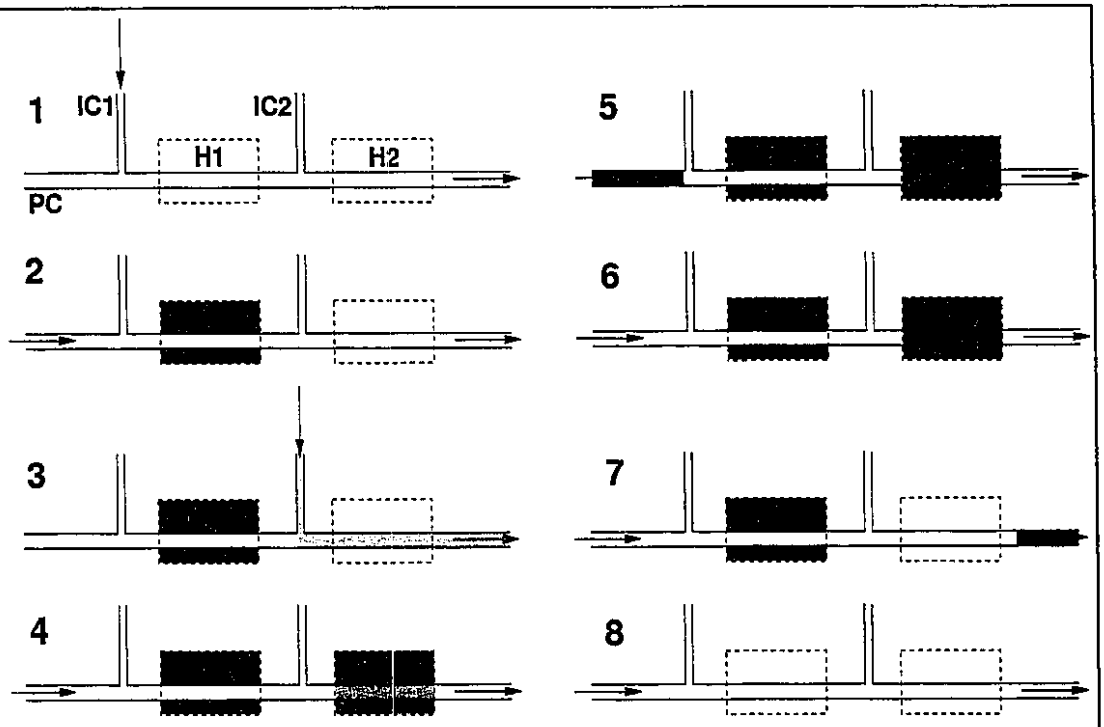

Figure 6.2: A prospective microfluidic smart bead application, with which multiple biomolecular species could be separated in a single channel. This diagram shows a microfluidic channel layout, consisting of a primary channel (PC), two bead injection channels (IC1 and IC2), and two heated regions (H1 and H2). In this diagram, arrows represent the presence and direction of flow, and a red color indicates an elevated temperature in a heated region. Initially (1), a suspension of smart beads modified with an affinity moiety (pale yellow) is injected through IC1. The temperature in H1 is elevated, resulting in bead adhesion, and excess beads are washed out (2). Next, a suspension of smart beads bearing a different affinity moiety (pale blue) is injected through IC2 (3). Region H2 is heated, beads adhere, and unbound beads are washed through the channel (4). Two different affinity moieties are now immobilized in the two separate heated regions. A bolus of solution containing a mixture of target molecules (green) is then injected into the primary channel (5). Different components (dark yellow and dark blue) of this mixture bind the different affinity moieties; unbound molecules are washed through the channel (6). The temperature in H2 is then decreased, eluting the bound blue molecule (7). Finally, the temperature in H1 is decreased, eluting the bound yellow molecule (8). In this manner, two different molecules can be separated into two distinct product streams.

smart polymers; in addition to temperature-responsive polymers, polymers that undergo phase transition in response to pH, ionic strength, and light are available. By connecting a specific stimulus to a specific biochemical functionality, control of the environment in a

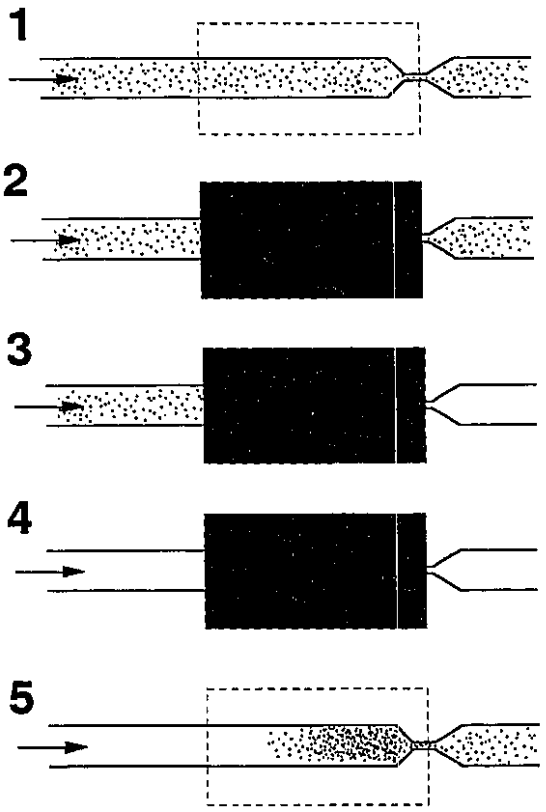

Figure 6.3: A diagram of a scheme for tightly packing a column with smart bead aggregates. This diagram shows a microfluidic channel with a constriction in it (solid lines) and a heated region (dashed lines). Flow is indicated with an arrow, and an elevated temperature in the heated region is indicated with a red color. Initially, suspended smart beads are flowing through the channel (1). They are smaller than the channel constriction, and are not obstructed by it. Then, the heater is activated and the smart beads aggregate (2). The aggregates are too large to pass through the channel constriction, and they begin to pack tightly into the space upstream of the constriction (3). The column is now packed, and fluid can be pushed through it (4). Components of the fluid can interact with the surfaces of the bead aggregates; tight packing provides a relatively high surface area. When the packed column is no longer needed, the heater is deactivated, lowering the channel temperature and leading to dissolution of the aggregates. The resuspended beads are washed away (5).

microfluidic channel can be coupled precisely to the biochemical functionalization of that channel.

Figure 6.3 contains a diagram of yet another application of smart beads in microfluidic devices. By using a microfluidic channel with a constriction that has a width on the same scale as the diameter of smart beads aggregate particles, it should be possible to pack that channel tightly with smart bead aggregates. Assuming that this channel packing material is sufficiently porous to facilitate high-pressure flow, smart beads could in this manner be used to form very high-surface-area columns in microfluidic devices in a controlled, on-demand manner. Upon reversing the phase aggregation stimulus of the beads, the aggregates will dissolve, and the beads will flow out of the channel. This system introduces all of the advantages of

reversibility and column renewal that come with the smart bead system to a densely packed column. Such a system would be useful in affinity chromatography applications requiring stringent and complete separation or separation of relatively large amounts of a target molecule, as well as in electrophoretic or physiochemical separation systems requiring a porous substrate.

The reversible immobilization of biomolecule-modified beads via grafted smart polymer phase transitions as an approach to biomolecular immobilization has many advantages over conventional microfluidic immobilization schemes. Immobilized biomolecules can be loaded into a device by the end user in an on-demand manner, allowing for improved flexibility and customizability in device use. On-demand immobilization also improves device shelf life, since devices need not be stored with fragile biomolecules pre-immobilized in them. The reversibility of this immobilization scheme allows the user to renew the immobilized substrate, increasing usable device lifetime. Finally, stimulus-dependant immobilization introduces a new control element into microfluidic devices: the location and timing of biomolecular immobilization can be controlled simply by controlling the polymer stimulus at various points on a device.

End Notes

(1) Manz, A.; Graber, N.; Widmer, H. M. "Miniaturized Total Chemical-Analysis Systems - a Novel Concept for Chemical Sensing" *Sensor Actuat B-Chem* **1990**, *1*, 244-248.

(2) Auroux, P. A.; Iossifidis, D.; Reyes, D. R.; Manz, A. "Micro total analysis systems. 2. Analytical standard operations and applications" *Anal Chem* **2002**, *74*, 2637-2652.

(3) Khandurina, J.; Guttman, A. "Bioanalysis in microfluidic devices" *J Chromatogr A* **2002**, *943*, 159-183.

(4) Chovan, T.; Guttman, A. "Microfabricated devices in biotechnology and biochemical processing" *Trends Biotechnol* **2002**, *20*, 116-122.

(5) Weigl, B. H.; Bardell, R. L.; Cabrera, C. R. "Lab-on-a-chip for drug development" *Adv. Drug Delivery Rev.* **2003**, *55*, 349-377.

(6) Landers, J. P. "Molecular diagnostics on electrophoretic microchips" *Anal Chem* **2003**, *75*, 2919-2927.

(7) Kopp, M. U.; Crabtree, H. J.; Manz, A. "Developments in technology and applications of microsystems" *Curr Opin Chem Biol* **1997**, *1*, 410-419.

(8) Beebe, D. J.; Mensing, G. A.; Walker, G. M. "Physics and applications of microfluidics in biology" *Annu Rev Biomed Eng* **2002**, *4*, 261-286.

(9) Reyes, D. R.; Iossifidis, D.; Auroux, P. A.; Manz, A. "Micro total analysis systems. 1. Introduction, theory, and technology" *Anal Chem* **2002**, *74*, 2623-2636.

(10) Szumski, M.; Buszewski, B. "State of the art in miniaturized separation techniques" *Crit Rev Anal Chem* **2002**, *32*, 1-46.

(11) Krishnan, M.; Namasivayam, V.; Lin, R. S.; Pal, R.; Burns, M. A. "Microfabricated reaction and separation systems" *Curr Opin Biotech* **2001**, *12*, 92-98.

(12) Harrison, D. J.; Manz, A.; Fan, Z. H.; Ludi, H.; Widmer, H. M. "Capillary Electrophoresis and Sample Injection Systems Integrated on a Planar Glass Chip" *Anal Chem* **1992**, *64*, 1926-1932.

(13) Lacher, N. A.; Garrison, K. E.; Martin, R. S.; Lunte, S. M. "Microchip capillary electrophoresis/electrochemistry" *Electrophoresis* **2001**, *22*, 2526-2536.

(14) Wang, J.; Pumera, M.; Chatrathi, M. P.; Escarpa, A.; Konrad, R.; Griebel, A.; Dorner, W.; Lowe, H. "Towards disposable lab-on-a-chip: Poly(methylmethacrylate)

microchip electrophoresis device with electrochemical detection" *Electrophoresis* **2002**, *23*, 596-601.

(15) Colyer, C. L.; Mangru, S. D.; Harrison, D. J. "Microchip-based capillary electrophoresis of human serum proteins" *J Chromatogr A* **1997**, *781*, 271-276.

(16) Woolley, A. T.; Mathies, R. A. "Ultra-High-Speed DNA-Sequencing Using Capillary Electrophoresis Chips" *Anal Chem* **1995**, *67*, 3676-3680.

(17) Brahmasandra, S. N.; Ugaz, V. M.; Burke, D. T.; Mastrangelo, C. H.; Burns, M. A. "Electrophoresis in microfabricated devices using photopolymerized polyacrylamide gels and electrode-defined sample injection" *Electrophoresis* **2001**, *22*, 300-311.

(18) Wang, P. C.; Gao, J.; Lee, C. S. "High-resolution chiral separation using microfluidics-based membrane chromatography" *J Chromatogr A* **2002**, *942*, 115-122.

(19) Desmet, G.; Vervoort, N.; Clicq, D.; Baron, G. V. "Experimental demonstration of the possibility to perform shear-driven chromatographic separations in micro-channels" *J Chromatogr A* **2001**, *924*, 111-122.

(20) Blom, M. T.; Chmela, E.; Gardeniers, J. G. E.; Tijssen, R.; Elwenspoek, M.; van den Berg, A. "Design and fabrication of a hydrodynamic chromatography chip" *Sensor Actuat B-Chem* **2002**, *82*, 111-116.

(21) Regnier, F. E.; He, B.; Lin, S.; Busse, J. "Chromatography and electrophoresis on chips: critical elements of future integrated, microfluidic analytical systems for life science" *Trends Biotechnol* **1999**, *17*, 101-106.

(22) Buranda, T.; Huang, J.; Perez-Luna, V. H.; Schreyer, B.; Sklar, L. A.; Lopez, G. P. "Biomolecular recognition on well-characterized beads packed in microfluidic channels" *Anal Chem* **2002**, *74*, 1149-1156.

(23) Ro, K. W.; Lim, K.; Kim, H.; Hahn, J. H. "Poly(dimethylsiloxane) microchip for precolumn reaction and micellar electrokinetic chromatography of biogenic amines" *Electrophoresis* **2002**, *23*, 1129-1137.

(24) Deng, T.; Prentiss, M.; Whitesides, G. M. "Fabrication of magnetic microfiltration systems using soft lithography" *Appl Phys Lett* **2002**, *80*, 461-463.

(25) Weigl, B. H.; Yager, P. "Microfluidics - Microfluidic diffusion-based separation and detection" *Science* **1999**, *283*, 346-347.

(26) Cabrera, C. R.; Finlayson, B.; Yager, P. "Formation of natural pH gradients in a microfluidic device under flow conditions: Model and experimental validation" *Anal Chem* **2001**, *73*, 658-666.

(27) Takahashi, T.; Ogata, S.; Nishizawa, M.; Matsue, T. "A valveless switch for microparticle sorting with laminar flow streams and electrophoresis perpendicular to the direction of fluid stream" *Electrochem. Comm.* **2003**, *5*, 175-177.

(28) Macounova, K.; Cabrera, C. R.; Yager, P. "Concentration and separation of proteins in microfluidic channels on the basis of transverse IEF" *Anal Chem* **2001**, *73*, 1627-1633.

(29) Cabrera, C. R.; Yager, P. "Continuous concentration of bacteria in a microfluidic flow cell using electrokinetic techniques" *Electrophoresis* **2001**, *22*, 355-362.

(30) Peterson, D. S.; Rohr, T.; Svec, F.; Fréchet, J. M. J. "Enzymatic microreactor-on-a-chip: protein mapping using trypsin immobilized on porous polymer monoliths molded in channels of microfluidic devices" *Anal Chem* **2002**, *74*, 4081-4088.

(31) Ekstrom, S.; Onnerfjord, P.; Nilsson, J.; Bengtsson, M.; Laurell, T.; Marko-Varga, G. "Integrated microanalytical technology enabling rapid and automated protein identification" *Anal Chem* **2000**, *72*, 286-293.

(32) Mao, H. B.; Yang, T. L.; Cremer, P. S. "Design and characterization of immobilized enzymes in microfluidic systems" *Anal Chem* **2002**, *74*, 379-385.

(33) Slentz, B. E.; Penner, N. A.; Regnier, F. E. "Protein proteolysis and the multi-dimensional electrochromatographic separation of histidine-containing peptide fragments on a chip" *J Chromatogr A* **2003**, *984*, 97-107.

(34) L'Hostis, E.; Michel, P. E.; Fiaccabrino, G. C.; Strike, D. J.; de Rooij, N. F.; Koudelka-Hep, M. "Microreactor and electrochemical detectors fabricated using Si and EPON SU-8" *Sensor Actuat B-Chem* **2000**, *64*, 156-162.

(35) Wang, C.; Oleschuk, R. D.; Ouchen, F.; Li, J. J.; Thibault, P.; Harrison, D. J. "Integration of immobilized trypsin bead beds for protein digestion within a microfluidic chip incorporating capillary electrophoresis separations and an electrospray mass spectrometry interface" *Rap. Comm. Mass Spec.* **2000**, *14*, 1377-1383.

(36) Lazar, I. M.; Ramsey, R. S.; Ramsey, J. M. "On-chip proteolytic digestion and analysis using "wrong-way-round" electrospray time-of-flight mass spectrometry" *Anal Chem* **2001**, *73*, 1733-1739.

(37) Gottschlich, N.; Culbertson, C. T.; McKnight, T. E.; Jacobson, S. C.; Ramsey, J. M. "Integrated microchip-device for the digestion, separation and postcolumn labeling of proteins and peptides" *J Chromatogr B* **2000**, *745*, 243-249.

(38) Hadd, A. G.; Raymond, D. E.; Halliwell, J. W.; Jacobson, S. C.; Ramsey, J. M. "Microchip device for performing enzyme assays" *Anal Chem* **1997**, *69*, 3407-3412.

(39) Hadd, A. G.; Jacobson, S. C.; Ramsey, J. M. "Microfluidic assays of acetylcholinesterase inhibitors" *Anal Chem* **1999**, *71*, 5206-5212.

(40) Starkey, D. E.; Han, A.; Bao, J. J.; Ahn, C. H.; Wehmeyer, K. R.; Prenger, M. C.; Halsall, H. B.; Heineman, W. R. "Fluorogenic assay for beta-glucuronidase using microchip-based capillary electrophoresis" *J Chromatogr B* **2001**, *762*, 33-41.

(41) Seong, G. H.; Heo, J.; Crooks, R. M. "Measurement of enzyme kinetics using a continuous-flow microfluidic system" *Anal Chem* **2003**, *75*, 3161-3167.

(42) Liu, J.; Enzelberger, M.; Quake, S. R. "A nanoliter rotary device for polymerase chain reaction" *Electrophoresis* **2002**, *23*, 1531-1536.

(43) Northrup, M. A.; Benett, B.; Hadley, D.; Landre, P.; Lehew, S.; Richards, J.; Stratton, P. "A miniature analytical instrument for nucleic acids based on micromachined silicon reaction chambers" *Anal Chem* **1998**, *70*, 918-922.

(44) Waters, L. C.; Jacobson, S. C.; Kroutchinina, N.; Khandurina, J.; Foote, R. S.; Ramsey, J. M. "Microchip device for cell lysis, multiplex PCR amplification, and electrophoretic sizing" *Anal Chem* **1998**, *70*, 158-162.

(45) Kopp, M. U.; de Mello, A. J.; Manz, A. "Chemical amplification: Continuous-flow PCR on a chip" *Science* **1998**, *280*, 1046-1048.

(46) Lu, L.-H.; Ryu, K. S.; Liu, C. "A magnetic microstirrer and array for microfluidic mixing" *J. MEMS* **2002**, *11*, 462-469.

(47) Liu, R. H.; Stremler, M. A.; Sharp, K. V.; Olsen, M. G.; Santiago, J. G.; Adrian, R. J.; Aref, H.; Beebe, D. J. "Passive mixing in a three-dimensional serpentine microchannel" *J. MEMS* **2000**, *9*, 190-197.

(48) Johnson, T. J.; Ross, D.; Locascio, L. E. "Rapid microfluidic mixing" *Anal Chem* **2002**, *74*, 45-51.

(49) Oddy, M. H.; Santiago, J. G.; Mikkelsen, J. C. "Electrokinetic instability micromixing" *Anal Chem* **2001**, *73*, 5822-5832.

(50) Jacobson, S. C.; McKnight, T. E.; Ramsey, J. M. "Microfluidic devices for electrokinetically driven parallel and serial mixing" *Anal Chem* **1999**, *71*, 4455-4459.

(51) Lao, A. I. K.; Lee, T. M. H.; Hsing, I. M.; Ip, N. Y. "Precise temperature control of microfluidic chamber for gas and liquid phase reactions" *Sensor Actuat a-Phys* **2000**, *84*, 11-17.

(52) Jiang, G. F.; Attiya, S.; Ocvirk, G.; Lee, W. E.; Harrison, D. J. "Red diode laser induced fluorescence detection with a confocal microscope on a microchip for capillary electrophoresis" *Biosens Bioelectron* **2000**, *14*, 861-869.

(53) Hubner, J.; Mogensen, K. B.; Jorgensen, A. M.; Friis, P.; Telleman, P.; Kutter, J. P. "Integrated optical measurement system for fluorescence spectroscopy in microfluidic channels" *Rev Sci Instrum* **2001**, *72*, 229-233.

(54) Wang, J. "Electrochemical detection for microscale analytical systems: a review" *Talanta* **2002**, *56*, 223-231.

(55) Zhan, W.; Alvarez, J.; Sun, L.; Crooks, R. M. "A multichannel microfluidic sensor that detects anodic redox reactions indirectly using anodic electrogenerated chemiluminescence" *Anal Chem* **2003**, *75*, 1233-1238.

(56) Lee, H. J.; Goodrich, T. T.; Corn, R. M. "SPR imaging measurements of 1-D and 2-D DNA microarrays created from microfluidic channels on gold thin films" *Anal Chem* **2001**, *73*, 5525-5531.

(57) Verpoorte, E. M. J.; Vanderschoot, B. H.; Jeanneret, S.; Manz, A.; Widmer, H. M.; Derooij, N. F. "3-Dimensional Micro-Flow Manifolds for Miniaturized Chemical-Analysis Systems" *J Micromech Microeng* **1994**, *4*, 246-256.

(58) Kim, E.; Xia, Y. N.; Whitesides, G. M. "Polymer Microstructures Formed by Molding in Capillaries" *Nature* **1995**, *376*, 581-584.

(59) Beebe, D. J.; Moore, J. S.; Yu, Q.; Liu, R. H.; Kraft, M. L.; Jo, B. H.; Devadoss, C. "Microfluidic tectonics: A comprehensive construction platform for microfluidic systems" *P Natl Acad Sci USA* **2000**, *97*, 13488-13493.

(60) Roberts, M. A.; Rossier, J. S.; Bercier, P.; Girault, H. "UV laser machined polymer substrates for the development of microdiagnostic systems" *Anal Chem* **1997**, *69*, 2035-2042.

(61) Bruin, G. J. M. "Recent developments in electrokinetically driven analysis on microfabricated devices" *Electrophoresis* **2000**, *21*, 3931-3951.

(62) McKnight, T. E.; Culbertson, C. T.; Jacobson, S. C.; Ramsey, J. M. "Electroosmotically induced hydraulic pumping with integrated electrodes on microfluidic devices" *Anal Chem* **2001**, *73*, 4045-4049.

(63) Duffy, D. C.; Gillis, H. L.; Lin, J.; Sheppard, N. F.; Kellogg, G. J. "Microfabricated centrifugal microfluidic systems: Characterization and multiple enzymatic assays" *Anal Chem* **1999**, *71*, 4669-4678.

(64) Nguyen, N. T.; Huang, X. Y.; Chuan, T. K. "MEMS-micropumps: A review" *J. Fluids Eng.* **2002**, *124*, 384-392.

(65) Shoji, S. "Fluids for sensor systems" *Top. Curr. Chem.* **1998**, *194*, 163-188.

(66) Thorsen, T.; Maerkl, S. J.; Quake, S. R. "Microfluidic large-scale integration" *Science* **2002**, *298*, 580-584.

(67) Unger, M. A.; Chou, H.-P.; Thorsen, T.; Scherer, A.; Quake, S. R. "Monolithic microfabricated valves and pumps by multilayer soft lithography" *Science* **2000**, *288*, 113-116.

(68) Yu, Q.; Bauer, J. M.; Moore, J. S.; Beebe, D. J. "Responsive biomimetic hydrogel valve for microfluidics" *Appl Phys Lett* **2001**, *78*, 2589-2591.

(69) Yu, C.; Mutlu, S.; Selvaganapathy, P.; Mastrangelo, C. H.; Svec, F.; Frechet, J. M. J. "Flow control valves for analytical microfluidic chips without mechanical parts based on thermally responsive monolithic polymers" *Anal Chem* **2003**, *75*, 1958-1961.

(70) Andersson, H.; van der Wijngaart, W.; Enoksson, P.; Stemme, G. "Micromachined flow-through filter-chamber for chemical reactions on beads" *Sensor Actuat B-Chem* **2000**, *67*, 203-208.

(71) Li, J. J.; Thibault, P.; Bings, N. H.; Skinner, C. D.; Wang, C.; Colyer, C.; Harrison, J. "Integration of microfabricated devices to capillary electrophoresis-electrospray mass spectrometry using a low dead volume connection: Application to rapid analyses of proteolytic digests" *Anal Chem* **1999**, *71*, 3036-3045.

(72) Deng, Y. Z.; Henion, J.; Li, J. J.; Thibault, P.; Wang, C.; Harrison, D. J. "Chip-based capillary electrophoresis/mass spectrometry determination of carnitines in human urine" *Anal Chem* **2001**, *73*, 639-646.

(73) Licklider, L.; Wang, X. Q.; Desai, A.; Tai, Y. C.; Lee, T. D. "A micromachined chip-based electrospray source for mass spectrometry" *Anal Chem* **2000**, *72*, 367-375.

(74) Hatch, A.; Kamholz, A. E.; Hawkins, K. R.; Munson, M. S.; Schilling, E. A.; Weigl, B. H.; Yager, P. "A rapid diffusion immunoassay in a T-sensor" *Nat Biotechnol* **2001**, *19*, 461-465.

(75) Yang, T. L.; Jung, S. Y.; Mao, H. B.; Cremer, P. S. "Fabrication of phospholipid bilayer-coated microchannels for on-chip immunoassays" *Anal Chem* **2001**, *73*, 165-169.

(76) Dodge, A.; Fluri, K.; Verpoorte, E.; de Rooij, N. F. "Electrokinetically driven microfluidic chips with surface-modified chambers for heterogenous immunoassays" *Anal Chem* **2001**, *73*, 3400-3409.

(77) Yakovleva, J.; Davidsson, R.; Lobanova, A.; Bengtsson, M.; Eremin, S.; Laurell, T.; Emneus, J. "Microfluidic enzyme immunoassay using silicon microchip with immobilized antibodies and chemiluminescence detection" *Anal Chem* **2002**, *74*, 2994-3004.

(78) Sato, K.; Tokeshi, M.; Odake, T.; Kimura, H.; Ooi, T.; Nakao, M.; Kitamori, T. "Integration of an immunosorbent assay system: Analysis of secretory human immunoglobulin A on polystyrene beads in a microchip" *Anal Chem* **2000**, *72*, 1144-1147.

(79) Hansen, C. L.; Skordalakes, E.; Berger, J. M.; Quake, S. R. "A robust and scalable microfluidic metering method that allows protein crystal growth by free interface diffusion" *P Natl Acad Sci USA* **2002**, *99*, 16531-16536.

(80) Sanjoh, A.; Tsukihara, T. "Spatiotemporal protein crystal growth studies using microfluidic silicon devices" *J. Cryst. Growth* **1999**, *194*, 691-702.

(81) Geschwind, D. H. "DNA microarrays: translation of the genome from laboratory to clinic" *Lancet Neurology* **2003**, *2*, 275-282.

(82) Cutler, P. "Protein arrays: The current state-of-the-art" *Proteomics* **2003**, *3*, 3-18.

(83) Templin, M. F.; Stoll, D.; Schrenk, M.; Traub, P. C.; Vohringer, C. F.; Joos, T. O. "Protein microarray technology" *Trends Biotechnol* **2002**, *20*, 160-166.

(84) Henry, A. C.; Tutt, T. J.; Galloway, M.; Davidson, Y. Y.; McWhorter, C. S.; Soper, S. A.; McCarley, R. L. "Surface modification of poly(methyl methacrylate) used in the fabrication of microanalytical devices" *Anal Chem* **2000**, *72*, 5331-5337.

(85) Barker, S. L. R.; Ross, D.; Tarlov, M. J.; Gaitan, M.; Locascio, L. E. "Control of flow direction in microfluidic devices with polyelectrolyte multilayers" *Anal Chem* **2000**, *72*, 5925-5929.

(86) Barker, S. L. R.; Tarlov, M. J.; Canavan, H.; Hickman, J. J.; Locascio, L. E. "Plastic microfluidic devices modified with polyelectrolyte multilayers" *Anal Chem* **2000**, *72*, 4899-4903.

(87) Liu, Y.; Fanguy, J. C.; Bledsoe, J. M.; Henry, C. S. "Dynamic coating using polyelectrolyte multilayers for chemical control of electroosmotic flow in capillary electrophoresis microchips" *Anal Chem* **2000**, *72*, 5939-5944.

(88) Linder, V.; Verpoorte, E.; Thormann, W.; de Rooij, N. F.; Sigrist, H. "Surface biopassivation of replicated poly(dimethylsiloxane) microfluidic channels and application to heterogeneous immunoreaction with on-chip fluorescence detection." *Anal Chem* **2001**, *73*, 4181-4189.

(89) Schwarz, A.; Rossier, J. S.; Roulet, E.; Mermod, N.; Roberts, M. A.; Girault, H. H. "Micropatterning of biomolecules on polymer substrates" *Langmuir* **1998**, *14*, 5526-5531.

(90) Papra, A.; Bernard, A.; Juncker, D.; Larsen, N. B.; Michel, B.; Delamarche, E. "Microfluidic networks made of poly(dimethylsiloxane), Si, and Au coated with polyethylene glycol for patterning proteins onto surfaces" *Langmuir* **2001**, *17*, 4090-4095.

(91) Xu, Y.; Vaidya, B.; Patel, A. B.; Ford, S. M.; McCarley, R. L.; Soper, S. A. "Solid-phase reversible immobilization in microfluidic chips for the purification of dye-labeled DNA sequencing fragments" *Anal Chem* **2003**, *In press, published on www.*

(92) Shamansky, L. M.; Davis, C. B.; Stuart, J. K.; Kuhr, W. G. "Immobilization and detection of DNA on microfluidic chips" *Talanta* **2001**, *55*, 909-918.

(93) Xiong, L.; Regnier, F. E. "Channel-specific coatings on microfabricated chips" *J Chromatogr A* **2001**, *924*, 165-176.

(94) Lahann, J.; Balcells, M.; Lu, H.; Rodon, T.; Jensen, K. F.; Langer, R. "Reactive polymer coatings: A first step toward surface engineering of microfluidic devices" *Anal Chem* **2003**, *In Press*.

(95) Knox, J. H. "Practical Aspects of LC Theory" *J. Chrom. Sci.* **1977**, *15*, 352-364.

(96) Chen, L. X.; Ma, J. P.; Tan, F.; Guan, Y. F. "Generating high-pressure sub-microliter flow rate in packed microchannel by electroosmotic force: potential applications in microfluidic systems" *Sensor Actuat B-Chem* **2003**, *88*, 260-265.

(97) Bergkvist, J.; Ekstrom, S.; Wallman, L.; Lofgren, M.; Marko-Varga, G.; Nilsson, J.; Laurell, T. "Improved chip design for integrated solid-phase microextraction in on-line proteomic sample preparation" *Proteomics* **2002**, *2*, 422-429.

(98) Ocvirk, G.; Verpoorte, E.; Manz, A.; Grasserbauer, M.; Widmer, H. M. "High-Performance Liquid-Chromatography Partially Integrated onto a Silicon Chip" *Anal Method Instrum* **1995**, *2*, 74-82.

(99) Ekstrom, S.; Malmstrom, J.; Wallman, L.; Lofgren, M.; Nilsson, J.; Laurell, T.; Marko-Varga, G. "On-chip microextraction for proteomic sample preparation of in-gel digests" *Proteomics* **2002**, *2*, 413-421.

(100) Nakamura, H.; Murakami, Y.; Yokoyama, K.; Tamiya, E.; Karube, I. "A compactly integrated flow cell with a chemiluminescent FIA system for determining lactate concentration in serum" *Anal Chem* **2001**, *73*, 373-378.

(101) Oleschuk, R. D.; Shultz-Lockyear, L. L.; Ning, Y. B.; Harrison, D. J. "Trapping of bead-based reagents within microfluidic systems: On-chip solid-phase extraction and electrochromatography" *Anal Chem* **2000**, *72*, 585-590.

(102) Richter, T.; Shultz-Lockyear, L. L.; Oleschuk, R. D.; Bilitewski, U.; Harrison, D. J. "Bi-enzymatic and capillary electrophoretic analysis of non-fluorescent compounds in microfluidic devices - Determination of xanthine" *Sensor Actuat B-Chem* **2002**, *81*, 369-376.

(103) Ceriotti, L.; de Rooij, N. F.; Verpoorte, E. "An integrated fritless column for on-chip capillary electrochromatography with conventional stationary phases" *Anal Chem* **2002**, *74*, 639-647.

(104) Lettieri, G. L.; Dodge, A.; Boer, G.; de Rooij, N. F.; Verpoorte, E. "A novel microfluidic concept for bioanalysis using freely moving beads trapped in recirculating flows" *Lab Chip* **2003**, *3*, 34-39.

(105) Rohr, T.; Yu, C.; Davey, M. H.; Svec, F.; Frechet, J. M. J. "Porous polymer monoliths: Simple and efficient mixers prepared by direct polymerization in the channels of microfluidic chips" *Electrophoresis* **2001**, *22*, 3959-3967.

(106) Yu, C.; Xu, M. C.; Svec, F.; Frechet, J. M. J. "Preparation of monolithic polymers with controlled porous properties for microfluidic chip applications using photoinitiated free-radical polymerization" *J Polym Sci Pol Chem* **2002**, *40*, 755-769.

(107) Josic, D.; Buchacher, A.; Jungbauer, A. "Monoliths as stationary phases for separation of proteins and polynucleotides and enzymatic conversion" *J Chromatogr B* **2001**, *752*, 191-205.

(108) Ericson, C.; Holm, J.; Ericson, T.; Hjerten, S. "Electroosmosis- and pressure-driven chromatography in chips using continuous beds" *Anal Chem* **2000**, *72*, 81-87.

(109) Ngola, S. M.; Fintschenko, Y.; Choi, W. Y.; Shepodd, T. J. "Conduct-as-cast polymer monoliths as separation media for capillary electrochromatography" *Anal Chem* **2001**, *73*, 849-856.

(110) Yu, C.; Davey, M. H.; Svec, F.; Frechet, J. M. J. "Monolithic porous polymer for on-chip solid-phase extraction and preconcentration prepared by photoinitiated in situ polymerization within a microfluidic device" *Anal Chem* **2001**, *73*, 5088-5096.

(111) Hoffman, A. S.; Stayton, P. S.; Bulmus, V.; Chen, G. H.; Chen, J. P.; Cheung, C.; Chilkoti, A.; Ding, Z. L.; Dong, L. C.; Fong, R.; Lackey, C. A.; Long, C. J.; Miura, M.;

Morris, J. E.; Murthy, N.; Nabeshima, Y.; Park, T. G.; Press, O. W.; Shimoboji, T.; Shoemaker, S.; Yang, H. J.; Monji, N.; Nowinski, R. C.; Cole, C. A.; Priest, J. H.; Harris, J. M.; Nakamae, K.; Nishino, T.; Miyata, T. "Really smart bioconjugates of smart polymers and receptor proteins" *J Biomed Mater Res* **2000**, *52*, 577-586.

(112) Heskins, M.; Guillet, J. E. "Solution Properties of Poly(N-isopropylacrylamide)" *J. Macromol. Sci.-Chem.* **1968**, *A2*, 1441-1455.

(113) Schild, H. G. "Poly (N-Isopropylacrylamide) - Experiment, Theory and Application" *Prog Polym Sci* **1992**, *17*, 163-249.

(114) Feil, H.; Bae, Y. H.; Jan, F. J.; Kim, S. W. "Effect of Comonomer Hydrophilicity and Ionization on the Lower Critical Solution Temperature of N-Isopropylacrylamide Copolymers" *Macromolecules* **1993**, *26*, 2496-2500.

(115) Hahn, M.; Gornitz, E.; Dautzenberg, H. "Synthesis and properties of ionically modified polymers with LCST behavior" *Macromolecules* **1998**, *31*, 5616-5623.

(116) de Azevedo, R. G.; Rebelo, L. P. N.; Ramos, A. M.; Szydlowski, J.; de Sousa, H. C.; Klein, J. "Phase behavior of (polyacrylamides plus water) solutions: concentration, pressure and isotope effects" *Fluid Phase Equilibr* **2001**, *185*, 189-198.

(117) Ding, Z. L.; Chen, G. H.; Hoffman, A. S. "Synthesis and purification of thermally sensitive oligomer-enzyme conjugates of poly(N-isopropylacrylamide)-trypsin" *Bioconjugate Chem* **1996**, *7*, 121-125.

(118) Chen, J. P.; Yang, H. J.; Hoffman, A. S. "Polymer Protein Conjugates .1. Effect of Protein Conjugation on the Cloud Point of Poly(N-Isopropylacrylamide)" *Biomaterials* **1990**, *11*, 625-630.

(119) Bae, Y. H.; Okano, T.; Kim, S. W. "Temperature dependance of swelling of crosslinked poly(N,N'-alkyl substituted acrylamides) in water" *J. Polym. Sci.* **1990**, *28*, 923-936.

(120) Luan, C.-H.; Urry, D. W. "Solvent deuteration enhancement of hydrophobicity: DSC study of the inverse temperature transition of elastin-based polypeptides" *J. Phys. Chem.* **1991**, *95*, 7896-7900.

(121) Wu, C.; Zhou, S. Q. "Laser-Light Scattering Study of the Phase-Transition of Poly(N-Isopropylacrylamide) in Water .1. Single-Chain" *Macromolecules* **1995**, *28*, 8381-8387.

(122) Winnik, F. M. "Quenching of fluorescence from pyrene-labeled poly(N-isopropylacrylamide) solutions heated above their lower critical solution temperature" *Macromolecules* **1990**, *23*, 1647-1649.

(123) Winnik, F. M. "Fluorescence studies of aqueous solutions of poly(N-isopropylacrylamide) below and above their LCST" *Macromolecules* **1990**, *23*, 233-242.

(124) Otake, K.; Inomata, H.; Konno, M.; Saito, S. "Thermal analysis of the volume phase transition with N-isopropylacrylamide gels" *Macromolecules* **1990**, *23*, 283-289.

(125) Garret-Flaudy, F.; Freitag, R. "Unusual thermoprecipitation behavior of poly(N,N-diethylacrylamide) from aqueous solution in the presence of anionic surfactants" *Langmuir* **2001**, *17*, 4711-4716.

(126) Zareie, H. M.; Bulmus, E. V.; Gunning, A. P.; Hoffman, A. S.; Piskin, E.; Morris, V. J. "Investigation of a stimuli-responsive copolymer by atomic force microscopy" *Polymer* **2000**, *41*, 6723-6727.

(127) Hsu, S. H.; Yu, T. L. "Dynamic viscoelasticity study of the phase transition of poly(N-isopropylacrylamide)" *Macromol Rapid Comm* **2000**, *21*, 476-480.

(128) Tiktopulo, E. I.; Bychkova, V. E.; Ricka, J.; Ptitsyn, O. B. "Cooperativity of the Coil-Globule Transition in a Homopolymer - Microcalorimetric Study of Poly(N-Isopropylacrylamide)" *Macromolecules* **1994**, *27*, 2879-2882.

(129) Dawson, K. A.; Gorelov, A. V.; Timoshenko, E. G.; Kuznetsov, Y. A.; DuChesne, A. "Formation of mesoglobules from phase separation in dilute polymer solutions: a study in experiment, theory, and applications" *Physica A* **1997**, *244*, 68-80.

(130) Gorelov, A. V.; DuChesne, A.; Dawson, K. A. "Phase separation in dilute solutions of poly (N-isopropylacrylamide)" *Physica A* **1997**, *240*, 443-452.

(131) Timoshenko, E. G.; Basovsky, R.; Kuznetsov, Y. A. "Micellesation vs aggregation in dilute solutions of amphiphilic heteropolymers" *Colloid Surface A* **2001**, *190*, 129-134.

(132) Galaev, I. Y.; Mattiasson, B. "'Smart' polymers and what they could do in biotechnology and medicine" *Trends Biotechnol* **1999**, *17*, 335-340.

(133) Fujii, M.; Taniguchi, M. "Application of Reversibly Soluble Polymers in Bioprocessing" *Trends Biotechnol* **1991**, *9*, 191-196.

(134) Niederauer, M. Q.; Glatz, C. E. In *Bioseparation*; Tsao, G. T., Belfort, G., Eds.; Springer-Verlag: Berlin ; Hong Kong, 1992, pp 159-188.

(135) Galaev, I. Y.; Mattiasson, B. "New methods for affinity purification of proteins. Affinity precipitation: a review" *Biochemistry-Moscow+* **1997**, *62*, 571-577.

(136) Chen, J. P.; Hoffman, A. S. "Polymer Protein Conjugates .2. Affinity Precipitation Separation of Human Immuno-Gamma-Globulin by a Poly(N-Isopropylacrylamide)-Protein-a Conjugate" *Biomaterials* **1990**, *11*, 631-634.

(137) Monji, N.; Hoffman, A. S. "A Novel Immunoassay System and Bioseparation Process Based on Thermal Phase Separating Polymers" *Appl Biochem Biotech* **1987**, *14*, 107-120.

(138) Takei, Y. G.; Matsukata, M.; Aoki, T.; Sanui, K.; Ogata, N.; Kikuchi, A.; Sakurai, Y.; Okano, T. "Temperature-responsive bioconjugates. 3. Antibody-poly (N-isopropylacrylamide) conjugates for temperature-modulated precipitations and affinity bioseparations" *Bioconjug Chem* **1994**, *5*, 577-582.

(139) Anastase-Ravion, S.; Ding, Z.; Pelle, A.; Hoffman, A. S.; Letourneur, D. "New antibody purification procedure using a thermally responsive poly(N-isopropylacrylamide)-dextran derivative conjugate" *J Chromatogr B* **2001**, *761*, 247-254.

(140) Umeno, D.; Kawasaki, M.; Maeda, M. "Water-soluble conjugate of double-stranded DNA and poly(N-isopropylacrylamide) for one-pot affinity precipitation separation of DNA-binding proteins" *Bioconjugate Chem* **1998**, *9*, 719-724.

(141) Fong, R. B.; Ding, Z. L.; Long, C. J.; Hoffman, A. S.; Stayton, P. S. "Thermoprecipitation of streptavidin via oligonucleotide-mediated self-assembly with poly (N-isopropylacrylamide)" *Bioconjugate Chem* **1999**, *10*, 720-725.

(142) Vaidya, A. A.; Lele, B. S.; Deshmukh, M. V.; Kulkarni, M. G. "Design and evaluation of new ligands for lysozyme recovery by affinity thermoprecipitation" *Chem Eng Sci* **2001**, *56*, 5681-5692.

(143) Vaidya, A. A.; Lele, B. S.; Kulkarni, M. G.; Mashelkar, R. A. "Thermoprecipitation of lysozyme from egg white using copolymers of N-isopropylacrylamide and acidic monomers" *J Biotechnol* **2001**, *87*, 95-107.

(144) Fong, R. B.; Ding, Z. L.; Hoffman, A. S.; Stayton, P. S. "Affinity separation using an Fv antibody fragment-"smart" polymer conjugate" *Biotechnol Bioeng* **2002**, *79*, 271-276.

(145) Garret-Flaudy, F.; Freitag, R. "Use of the avidin (imino)biotin system as a general approach to affinity precipitation" *Biotechnol Bioeng* **2001**, *71*, 223-234.

(146) Eggert, M.; Baltes, T.; Garret-Flaudy, F.; Freitag, R. "Affinity precipitation - an alternative to fluidized bed adsorption?" *J Chromatogr A* **1998**, *827*, 269-280.

(147) Wahlund, P. O.; Galaev, I. Y.; Kazakov, S. A.; Lozinsky, V. I.; Mattiasson, B. ""Protein-like" copolymers: Effect of polymer architecture on the performance in bioseparation process" *Macromol Biosci* **2002**, *2*, 33-42.

(148) Yang, H. H.; Zhu, Q. Z.; Chen, S.; Li, D. H.; Chen, X. L.; Ding, M. T.; Xu, J. G. "Fluorescence immunoassay system based on the use of a pH-sensitive phase-separating polymer" *Anal. Biochem.* **2001**, *296*, 167-173.

(149) Chern, C. S.; Lee, C. K.; Chen, C. Y. "Biotin-modified submicron latex particles for affinity precipitation of avidin" *Colloid Surface B* **1996**, *7*, 55-64.

(150) Buchholz, B. A.; Doherty, E. A. S.; Albarghouthi, M. N.; Bogdan, F. M.; Zahn, J. M.; Barron, A. E. "Microchannel DNA sequencing matrices with a thermally controlled "viscosity switch"" *Anal Chem* **2001**, *73*, 157-164.

(151) Kan, C. W.; Barron, A. E. "A DNA sieving matrix with thermally tunable mesh size" *Electrophoresis* **2003**, *24*, 55-62.

(152) Kobayashi, J.; Kikuchi, A.; Sakai, K.; Okano, T. "Aqueous chromatography utilizing pH-/temperature responsive polymer stationary phases to separate ionic bioactive compounds" *Anal Chem* **2001**, *73*, 2027-2033.

(153) Kobayashi, J.; Kikuchi, A.; Sakai, K.; Okano, T. "Cross-linked thermoresponsive anionic polymer-grafted surfaces to separate bioactive basic peptides" *Anal Chem* **2003**, *75*, 3244-3249.

(154) Kanazawa, H.; Kashiwase, Y.; Yamamoto, K.; Matsushima, Y.; Kikuchi, A.; Sakurai, Y.; Okano, T. "Temperature-responsive liquid chromatography .2. Effects of hydrophobic groups in N-isopropylacrylamide copolymer-modified silica" *Anal Chem* **1997**, *69*, 823-830.

(155) Kanazawa, H.; Yamamoto, K.; Matsushima, Y.; Takai, N.; Kikuchi, A.; Sakurai, Y.; Okano, T. "Temperature-responsive chromatography using poly(N-isopropylacrylamide)-modified silica" *Anal Chem* **1996**, *68*, 100-105.

(156) Yakushiji, T.; Sakai, K.; Kikuchi, A.; Aoyagi, T.; Sakurai, Y.; Okano, T. "Effects of cross-linked structure on temperature-responsive hydrophobic interaction of poly(N-isopropylacrylamide) hydrogel-modified surfaces with steroids" *Anal Chem* **1999**, *71*, 1125-1130.

(157) Teal, H. E.; Hu, Z. B.; Root, D. D. "Native purification of biomolecules with temperature-mediated hydrophobic modulation liquid chromatography" *Anal. Biochem.* **2000**, *283*, 159-165.

(158) Gewehr, M.; Nakamura, K.; Ise, N.; Kitano, H. "Gel-Permeation Chromatography Using Porous-Glass Beads Modified with Temperature-Responsive Polymers" *Makromol Chem* **1992**, *193*, 249-256.

(159) Hosoya, K.; Sawada, E.; Kimata, K.; Araki, T.; Tanaka, N.; Frechet, J. M. J. "In-Situ Surface-Selective Modification of Uniform Size Macroporous Polymer Particles with Temperature-Responsive Poly-N-Isopropylacrylamide" *Macromolecules* **1994**, *27*, 3973-3976.

(160) Lakhiari, H.; Okano, T.; Nurdin, N.; Luthi, C.; Descouts, P.; Muller, D.; Jozefonvicz, J. "Temperature-responsive size-exclusion chromatography using poly(N-isopropylacrylamide) grafted silica" *Bba-Gen Subjects* **1998**, *1379*, 303-313.

(161) Adrados, B. P.; Galaev, I. Y.; Nilsson, K.; Mattiasson, B. "Size exclusion behavior of hydroxypropylcellulose beads with temperature-dependent porosity" *J Chromatogr A* **2001**, *930*, 73-78.

(162) Galaev, I. Y.; Warrol, C.; Mattiasson, B. "Temperature-Induced Displacement of Proteins from Dye-Affinity Columns Using an Immobilized Polymeric Displacer" *J Chromatogr A* **1994**, *684*, 37-43.

(163) Yoshizako, K.; Akiyama, Y.; Yamanaka, H.; Shinohara, Y.; Hasegawa, Y.; Carredano, E.; Kikuchi, A.; Okano, T. "Regulation of protein binding toward a ligand on chromatographic matrixes by masking and forced-releasing effects using thermoresponsive polymer" *Anal Chem* **2002**, *74*, 4160-4166.

(164) Yamanaka, H.; Yoshizako, K.; Akiyama, Y.; Sota, H.; Hasegawa, Y.; Shinohara, Y.; Kikuchi, A.; Okano, T. "Affinity chromatography with collapsibly tethered ligands" *Anal Chem* **2003**.

(165) Hoffman, A. S.; Afrassiabi, A.; Dong, L. C. "Thermally Reversible Hydrogels: II. Delivery and Selective Removal of Substances From Aqueous Solutions" *J. Controlled Release* **1986**, *4*, 213-222.

(166) Dong, L. C.; Hoffman, A. S. "A novel approach for preparation of pH-sensitive hydrogels for enteric drug delivery" *J. Controlled Release* **1991**, *15*, 141-152.

(167) Wu, X. S.; Hoffman, A. S.; Yager, P. "Synthesis and characterization of thermally reversible macroporous poly(N-isopropylacrylamide) hydrogels" *J Polym Sci Pol Chem* **1992**, *30*, 2121-2129.

(168) Beebe, D. J.; Moore, J. S.; Bauer, J. M.; Yu, Q.; Liu, R. H.; Devadoss, C.; Jo, B. H. "Functional hydrogel structures for autonomous flow control inside microfluidic channels" *Nature* **2000**, *404*, 588+.

(169) Liu, R. H.; Yu, Q.; Beebe, D. J. "Fabrication and characterization of hydrogel-based microvalves" *J. MEMS* **2002**, *11*, 45-53.

(170) Eddington, D. T.; Liu, R. H.; Moore, J. S.; Beebe, D. J. "An organic self-regulating microfluidic system" *Lab Chip* **2001**, *1*, 96-99.

(171) Takei, Y. G.; Aoki, T.; Sanui, K.; Ogata, N.; Sakurai, Y.; Okano, T. "Dynamic Contact-Angle Measurement of Temperature-Responsive Surface-Properties for Poly(N-Isopropylacrylamide) Grafted Surfaces" *Macromolecules* **1994**, *27*, 6163-6166.

(172) Okano, T.; Yamada, N.; Okuhara, M.; Sakai, H.; Sakurai, Y. "Mechanism of Cell Detachment from Temperature-Modulated, Hydrophilic-Hydrophobic Polymer Surfaces" *Biomaterials* **1995**, *16*, 297-303.

(173) Ebara, M.; Yamoto, M.; Hirose, M.; Aoyagi, T.; Kikuchi, A.; Sakai, K.; Okano, T. "Copolymerization of 2-carboxyisopropylacrylamide with N-isopropylacrylamide accelerates cell detachment from grafted surfaces by reducing temperature" *Biomacromolecules* **2003**, *4*, 344-349.

(174) Matsukata, M.; Aoki, T.; Sanui, K.; Ogata, N.; Kikuchi, A.; Sakurai, Y.; Okano, T. "Effect of molecular architecture of poly(N-isopropylacrylamide)-trypsin conjugates on their solution and enzymatic properties" *Bioconjugate Chem* **1996**, *7*, 96-101.

(175) Ding, Z. L.; Chen, G. H.; Hoffman, A. S. "Unusual properties of thermally sensitive oligomer-enzyme conjugates of poly(N-isopropylacrylamide)-trypsin" *J Biomed Mater Res* **1998**, *39*, 498-505.

(176) Ding, Z. L.; Chen, G. H.; Hoffman, A. S. "Activity and Thermally-Induced Precipitation of Poly(Nipaam)-Enzyme Conjugates" *Abstr Pap Am Chem S* **1994**, *207*, 165-Btec.

(177) Shimoboji, T.; Larenas, E.; Fowler, T.; Kulkarni, S.; Hoffman, A. S.; Stayton, P. S. "Photoresponsive polymer-enzyme switches" *P Natl Acad Sci USA* **2002**, *99*, 16592-16596.

(178) Ding, Z. L.; Long, C. J.; Hayashi, Y.; Bulmus, E. V.; Hoffman, A. S.; Stayton, P. S. "Temperature control of biotin binding and release with a streptavidin-poly(N-isopropylacrylamide) site-specific conjugate" *Bioconjugate Chem* **1999**, *10*, 395-400.

(179) Bulmus, V.; Ding, Z. L.; Long, C. J.; Stayton, P. S.; Hoffman, A. S. "Site-specific polymer-streptavidin bioconjugate for pH-controlled binding and triggered release of biotin" *Bioconjugate Chem* **2000**, *11*, 78-83.

(180) Shimoboji, T.; Ding, Z. L.; Stayton, P. S.; Hoffman, A. S. "Mechanistic investigation of smart polymer-protein conjugates" *Bioconjugate Chem* **2001**, *12*, 314-319.

(181) Ding, Z. L.; Fong, R. B.; Long, C. J.; Stayton, P. S.; Hoffman, A. S. "Size-dependent control of the binding of biotinylated proteins to streptavidin using a polymer shield" *Nature* **2001**, *411*, 59-62.

(182) Shimoboji, T.; Ding, Z. L.; Stayton, P. S.; Hoffman, A. S. "Photoswitching of ligand association with a photoresponsive polymer-protein conjugate" *Bioconjugate Chem* **2002**, *13*.

(183) Lackey, C. A.; Murthy, N.; Press, O. W.; Tirrell, D. A.; Hoffman, A. S.; Stayton, P. S. "Hemolytic activity of pH-responsive polymer-streptavidin bioconjugates" *Bioconjugate Chem* **1999**, *10*, 401-405.

(184) Cheung, C. Y.; Murthy, N.; Stayton, P. S.; Hoffman, A. S. "A pH-sensitive polymer that enhances cationic lipid-mediated gene transfer" *Bioconjugate Chem* **2001**, *12*, 906-910.

(185) Kyriakides, T. R.; Cheung, C. Y.; Murthy, N.; Bornstein, P.; Stayton, P. S.; Hoffman, A. S. "pH-sensitive polymers that enhance intracellular drug delivery in vivo" *J. Controlled Release* **2002**, *78*, 295-303.

(186) Murthy, N.; Campbell, J.; Fausto, N.; Hoffman, A. S.; Stayton, P. S. "Bioinspired pH-responsive polymers for the intracellular delivery of biomolecular drugs" *Bioconjugate Chem* **2003**, *14*, 412-419.

(187) Lackey, C. A.; Press, O. W.; Hoffman, A. S.; Stayton, P. S. "A biomimetic pH-responsive polymer directs endosomal release and intracellular delivery of an endocytosed antibody complex" *Bioconjugate Chem* **2002**, *13*, 996-1001.

(188) Sun, Y. M.; Yu, C. W.; Liang, H. C.; Chen, J. P. "Temperature-sensitive latex particles for immobilization of alpha-amylase" *J Disper Sci Technol* **1999**, *20*, 907-920.

(189) Chen, J. P.; Su, D. R. "Latex particles with thermo-flocculation and magnetic properties for immobilization of alpha-chymotrypsin" *Biotechnol Progr* **2001**, *17*, 369-375.

(190) Taniguchi, T.; Duracher, D.; Delair, T.; Elaïssari, A.; Pichot, C. "Adsorption/desorption behavior and covalent grafting of an antibody onto cationic amino-functionalized poly(styrene-N-isopropylacrylamide) core-shell latex particles" *Colloid Surface B* **2003**, *29*, 53-65.

(191) Yasui, M.; Shiroya, T.; Fujimoto, K.; Kawaguchi, H. "Activity of enzymes immobilized on microspheres with thermosensitive hairs" *Colloid Surface B* **1997**, *8*, 311-319.

(192) Elmas, B.; Onur, M. A.; Senel, S.; Tuncel, A. "Temperature controlled RNA isolation by N-isopropylacrylamide-vinylphenyl boronic acid copolymer latex" *Colloid Polym Sci* **2002**, *280*, 1137-1146.

(193) Chaliet, L.; Miller, F. W.; Tausig, F.; Wolf, F. J. *Antimicrob. Ag. Chemother.* **1963**, *3*, 28.

(194) Green, N. M. "Avidin" *Adv Protein Chem* **1975**, *29*, 85-133.

(195) Green, N. M. "Avidin and streptavidin" *Methods Enzymol* **1990**, *184*, 51-67.

(196) Diamandis, E. P.; Christopoulos, T. K. "The Biotin (Strept)Avidin System - Principles and Applications in Biotechnology" *Clin Chem* **1991**, *37*, 625-636.

(197) Wilchek, M.; Bayer, E. A. "Applications of avidin-biotin technology: literature survey" *Methods Enzymol* **1990**, *184*, 14-45.

(198) Chilkoti, A.; Stayton, P. S. "Molecular-Origins of the Slow Streptavidin-Biotin Dissociation Kinetics" *J Am Chem Soc* **1995**, *117*, 10622-10628.

(199) Piran, U.; Riordan, W. J. "Dissociation rate constant of the biotin-streptavidin complex" *J Immunol Methods* **1990**, *133*, 141-143.

(200) Weber, P. C.; Ohlendorf, D. H.; Wendoloski, J. J.; Salemme, F. R. "Structural Origins of High-Affinity Biotin Binding to Streptavidin" *Science* **1989**, *243*, 85-88.

(201) Hendrickson, W. A.; Pahler, A.; Smith, J. L.; Satow, Y.; Merritt, E. A.; Phizackerley, R. P. "Crystal-Structure of Core Streptavidin Determined from Multiwavelength Anomalous Diffraction of Synchrotron Radiation" *P Natl Acad Sci USA* **1989**, *86*, 2190-2194.

(202) Chilkoti, A.; Tan, P. H.; Stayton, P. S. "Site-Directed Mutagenesis Studies of the High-Affinity Streptavidin-Biotin Complex - Contributions of Tryptophan Residue-79, Residue-108, and Residue-120" *P Natl Acad Sci USA* **1995**, *92*, 1754-1758.

(203) Klumb, L. A.; Chu, V.; Stayton, P. S. "Energetic roles of hydrogen bonds at the ureido oxygen binding pocket in the streptavidin-biotin complex" *Biochemistry-Us* **1998**, *37*, 7657-7663.

(204) Hyre, D. E.; Le Trong, I.; Freitag, S.; Stenkamp, R. E.; Stayton, P. S. "Ser45 plays an important role in managing both the equilibrium and transition state energetics of the streptavidin-biotin system" *Protein Sci* **2000**, *9*, 878-885.

(205) Malmstadt, N.; Hyre, D. E.; Ding, Z.; Hoffman, A. S.; Stayton, P. S. "Affinity Thermoprecipitation and Recovery of Biotinylated Biomolecules via a Mutant Streptavidin-Smart Polymer Conjugate" *Bioconjug Chem* **2003**, *14*, 575-580.

(206) Ladisch, M. R. *Bioseparations engineering : principles, practice, and economics*; Wiley: New York, 2001.

(207) Dechow, F. J. *Separation and purification techniques in biotechnology*; Noyes Publications: Park Ridge, N.J., U.S.A., 1989.

(208) Belter, P. A.; Cussler, E. L.; Hu, W.-S. *Bioseparations : downstream processing for biotechnology*; Wiley: New York, 1988.

(209) Campbell, D. H.; Lenscher, E. L.; Lerman, L. S. *P Natl Acad Sci USA* **1951**, *37*, 575.

(210) Lerman, L. S. *Nature* **1953**, *172*, 635.

(211) Cuatrecasas, P.; Wilchek, M.; Anfinsen, C. B. *P Natl Acad Sci USA* **1968**, *61*, 636.

(212) Porath, J.; Axen, R.; Ernback, S. *Nature* **1967**, *215*, 1491.

(213) Luong, J. H. T.; Nguyen, A.-L. In *Bioseparation*; Tsao, G. T., Belfort, G., Eds.; Springer-Verlag: Berlin ; Hong Kong, 1992, pp 137-158.

(214) Wilchek, M.; Miron, T.; Kohn, J. In *Methods in Enzymology, v. 104*; Jakoby, W. B., Ed.; Academic Press: New York, 1983, p 3.

(215) Holzman, T. F.; Baldwin, T. O. "Isolation of Bacterial Luciferases by Affinity-Chromatography on 2,2-Diphenylpropylamine-Sepharose - Phosphate-Mediated Binding to an Immobilized Substrate-Analog" *Biochemistry-Us* **1982**, *21*, 6194-6201.

(216) Goss, T. A.; Bard, M.; Jarrett, H. W. "High-Performance Affinity-Chromatography of DNA" *J Chromatogr* **1990**, *508*, 279-287.

(217) Flaschel, E.; Friehs, K. "Improvement of Downstream Processing of Recombinant Proteins by Means of Genetic-Engineering Methods" *Biotechnol Adv* **1993**, *11*, 31-77.

(218) Lopatin, S. A.; Varlamov, V. P. "New Trends in Immobilized Metal Affinity-Chromatography of Proteins - (Review)" *Appl Biochem Micro+* **1995**, *31*, 221-227.

(219) Smith, P. A.; Tripp, B. C.; DiBlasio-Smith, E. A.; Lu, Z. J.; LaVallie, E. R.; McCoy, J. M. "A plasmid expression system for quantitative in vivo biotinylation of thioredoxin fusion proteins in Escherichia coli" *Nucleic Acids Res* **1998**, *26*, 1414-1420.

(220) Taki, M.; Sawata, S. Y.; Taira, K. "Specific N-terminal biotinylation of a protein in vitro by a chemically modified tRNA(fmet) can support the native activity of the translated protein" *J Biosci Bioeng* **2001**, *92*, 149-153.

(221) Diamond, A. D.; Hsu, J. T. "Aqueous two-phase systems for biomolecule separation" *Adv Biochem Eng Biotechnol* **1992**, *47*, 89-135.

(222) Bandmann, N.; Collet, E.; Leijen, J.; Uhlen, M.; Veide, A.; Nygren, P. A. "Genetic engineering of the Fusarium solani pisi lipase cutinase for enhanced partitioning in PEG-phosphate aqueous two-phase systems" *J Biotechnol* **2000**, *79*, 161-172.

(223) Kwon, Y. J.; Hatti-Kaul, R. "Protein separation using metal ion-bound particles in aqueous two-phase system" *Biotech Techniques* **1999**, *13*, 145-148.

(224) Giovannini, R.; Freitag, R. "Continuous isolation of plasmid DNA by annular chromatography" *Biotechnol Bioeng* **2002**, *77*, 445-454.

(225) Giovannini, R.; Freitag, R. "Isolation of a recombinant antibody from cell culture supernatant: continuous annular versus batch and expanded-bed chromatography" *Biotechnol Bioeng* **2001**, *73*, 522-529.

(226) Kuo, M. H.; Allis, C. D. "In vivo cross-linking and immunoprecipitation for studying dynamic protein: DNA associations in chromatin environment" *Methods* **1999**, *19*, 425-433.

(227) Heney, G.; Orr, G. A. "The purification of avidin and its derivatives on 2-iminobiotin-6-aminohexyl-Sepharose 4B" *Anal Biochem* **1981**, *114*, 92-96.

(228) Green, N. M. "Spectrophotometric Determination of Avidin and Biotin" *Methods Enzymol.* **1970**, 418.

(229) Perez-Luna, V. H.; O'Brien, M. J.; Opperman, K. A.; Hampton, P. D.; Lopez, G. P.; Klumb, L. A.; Stayton, P. S. "Molecular recognition between genetically engineered streptavidin and surface-bound biotin" *J Am Chem Soc* **1999**, *121*, 6469-6478.

(230) Wilbur, D. S.; Chyan, M. K.; Pathare, P. M.; Hamlin, D. K.; Frownfelter, M. B.; Kegley, B. B. "Biotin reagents for antibody pretargeting. 4. Selection of biotin conjugates for in vivo application based on their dissociation rate from avidin and streptavidin" *Bioconjugate Chem* **2000**, *11*, 569-583.

(231) Malmstadt, N.; Yager, P.; Hoffman, A. S.; Stayton, P. S. "A Smart Microfluidic Affinity Chromatography Matrix Composed of Poly(N-isopropylacrylamide)-Coated Beads" *Anal Chem* **2003**, *75*, 2943-2949.

(232) Foust, A. S. *Principles of unit operations*; 2d ed.; Wiley: New York, 1980.

(233) Perry, R. H.; Maloney, J. O.; Green, D. W.; Knovel (Firm) *Perry's chemical engineers' handbook*; 7th / ed.; McGraw-Hill: New York, 1997.

(234) Richardson, J. F.; Zaki, W. N. *Trans. Inst. Chem. Eng.* **1954**, *32*, 38.

(235) Habeeb, A. F. S. A. "Determination of free amino groups in protein by trinitrobenzene sulfonic acid" *Anal. Biochem.* **1966**, *14*, 328.

(236) Taylor, G. "Dispersion of soluble matter in solvent flowing slowly through a tube" *Proc. Royal Soc., A* **1953**, *219*, 186-203.

(237) Diamandis, E. P.; Christopoulos, T. K., Eds. *Immunoassay;* Academic Press: San Diego, CA, 1996.

(238) Gosling, J. P.; Lawrence, V. B., Eds. *Immunoassay: Laboratory analysis and clinical application;* Butterworth-Heinemann: Newton, MA, 1994.

(239) Jortani, S. A.; Valdes, R. "Digoxin and its related endogenous factors" *Crit Rev Cl Lab Sci* **1997**, *34*, 225-274.

(240) Hafner, F. T.; Kautz, R. A.; Iverson, B. L.; Tim, R. C.; Karger, B. L. "Noncompetitive immunoassay of small analytes at the femtomolar level by affinity probe capillary electrophoresis: Direct analysis of digoxin using a uniform-labeled scFv immunoreagent" *Anal Chem* **2000**, *72*, 5779-5786.

(241) Szurdoki, F.; Michael, K. L.; Walt, D. R. "A duplexed microsphere-based fluorescent immunoassay" *Anal. Biochem.* **2001**, *291*, 219-228.

(242) Shim, Y. N.; Paeng, I. R. "Development of bioluminescence immunoassay using photoprotein, aequorin and site-directed immobilization" *B Kor Chem Soc* **2003**, *24*, 70-74.

Bibliography

Adrados, B. P.; Galaev, I. Y.; Nilsson, K.; Mattiasson, B. "Size exclusion behavior of hydroxypropylcellulose beads with temperature-dependent porosity" *J Chromatogr A* **2001**, *930*, 73-78.

Anastase-Ravion, S.; Ding, Z.; Pelle, A.; Hoffman, A. S.; Letourneur, D. "New antibody purification procedure using a thermally responsive poly(N-isopropylacrylamide)-dextran derivative conjugate" *J Chromatogr B* **2001**, *761*, 247-254.

Andersson, H.; van der Wijngaart, W.; Enoksson, P.; Stemme, G. "Micromachined flow-through filter-chamber for chemical reactions on beads" *Sensor Actuat B-Chem* **2000**, *67*, 203-208.

Auroux, P. A.; Iossifidis, D.; Reyes, D. R.; Manz, A. "Micro total analysis systems. 2. Analytical standard operations and applications" *Anal Chem* **2002**, *74*, 2637-2652.

Bae, Y. H.; Okano, T.; Kim, S. W. "Temperature dependance of swelling of crosslinked poly(N,N'-alkyl substituted acrylamides) in water" *J. Polym. Sci.* **1990**, *28*, 923-936.

Bandmann, N.; Collet, E.; Leijen, J.; Uhlen, M.; Veide, A.; Nygren, P. A. "Genetic engineering of the Fusarium solani pisi lipase cutinase for enhanced partitioning in PEG-phosphate aqueous two-phase systems" *J Biotechnol* **2000**, *79*, 161-172.

Barker, S. L. R.; Ross, D.; Tarlov, M. J.; Gaitan, M.; Locascio, L. E. "Control of flow direction in microfluidic devices with polyelectrolyte multilayers" *Anal Chem* **2000**, *72*, 5925-5929.

Barker, S. L. R.; Tarlov, M. J.; Canavan, H.; Hickman, J. J.; Locascio, L. E. "Plastic microfluidic devices modified with polyelectrolyte multilayers" *Anal Chem* **2000**, *72*, 4899-4903.

Beebe, D. J.; Mensing, G. A.; Walker, G. M. "Physics and applications of microfluidics in biology" *Annu Rev Biomed Eng* **2002**, *4*, 261-286.

Beebe, D. J.; Moore, J. S.; Bauer, J. M.; Yu, Q.; Liu, R. H.; Devadoss, C.; Jo, B. H. "Functional hydrogel structures for autonomous flow control inside microfluidic channels" *Nature* **2000**, *404*, 588+.

Beebe, D. J.; Moore, J. S.; Yu, Q.; Liu, R. H.; Kraft, M. L.; Jo, B. H.; Devadoss, C. "Microfluidic tectonics: A comprehensive construction platform for microfluidic systems" *P Natl Acad Sci USA* **2000**, *97*, 13488-13493.

Belter, P. A.; Cussler, E. L.; Hu, W.-S. *Bioseparations : downstream processing for biotechnology*; Wiley: New York, 1988.

Berg, J. M.; Anderson, R.; Anaya, M.; Lahlouh, B.; Holtz, M.; Dallas, T. "A two-stage discrete peristaltic micropump" *Sensor Actuat a-Phys* **2003**, *104*, 6-10.

Bergkvist, J.; Ekstrom, S.; Wallman, L.; Lofgren, M.; Marko-Varga, G.; Nilsson, J.; Laurell, T. "Improved chip design for integrated solid-phase microextraction in on-line proteomic sample preparation" *Proteomics* **2002**, *2*, 422-429.

Blom, M. T.; Chmela, E.; Gardeniers, J. G. E.; Tijssen, R.; Elwenspoek, M.; van den Berg, A. "Design and fabrication of a hydrodynamic chromatography chip" *Sensor Actuat B-Chem* **2002**, *82*, 111-116.

Brahmasandra, S. N.; Ugaz, V. M.; Burke, D. T.; Mastrangelo, C. H.; Burns, M. A. "Electrophoresis in microfabricated devices using photopolymerized polyacrylamide gels and electrode-defined sample injection" *Electrophoresis* **2001**, *22*, 300-311.

Bruin, G. J. M. "Recent developments in electrokinetically driven analysis on microfabricated devices" *Electrophoresis* **2000**, *21*, 3931-3951.

Buchholz, B. A.; Doherty, E. A. S.; Albarghouthi, M. N.; Bogdan, F. M.; Zahn, J. M.; Barron, A. E. "Microchannel DNA sequencing matrices with a thermally controlled "viscosity switch"" *Anal Chem* **2001**, *73*, 157-164.

Bulmus, V.; Ding, Z. L.; Long, C. J.; Stayton, P. S.; Hoffman, A. S. "Site-specific polymer-streptavidin bioconjugate for pH-controlled binding and triggered release of biotin" *Bioconjugate Chem* **2000**, *11*, 78-83.

Buranda, T.; Huang, J.; Perez-Luna, V. H.; Schreyer, B.; Sklar, L. A.; Lopez, G. P. "Biomolecular recognition on well-characterized beads packed in microfluidic channels" *Anal Chem* **2002**, *74*, 1149-1156.

Cabrera, C. R.; Finlayson, B.; Yager, P. "Formation of natural pH gradients in a microfluidic device under flow conditions: Model and experimental validation" *Anal Chem* **2001**, *73*, 658-666.

Cabrera, C. R.; Yager, P. "Continuous concentration of bacteria in a microfluidic flow cell using electrokinetic techniques" *Electrophoresis* **2001**, *22*, 355-362.

Campbell, D. H.; Lenscher, E. L.; Lerman, L. S. *P Natl Acad Sci USA* **1951**, *37*, 575.

Ceriotti, L.; de Rooij, N. F.; Verpoorte, E. "An integrated fritless column for on-chip capillary electrochromatography with conventional stationary phases" *Anal Chem* **2002**, *74*, 639-647.

Chaliet, L.; Miller, F. W.; Tausig, F.; Wolf, F. J. *Antimicrob. Ag. Chemother.* **1963**, *3*, 28.

Chen, J. P.; Hoffman, A. S. "Polymer Protein Conjugates .2. Affinity Precipitation Separation of Human Immuno-Gamma-Globulin by a Poly(N-Isopropylacrylamide)-Protein-a Conjugate" *Biomaterials* **1990**, *11*, 631-634.

Chen, J. P.; Su, D. R. "Latex particles with thermo-flocculation and magnetic properties for immobilization of alpha-chymotrypsin" *Biotechnol Progr* **2001**, *17*, 369-375.

Chen, J. P.; Yang, H. J.; Hoffman, A. S. "Polymer Protein Conjugates .1. Effect of Protein Conjugation on the Cloud Point of Poly(N-Isopropylacrylamide)" *Biomaterials* **1990**, *11*, 625-630.

Chen, L. X.; Ma, J. P.; Tan, F.; Guan, Y. F. "Generating high-pressure sub-microliter flow rate in packed microchannel by electroosmotic force: potential applications in microfluidic systems" *Sensor Actuat B-Chem* **2003**, *88*, 260-265.

Chern, C. S.; Lee, C. K.; Chen, C. Y. "Biotin-modified submicron latex particles for affinity precipitation of avidin" *Colloid Surface B* **1996**, *7*, 55-64.

Chern, C. S.; Lee, C. K.; Chen, C. Y.; Yeh, M. J. "Characterization of pH-sensitive polymeric supports for selective precipitation of proteins" *Colloid Surface B* **1996**, *6*, 37-49.

Cheung, C. Y.; Murthy, N.; Stayton, P. S.; Hoffman, A. S. "A pH-sensitive polymer that enhances cationic lipid-mediated gene transfer" *Bioconjugate Chem* **2001**, *12*, 906-910.

Chilkoti, A.; Stayton, P. S. "Molecular-Origins of the Slow Streptavidin-Biotin Dissociation Kinetics" *J Am Chem Soc* **1995**, *117*, 10622-10628.

Chilkoti, A.; Tan, P. H.; Stayton, P. S. "Site-Directed Mutagenesis Studies of the High-Affinity Streptavidin-Biotin Complex - Contributions of Tryptophan Residue-79, Residue-108, and Residue-120" *P Natl Acad Sci USA* **1995**, *92*, 1754-1758.

Chovan, T.; Guttman, A. "Microfabricated devices in biotechnology and biochemical processing" *Trends Biotechnol* **2002**, *20*, 116-122.

Colyer, C. L.; Mangru, S. D.; Harrison, D. J. "Microchip-based capillary electrophoresis of human serum proteins" *J Chromatogr A* **1997**, *781*, 271-276.

Cuatrecasas, P.; Wilchek, M.; Anfinsen, C. B. *P Natl Acad Sci USA* **1968**, *61*, 636.

Cutler, P. "Protein arrays: The current state-of-the-art" *Proteomics* **2003**, *3*, 3-18.

Dawson, K. A.; Gorelov, A. V.; Timoshenko, E. G.; Kuznetsov, Y. A.; DuChesne, A. "Formation of mesoglobules from phase separation in dilute polymer solutions: a study in experiment, theory, and applications" *Physica A* **1997**, *244*, 68-80.

de Azevedo, R. G.; Rebelo, L. P. N.; Ramos, A. M.; Szydlowski, J.; de Sousa, H. C.; Klein, J. "Phase behavior of (polyacrylamides plus water) solutions: concentration, pressure and isotope effects" *Fluid Phase Equilibr* **2001**, *185*, 189-198.

Dechow, F. J. *Separation and purification techniques in biotechnology*; Noyes Publications: Park Ridge, N.J., U.S.A., 1989.

Deng, T.; Prentiss, M.; Whitesides, G. M. "Fabrication of magnetic microfiltration systems using soft lithography" *Appl Phys Lett* **2002**, *80*, 461-463.

Deng, Y. L.; Xiao, H. N.; Pelton, R. "Temperature-sensitive flocculants based on poly(N-isopropylacrylamide-co-diallyldimethylammonium chloride)" *J Colloid Interf Sci* **1996**, *179*, 188-193.

Deng, Y. Z.; Henion, J.; Li, J. J.; Thibault, P.; Wang, C.; Harrison, D. J. "Chip-based capillary electrophoresis/mass spectrometry determination of carnitines in human urine" *Anal Chem* **2001**, *73*, 639-646.

Desmet, G.; Vervoort, N.; Clicq, D.; Baron, G. V. "Experimental demonstration of the possibility to perform shear-driven chromatographic separations in micro-channels" *J Chromatogr A* **2001**, *924*, 111-122.

Diamandis, E. P.; Christopoulos, T. K. "The Biotin (Strept)Avidin System - Principles and Applications in Biotechnology" *Clin Chem* **1991**, *37*, 625-636.

Diamandis, E. P.; Christopoulos, T. K., Eds. *Immunoassay*; Academic Press: San Diego, CA, 1996.

Diamond, A. D.; Hsu, J. T. "Aqueous two-phase systems for biomolecule separation" *Adv Biochem Eng Biotechnol* **1992**, *47*, 89-135.

Ding, Z. L.; Chen, G. H.; Hoffman, A. S. "Activity and Thermally-Induced Precipitation of Poly(Nipaam)-Enzyme Conjugates" *Abstr Pap Am Chem S* **1994**, *207*, 165-Btec.

Ding, Z. L.; Chen, G. H.; Hoffman, A. S. "Synthesis and purification of thermally sensitive oligomer-enzyme conjugates of poly(N-isopropylacrylamide)-trypsin" *Bioconjugate Chem* **1996**, *7*, 121-125.

Ding, Z. L.; Chen, G. H.; Hoffman, A. S. "Unusual properties of thermally sensitive oligomer-enzyme conjugates of poly(N-isopropylacrylamide)-trypsin" *J Biomed Mater Res* **1998**, *39*, 498-505.

Ding, Z. L.; Fong, R. B.; Long, C. J.; Stayton, P. S.; Hoffman, A. S. "Size-dependent control of the binding of biotinylated proteins to streptavidin using a polymer shield" *Nature* **2001**, *411*, 59-62.

Ding, Z. L.; Long, C. J.; Hayashi, Y.; Bulmus, E. V.; Hoffman, A. S.; Stayton, P. S. "Temperature control of biotin binding and release with a streptavidin-poly(N-isopropylacrylamide) site-specific conjugate" *Bioconjugate Chem* **1999**, *10*, 395-400.

Dodge, A.; Fluri, K.; Verpoorte, E.; de Rooij, N. F. "Electrokinetically driven microfluidic chips with surface-modified chambers for heterogenous immunoassays" *Anal Chem* **2001**, *73*, 3400-3409.

Dong, L. C.; Hoffman, A. S. "A novel approach for preparation of pH-sensitive hydrogels for enteric drug delivery" *J. Controlled Release* **1991**, *15*, 141-152.

Duffy, D. C.; Gillis, H. L.; Lin, J.; Sheppard, N. F.; Kellogg, G. J. "Microfabricated centrifugal microfluidic systems: Characterization and multiple enzymatic assays" *Anal Chem* **1999**, *71*, 4669-4678.

Ebara, M.; Yamoto, M.; Hirose, M.; Aoyagi, T.; Kikuchi, A.; Sakai, K.; Okano, T. "Copolymerization of 2-carboxyisopropylacrylamide with N-isopropylacrylamide accelerates cell detachment from grafted surfaces by reducing temperature" *Biomacromolecules* **2003**, *4*, 344-349.

Eddington, D. T.; Liu, R. H.; Moore, J. S.; Beebe, D. J. "An organic self-regulating microfluidic system" *Lab Chip* **2001**, *1*, 96-99.

Eggert, M.; Baltes, T.; Garret-Flaudy, F.; Freitag, R. "Affinity precipitation - an alternative to fluidized bed adsorption?" *J Chromatogr A* **1998**, *827*, 269-280.

Ekstrom, S.; Malmstrom, J.; Wallman, L.; Lofgren, M.; Nilsson, J.; Laurell, T.; Marko-Varga, G. "On-chip microextraction for proteomic sample preparation of in-gel digests" *Proteomics* **2002**, *2*, 413-421.

Ekstrom, S.; Onnerfjord, P.; Nilsson, J.; Bengtsson, M.; Laurell, T.; Marko-Varga, G. "Integrated microanalytical technology enabling rapid and automated protein identification" *Anal Chem* **2000**, *72*, 286-293.

Elmas, B.; Onur, M. A.; Senel, S.; Tuncel, A. "Temperature controlled RNA isolation by N-isopropylacrylamide-vinylphenyl boronic acid copolymer latex" *Colloid Polym Sci* **2002**, *280*, 1137-1146.

Ericson, C.; Holm, J.; Ericson, T.; Hjerten, S. "Electroosmosis- and pressure-driven chromatography in chips using continuous beds" *Anal Chem* **2000**, *72*, 81-87.

Feil, H.; Bae, Y. H.; Jan, F. J.; Kim, S. W. "Effect of Comonomer Hydrophilicity and Ionization on the Lower Critical Solution Temperature of N-Isopropylacrylamide Copolymers" *Macromolecules* **1993**, *26*, 2496-2500.

Flaschel, E.; Friehs, K. "Improvement of Downstream Processing of Recombinant Proteins by Means of Genetic-Engineering Methods" *Biotechnol Adv* **1993**, *11*, 31-77.

Fong, R. B.; Ding, Z. L.; Hoffman, A. S.; Stayton, P. S. "Affinity separation using an Fv antibody fragment-"smart" polymer conjugate" *Biotechnol Bioeng* **2002**, *79*, 271-276.

Fong, R. B.; Ding, Z. L.; Long, C. J.; Hoffman, A. S.; Stayton, P. S. "Thermoprecipitation of streptavidin via oligonucleotide-mediated self-assembly with poly (N-isopropylacrylamide)" *Bioconjugate Chem* **1999**, *10*, 720-725.

Foust, A. S. *Principles of unit operations*; 2d ed.; Wiley: New York, 1980.

Fujii, M.; Taniguchi, M. "Application of Reversibly Soluble Polymers in Bioprocessing" *Trends Biotechnol* **1991**, *9*, 191-196.

Galaev, I. Y.; Kumar, A.; Agarwal, R.; Gupta, M. N.; Mattiasson, B. "Imidazole - A new ligand for metal affinity precipitation - Precipitation of kunitz soybean trypsin inhibitor using Cu(II)-loaded copolymers of 1-vinylimidazole with N-vinylcaprolactam or N-isopropylacrylamide" *Appl Biochem Biotech* **1997**, *68*, 121-133.

Galaev, I. Y.; Mattiasson, B. "New methods for affinity purification of proteins. Affinity precipitation: a review" *Biochemistry-Moscow+* **1997**, *62*, 571-577.

Galaev, I. Y.; Mattiasson, B. "'Smart' polymers and what they could do in biotechnology and medicine" *Trends Biotechnol* **1999**, *17*, 335-340.

Galaev, I. Y.; Warrol, C.; Mattiasson, B. "Temperature-Induced Displacement of Proteins from Dye-Affinity Columns Using an Immobilized Polymeric Displacer" *J Chromatogr A* **1994**, *684*, 37-43.

Garret-Flaudy, F.; Freitag, R. "Unusual thermoprecipitation behavior of poly(N,N-diethylacrylamide) from aqueous solution in the presence of anionic surfactants" *Langmuir* **2001**, *17*, 4711-4716.

Garret-Flaudy, F.; Freitag, R. "Use of the avidin (imino)biotin system as a general approach to affinity precipitation" *Biotechnol Bioeng* **2001**, *71*, 223-234.

Geschwind, D. H. "DNA microarrays: translation of the genome from laboratory to clinic" *Lancet Neurology* **2003**, *2*, 275-282.

Gewehr, M.; Nakamura, K.; Ise, N.; Kitano, H. "Gel-Permeation Chromatography Using Porous-Glass Beads Modified with Temperature-Responsive Polymers" *Makromol Chem* **1992**, *193*, 249-256.

Giovannini, R.; Freitag, R. "Isolation of a recombinant antibody from cell culture supernatant: continuous annular versus batch and expanded-bed chromatography" *Biotechnol Bioeng* **2001**, *73*, 522-529.

Giovannini, R.; Freitag, R. "Continuous isolation of plasmid DNA by annular chromatography" *Biotechnol Bioeng* **2002**, *77*, 445-454.

Gorelov, A. V.; DuChesne, A.; Dawson, K. A. "Phase separation in dilute solutions of poly (N-isopropylacrylamide)" *Physica A* **1997**, *240*, 443-452.

Gosling, J. P.; Lawrence, V. B., Eds. *Immunoassay: Laboratory analysis and clinical application*; Butterworth-Heinemann: Newton, MA, 1994.

Goss, T. A.; Bard, M.; Jarrett, H. W. "High-Performance Affinity-Chromatography of DNA" *J Chromatogr* **1990**, *508*, 279-287.

Gottschlich, N.; Culbertson, C. T.; McKnight, T. E.; Jacobson, S. C.; Ramsey, J. M. "Integrated microchip-device for the digestion, separation and postcolumn labeling of proteins and peptides" *J Chromatogr B* **2000**, *745*, 243-249.

Green, N. M. "Avidin: 1. The Use of [14C]Biotin for Kinetic Studies and for Assay" *Biochem. J.* **1963**, *89*, 585-591.

Green, N. M. "Spectrophotometric Determination of Avidin and Biotin" *Methods Enzymol.* **1970**, 418.

Green, N. M. "Avidin" *Adv Protein Chem* **1975**, *29*, 85-133.

Green, N. M. "Avidin and streptavidin" *Methods Enzymol* **1990**, *184*, 51-67.

Habeeb, A. F. S. A. "Determination of free amino groups in protein by trinitrobenzene sulfonic acid" *Anal. Biochem.* **1966**, *14*, 328.

Hadd, A. G.; Jacobson, S. C.; Ramsey, J. M. "Microfluidic assays of acetylcholinesterase inhibitors" *Anal Chem* **1999**, *71*, 5206-5212.

Hadd, A. G.; Raymond, D. E.; Halliwell, J. W.; Jacobson, S. C.; Ramsey, J. M. "Microchip device for performing enzyme assays" *Anal Chem* **1997**, *69*, 3407-3412.

Hafner, F. T.; Kautz, R. A.; Iverson, B. L.; Tim, R. C.; Karger, B. L. "Noncompetitive immunoassay of small analytes at the femtomolar level by affinity probe capillary electrophoresis: Direct analysis of digoxin using a uniform-labeled scFv immunoreagent" *Anal Chem* **2000**, *72*, 5779-5786.

Hahn, M.; Gornitz, E.; Dautzenberg, H. "Synthesis and properties of ionically modified polymers with LCST behavior" *Macromolecules* **1998**, *31*, 5616-5623.

Hansen, C. L.; Skordalakes, E.; Berger, J. M.; Quake, S. R. "A robust and scalable microfluidic metering method that allows protein crystal growth by free interface diffusion" *P Natl Acad Sci USA* **2002**, *99*, 16531-16536.

Harrison, D. J.; Manz, A.; Fan, Z. H.; Ludi, H.; Widmer, H. M. "Capillary Electrophoresis and Sample Injection Systems Integrated on a Planar Glass Chip" *Anal Chem* **1992**, *64*, 1926-1932.

Hatch, A.; Kamholz, A. E.; Hawkins, K. R.; Munson, M. S.; Schilling, E. A.; Weigl, B. H.; Yager, P. "A rapid diffusion immunoassay in a T-sensor" *Nat Biotechnol* **2001**, *19*, 461-465.

Hendrickson, W. A.; Pahler, A.; Smith, J. L.; Satow, Y.; Merritt, E. A.; Phizackerley, R. P. "Crystal-Structure of Core Streptavidin Determined from Multiwavelength Anomalous Diffraction of Synchrotron Radiation" *P Natl Acad Sci USA* **1989**, *86*, 2190-2194.

Heney, G.; Orr, G. A. "The purification of avidin and its derivatives on 2-iminobiotin-6-aminohexyl-Sepharose 4B" *Anal Biochem* **1981**, *114*, 92-96.

Henry, A. C.; Tutt, T. J.; Galloway, M.; Davidson, Y. Y.; McWhorter, C. S.; Soper, S. A.; McCarley, R. L. "Surface modification of poly(methyl methacrylate) used in the fabrication of microanalytical devices" *Anal Chem* **2000**, *72*, 5331-5337.

Heskins, M.; Guillet, J. E. "Solution Properties of Poly(N-isopropylacrylamide)" *J. Macromol. Sci.-Chem.* **1968**, *A2*, 1441-1455.

Hoffman, A. S.; Afrassiabi, A.; Dong, L. C. "Thermally Reversible Hydrogels: II. Delivery and Selective Removal of Substances From Aqueous Solutions" *J. Controlled Release* **1986**, *4*, 213-222.

Hoffman, A. S.; Stayton, P. S.; Bulmus, V.; Chen, G. H.; Chen, J. P.; Cheung, C.; Chilkoti, A.; Ding, Z. L.; Dong, L. C.; Fong, R.; Lackey, C. A.; Long, C. J.; Miura, M.; Morris, J. E.; Murthy, N.; Nabeshima, Y.; Park, T. G.; Press, O. W.; Shimoboji, T.; Shoemaker, S.; Yang, H. J.; Monji, N.; Nowinski, R. C.; Cole, C. A.; Priest, J. H.; Harris, J. M.; Nakamae, K.; Nishino, T.; Miyata, T. "Really smart bioconjugates of smart polymers and receptor proteins" *J Biomed Mater Res* **2000**, *52*, 577-586.

Holzman, T. F.; Baldwin, T. O. "Isolation of Bacterial Luciferases by Affinity-Chromatography on 2,2-Diphenylpropylamine-Sepharose - Phosphate-Mediated Binding to an Immobilized Substrate-Analog" *Biochemistry-Us* **1982**, *21*, 6194-6201.

Hosoya, K.; Sawada, E.; Kimata, K.; Araki, T.; Tanaka, N.; Frechet, J. M. J. "In-Situ Surface-Selective Modification of Uniform Size Macroporous Polymer Particles with Temperature-Responsive Poly-N-Isopropylacrylamide" *Macromolecules* **1994**, *27*, 3973-3976.

Hsu, S. H.; Yu, T. L. "Dynamic viscoelasticity study of the phase transition of poly(N-isopropylacrylamide)" *Macromol Rapid Comm* **2000**, *21*, 476-480.

Hubner, J.; Mogensen, K. B.; Jorgensen, A. M.; Friis, P.; Telleman, P.; Kutter, J. P. "Integrated optical measurement system for fluorescence spectroscopy in microfluidic channels" *Rev Sci Instrum* **2001**, *72*, 229-233.

Hyre, D. E.; Le Trong, I.; Freitag, S.; Stenkamp, R. E.; Stayton, P. S. "Ser45 plays an important role in managing both the equilibrium and transition state energetics of the streptavidin-biotin system" *Protein Sci* **2000**, *9*, 878-885.

Jacobson, S. C.; McKnight, T. E.; Ramsey, J. M. "Microfluidic devices for electrokinetically driven parallel and serial mixing" *Anal Chem* **1999**, *71*, 4455-4459.

Jiang, G. F.; Attiya, S.; Ocvirk, G.; Lee, W. E.; Harrison, D. J. "Red diode laser induced fluorescence detection with a confocal microscope on a microchip for capillary electrophoresis" *Biosens Bioelectron* **2000**, *14*, 861-869.

Johnson, T. J.; Ross, D.; Locascio, L. E. "Rapid microfluidic mixing" *Anal Chem* **2002**, *74*, 45-51.

Jortani, S. A.; Valdes, R. "Digoxin and its related endogenous factors" *Crit Rev Cl Lab Sci* **1997**, *34*, 225-274.

Josic, D.; Buchacher, A.; Jungbauer, A. "Monoliths as stationary phases for separation of proteins and polynucleotides and enzymatic conversion" *J Chromatogr B* **2001**, *752*, 191-205.

Kan, C. W.; Barron, A. E. "A DNA sieving matrix with thermally tunable mesh size" *Electrophoresis* **2003**, *24*, 55-62.

Kanazawa, H.; Kashiwase, Y.; Yamamoto, K.; Matsushima, Y.; Kikuchi, A.; Sakurai, Y.; Okano, T. "Temperature-responsive liquid chromatography .2. Effects of hydrophobic groups in N-isopropylacrylamide copolymer-modified silica" *Anal Chem* **1997**, *69*, 823-830.

Kanazawa, H.; Yamamoto, K.; Matsushima, Y.; Takai, N.; Kikuchi, A.; Sakurai, Y.; Okano, T. "Temperature-responsive chromatography using poly(N-isopropylacrylamide)-modified silica" *Anal Chem* **1996**, *68*, 100-105.

Khandurina, J.; Guttman, A. "Bioanalysis in microfluidic devices" *J Chromatogr A* **2002**, *943*, 159-183.

Kim, E.; Xia, Y. N.; Whitesides, G. M. "Polymer Microstructures Formed by Molding in Capillaries" *Nature* **1995**, *376*, 581-584.

Klumb, L. A.; Chu, V.; Stayton, P. S. "Energetic roles of hydrogen bonds at the ureido oxygen binding pocket in the streptavidin-biotin complex" *Biochemistry-Us* **1998**, *37*, 7657-7663.

Knox, J. H. "Practical Aspects of LC Theory" *J. Chrom. Sci.* **1977**, *15*, 352-364.

Kobayashi, J.; Kikuchi, A.; Sakai, K.; Okano, T. "Aqueous chromatography utilizing pH-/temperature responsive polymer stationary phases to separate ionic bioactive compounds" *Anal Chem* **2001**, *73*, 2027-2033.

Kobayashi, J.; Kikuchi, A.; Sakai, K.; Okano, T. "Cross-linked thermoresponsive anionic polymer-grafted surfaces to separate bioactive basic peptides" *Anal Chem* **2003**, *75*, 3244-3249.

Kondo, A.; Fukuda, H. "Preparation of thermo-sensitive magnetic microspheres and their application to bioprocesses" *Colloid Surface A* **1999**, *153*, 435-438.

Kopp, M. U.; Crabtree, H. J.; Manz, A. "Developments in technology and applications of microsystems" *Curr Opin Chem Biol* **1997**, *1*, 410-419.

Kopp, M. U.; de Mello, A. J.; Manz, A. "Chemical amplification: Continuous-flow PCR on a chip" *Science* **1998**, *280*, 1046-1048.

Krishnan, M.; Namasivayam, V.; Lin, R. S.; Pal, R.; Burns, M. A. "Microfabricated reaction and separation systems" *Curr Opin Biotech* **2001**, *12*, 92-98.

Kuo, M. H.; Allis, C. D. "In vivo cross-linking and immunoprecipitation for studying dynamic protein: DNA associations in chromatin environment" *Methods* **1999**, *19*, 425-433.

Kwon, Y. J.; Hatti-Kaul, R. "Protein separation using metal ion-bound particles in aqueous two-phase system" *Biotech Techniques* **1999**, *13*, 145-148.

Kyriakides, T. R.; Cheung, C. Y.; Murthy, N.; Bornstein, P.; Stayton, P. S.; Hoffman, A. S. "pH-sensitive polymers that enhance intracellular drug delivery in vivo" *J. Controlled Release* **2002**, *78*, 295-303.

Lacher, N. A.; Garrison, K. E.; Martin, R. S.; Lunte, S. M. "Microchip capillary electrophoresis/electrochemistry" *Electrophoresis* **2001**, *22*, 2526-2536.

Lackey, C. A.; Murthy, N.; Press, O. W.; Tirrell, D. A.; Hoffman, A. S.; Stayton, P. S. "Hemolytic activity of pH-responsive polymer-streptavidin bioconjugates" *Bioconjugate Chem* **1999**, *10*, 401-405.

Lackey, C. A.; Press, O. W.; Hoffman, A. S.; Stayton, P. S. "A biomimetic pH-responsive polymer directs endosomal release and intracellular delivery of an endocytosed antibody complex" *Bioconjugate Chem* **2002**, *13*, 996-1001.

Ladisch, M. R. *Bioseparations engineering : principles, practice, and economics*; Wiley: New York, 2001.

Lahann, J.; Balcells, M.; Lu, H.; Rodon, T.; Jensen, K. F.; Langer, R. "Reactive polymer coatings: A first step toward surface engineering of microfluidic devices" *Anal Chem* **2003**, *In Press.*

Lahann, J.; Choi, I. S.; Lee, J.; Jensen, K. F.; Langer, R. "A new method toward microengineered surfaces based on reactive coating" *Angew. Chem. Int. Ed.* **2001**, *40*, 3166-3169.

Lakhiari, H.; Okano, T.; Nurdin, N.; Luthi, C.; Descouts, P.; Muller, D.; Jozefonvicz, J. "Temperature-responsive size-exclusion chromatography using poly(N-isopropylacrylamide) grafted silica" *Bba-Gen Subjects* **1998**, *1379*, 303-313.

Landers, J. P. "Molecular diagnostics on electrophoretic microchips" *Anal Chem* **2003**, *75*, 2919-2927.

Lao, A. I. K.; Lee, T. M. H.; Hsing, I. M.; Ip, N. Y. "Precise temperature control of microfluidic chamber for gas and liquid phase reactions" *Sensor Actuat a-Phys* **2000**, *84*, 11-17.

Lazar, I. M.; Ramsey, R. S.; Ramsey, J. M. "On-chip proteolytic digestion and analysis using "wrong-way-round" electrospray time-of-flight mass spectrometry" *Anal Chem* **2001**, *73*, 1733-1739.

Lee, H. J.; Goodrich, T. T.; Corn, R. M. "SPR imaging measurements of 1-D and 2-D DNA microarrays created from microfluidic channels on gold thin films" *Anal Chem* **2001**, *73*, 5525-5531.

Lerman, L. S. *Nature* **1953**, *172*, 635.

Lettieri, G. L.; Dodge, A.; Boer, G.; de Rooij, N. F.; Verpoorte, E. "A novel microfluidic concept for bioanalysis using freely moving beads trapped in recirculating flows" *Lab Chip* **2003**, *3*, 34-39.

L'Hostis, E.; Michel, P. E.; Fiaccabrino, G. C.; Strike, D. J.; de Rooij, N. F.; Koudelka-Hep, M. "Microreactor and electrochemical detectors fabricated using Si and EPON SU-8" *Sensor Actuat B-Chem* **2000**, *64*, 156-162.

Li, J. J.; Thibault, P.; Bings, N. H.; Skinner, C. D.; Wang, C.; Colyer, C.; Harrison, J. "Integration of microfabricated devices to capillary electrophoresis-electrospray mass spectrometry using a low dead volume connection: Application to rapid analyses of proteolytic digests" *Anal Chem* **1999**, *71*, 3036-3045.

Licklider, L.; Wang, X. Q.; Desai, A.; Tai, Y. C.; Lee, T. D. "A micromachined chip-based electrospray source for mass spectrometry" *Anal Chem* **2000**, *72*, 367-375.

Linder, V.; Verpoorte, E.; Thormann, W.; de Rooij, N. F.; Sigrist, H. "Surface biopassivation of replicated poly(dimethylsiloxane) microfluidic channels and application to heterogeneous immunoreaction with on-chip fluorescence detection." *Anal Chem* **2001**, *73*, 4181-4189.

Liu, J.; Enzelberger, M.; Quake, S. R. "A nanoliter rotary device for polymerase chain reaction" *Electrophoresis* **2002**, *23*, 1531-1536.

Liu, R. H.; Stremler, M. A.; Sharp, K. V.; Olsen, M. G.; Santiago, J. G.; Adrian, R. J.; Aref, H.; Beebe, D. J. "Passive mixing in a three-dimensional serpentine microchannel" *J. MEMS* **2000**, *9*, 190-197.

Liu, R. H.; Yu, Q.; Beebe, D. J. "Fabrication and characterization of hydrogel-based microvalves" *J. MEMS* **2002**, *11*, 45-53.

Liu, Y.; Fanguy, J. C.; Bledsoe, J. M.; Henry, C. S. "Dynamic coating using polyelectrolyte multilayers for chemical control of electroosmotic flow in capillary electrophoresis microchips" *Anal Chem* **2000**, *72*, 5939-5944.

Lopatin, S. A.; Varlamov, V. P. "New Trends in Immobilized Metal Affinity-Chromatography of Proteins - (Review)" *Appl Biochem Micro+* **1995**, *31*, 221-227.

Lu, L.-H.; Ryu, K. S.; Liu, C. "A magnetic microstirrer and array for microfluidic mixing" *J. MEMS* **2002**, *11*, 462-469.

Luan, C.-H.; Urry, D. W. "Solvent deuteration enhancement of hydrophobicity: DSC study of the inverse temperature transition of elastin-based polypeptides" *J. Phys. Chem.* **1991**, *95*, 7896-7900.

Luong, J. H. T.; Nguyen, A.-L. In *Bioseparation*; Tsao, G. T., Belfort, G., Eds.; Springer-Verlag: Berlin ; Hong Kong, 1992, pp 137-158.

Luong, J. H. T.; Nguyen, A. L.; Male, K. B. "Recent Developments in Downstream Processing Based on Affinity Interactions" *Trends Biotechnol* **1987**, *5*, 281-286.

Macounova, K.; Cabrera, C. R.; Yager, P. "Concentration and separation of proteins in microfluidic channels on the basis of transverse IEF" *Anal Chem* **2001**, *73*, 1627-1633.

Malmstadt, N.; Hyre, D. E.; Ding, Z.; Hoffman, A. S.; Stayton, P. S. "Affinity Thermoprecipitation and Recovery of Biotinylated Biomolecules via a Mutant Streptavidin-Smart Polymer Conjugate" *Bioconjug Chem* **2003**, *14*, 575-580.

Malmstadt, N.; Yager, P.; Hoffman, A. S.; Stayton, P. S. "A Smart Microfluidic Affinity Chromatography Matrix Composed of Poly(N-isopropylacrylamide)-Coated Beads" *Anal Chem* **2003**, *75*, 2943-2949.

Manz, A.; Graber, N.; Widmer, H. M. "Miniaturized Total Chemical-Analysis Systems - a Novel Concept for Chemical Sensing" *Sensor Actuat B-Chem* **1990**, *1*, 244-248.

Mao, H. B.; Yang, T. L.; Cremer, P. S. "Design and characterization of immobilized enzymes in microfluidic systems" *Anal Chem* **2002**, *74*, 379-385.

Matsukata, M.; Aoki, T.; Sanui, K.; Ogata, N.; Kikuchi, A.; Sakurai, Y.; Okano, T. "Effect of molecular architecture of poly(N-isopropylacrylamide)-trypsin conjugates on their solution and enzymatic properties" *Bioconjugate Chem* **1996**, *7*, 96-101.

Mattiasson, B.; Kumar, A.; Galaev, I. Y. "Affinity precipitation of proteins: design criteria for an efficient polymer" *J Mol Recognit* **1998**, *11*, 211-216.

McKnight, T. E.; Culbertson, C. T.; Jacobson, S. C.; Ramsey, J. M. "Electroosmotically induced hydraulic pumping with integrated electrodes on microfluidic devices" *Anal Chem* **2001**, *73*, 4045-4049.

Monji, N.; Hoffman, A. S. "A Novel Immunoassay System and Bioseparation Process Based on Thermal Phase Separating Polymers" *Appl Biochem Biotech* **1987**, *14*, 107-120.

Murthy, N.; Campbell, J.; Fausto, N.; Hoffman, A. S.; Stayton, P. S. "Bioinspired pH-responsive polymers for the intracellular delivery of biomolecular drugs" *Bioconjugate Chem* **2003**, *14*, 412-419.

Nakamura, H.; Murakami, Y.; Yokoyama, K.; Tamiya, E.; Karube, I. "A compactly integrated flow cell with a chemiluminescent FIA system for determining lactate concentration in serum" *Anal Chem* **2001**, *73*, 373-378.

Ngola, S. M.; Fintschenko, Y.; Choi, W. Y.; Shepodd, T. J. "Conduct-as-cast polymer monoliths as separation media for capillary electrochromatography" *Anal Chem* **2001**, *73*, 849-856.

Nguyen, N. T.; Huang, X. Y.; Chuan, T. K. "MEMS-micropumps: A review" *J. Fluids Eng.* **2002**, *124*, 384-392.

Niederauer, M. Q.; Glatz, C. E. In *Bioseparation*; Tsao, G. T., Belfort, G., Eds.; Springer-Verlag: Berlin ; Hong Kong, 1992, pp 159-188.

Northrup, M. A.; Benett, B.; Hadley, D.; Landre, P.; Lehew, S.; Richards, J.; Stratton, P. "A miniature analytical instrument for nucleic acids based on micromachined silicon reaction chambers" *Anal Chem* **1998**, *70*, 918-922.

Ocvirk, G.; Verpoorte, E.; Manz, A.; Grasserbauer, M.; Widmer, H. M. "High-Performance Liquid-Chromatography Partially Integrated onto a Silicon Chip" *Anal Method Instrum* **1995**, 2, 74-82.

Oddy, M. H.; Santiago, J. G.; Mikkelsen, J. C. "Electrokinetic instability micromixing" *Anal Chem* **2001**, *73*, 5822-5832.

Okano, T.; Yamada, N.; Okuhara, M.; Sakai, H.; Sakurai, Y. "Mechanism of Cell Detachment from Temperature-Modulated, Hydrophilic-Hydrophobic Polymer Surfaces" *Biomaterials* **1995**, *16*, 297-303.

Oleschuk, R. D.; Shultz-Lockyear, L. L.; Ning, Y. B.; Harrison, D. J. "Trapping of bead-based reagents within microfluidic systems: On-chip solid-phase extraction and electrochromatography" *Anal Chem* **2000**, *72*, 585-590.

Otake, K.; Inomata, H.; Konno, M.; Saito, S. "Thermal analysis of the volume phase transition with N-isopropylacrylamide gels" *Macromolecules* **1990**, *23*, 283-289.

Papra, A.; Bernard, A.; Juncker, D.; Larsen, N. B.; Michel, B.; Delamarche, E. "Microfluidic networks made of poly(dimethylsiloxane), Si, and Au coated with polyethylene glycol for patterning proteins onto surfaces" *Langmuir* **2001**, *17*, 4090-4095.

Perez-Luna, V. H.; O'Brien, M. J.; Opperman, K. A.; Hampton, P. D.; Lopez, G. P.; Klumb, L. A.; Stayton, P. S. "Molecular recognition between genetically engineered streptavidin and surface-bound biotin" *J Am Chem Soc* **1999**, *121*, 6469-6478.

Perry, R. H.; Maloney, J. O.; Green, D. W.; Knovel (Firm) *Perry's chemical engineers' handbook*; 7th / ed.; McGraw-Hill: New York, 1997.

Peterson, D. S.; Rohr, T.; Svec, F.; Fréchet, J. M. J. "Enzymatic microreactor-on-a-chip: protein mapping using trypsin immobilized on porous polymer monoliths molded in channels of microfluidic devices" *Anal Chem* **2002**, *74*, 4081-4088.

Piran, U.; Riordan, W. J. "Dissociation rate constant of the biotin-streptavidin complex" *J Immunol Methods* **1990**, *133*, 141-143.

Porath, J.; Axen, R.; Ernback, S. *Nature* **1967**, *215*, 1491.

Regnier, F. E.; He, B.; Lin, S.; Busse, J. "Chromatography and electrophoresis on chips: critical elements of future integrated, microfluidic analytical systems for life science" *Trends Biotechnol* **1999**, *17*, 101-106.

Reyes, D. R.; Iossifidis, D.; Auroux, P. A.; Manz, A. "Micro total analysis systems. 1. Introduction, theory, and technology" *Anal Chem* **2002**, *74*, 2623-2636.

Richardson, J. F.; Zaki, W. N. *Trans. Inst. Chem. Eng.* **1954**, *32*, 38.

Richter, T.; Shultz-Lockyear, L. L.; Oleschuk, R. D.; Bilitewski, U.; Harrison, D. J. "Bi-enzymatic and capillary electrophoretic analysis of non-fluorescent compounds in microfluidic devices - Determination of xanthine" *Sensor Actuat B-Chem* **2002**, *81*, 369-376.

Ro, K. W.; Lim, K.; Kim, H.; Hahn, J. H. "Poly(dimethylsiloxane) microchip for precolumn reaction and micellar electrokinetic chromatography of biogenic amines" *Electrophoresis* **2002**, *23*, 1129-1137.

Roberts, M. A.; Rossier, J. S.; Bercier, P.; Girault, H. "UV laser machined polymer substrates for the development of microdiagnostic systems" *Anal Chem* **1997**, *69*, 2035-2042.

Rohr, T.; Yu, C.; Davey, M. H.; Svec, F.; Frechet, J. M. J. "Porous polymer monoliths: Simple and efficient mixers prepared by direct polymerization in the channels of microfluidic chips" *Electrophoresis* **2001**, *22*, 3959-3967.

Sanjoh, A.; Tsukihara, T. "Spatiotemporal protein crystal growth studies using microfluidic silicon devices" *J. Cryst. Growth* **1999**, *194*, 691-702.

Sato, K.; Tokeshi, M.; Odake, T.; Kimura, H.; Ooi, T.; Nakao, M.; Kitamori, T. "Integration of an immunosorbent assay system: Analysis of secretory human immunoglobulin A on polystyrene beads in a microchip" *Anal Chem* **2000**, *72*, 1144-1147.

Schild, H. G. "Poly (N-Isopropylacrylamide) - Experiment, Theory and Application" *Prog Polym Sci* **1992**, *17*, 163-249.

Schwarz, A.; Rossier, J. S.; Roulet, E.; Mermod, N.; Roberts, M. A.; Girault, H. H. "Micropatterning of biomolecules on polymer substrates" *Langmuir* **1998**, *14*, 5526-5531.

Seong, G. H.; Heo, J.; Crooks, R. M. "Measurement of enzyme kinetics using a continuous-flow microfluidic system" *Anal Chem* **2003**, *75*, 3161-3167.

Shamansky, L. M.; Davis, C. B.; Stuart, J. K.; Kuhr, W. G. "Immobilization and detection of DNA on microfluidic chips" *Talanta* **2001**, *55*, 909-918.

Shim, Y. N.; Paeng, I. R. "Development of bioluminescence immunoassay using photoprotein, aequorin and site-directed immobilization" *B Kor Chem Soc* **2003**, *24*, 70-74.

Shimoboji, T.; Ding, Z. L.; Stayton, P. S.; Hoffman, A. S. "Mechanistic investigation of smart polymer-protein conjugates" *Bioconjugate Chem* **2001**, *12*, 314-319.

Shimoboji, T.; Ding, Z. L.; Stayton, P. S.; Hoffman, A. S. "Photoswitching of ligand association with a photoresponsive polymer-protein conjugate" *Bioconjugate Chem* **2002**, *13*.

Shimoboji, T.; Larenas, E.; Fowler, T.; Kulkarni, S.; Hoffman, A. S.; Stayton, P. S. "Photoresponsive polymer-enzyme switches" *P Natl Acad Sci USA* **2002**, *99*, 16592-16596.

Shoji, S. "Fluids for sensor systems" *Top. Curr. Chem.* **1998**, *194*, 163-188.

Slentz, B. E.; Penner, N. A.; Regnier, F. E. "Protein proteolysis and the multi-dimensional electrochromatographic separation of histidine-containing peptide fragments on a chip" *J Chromatogr A* **2003**, *984*, 97-107.

Smith, P. A.; Tripp, B. C.; DiBlasio-Smith, E. A.; Lu, Z. J.; LaVallie, E. R.; McCoy, J. M. "A plasmid expression system for quantitative in vivo biotinylation of thioredoxin fusion proteins in Escherichia coli" *Nucleic Acids Res* **1998**, *26*, 1414-1420.

Starkey, D. E.; Han, A.; Bao, J. J.; Ahn, C. H.; Wehmeyer, K. R.; Prenger, M. C.; Halsall, H. B.; Heineman, W. R. "Fluorogenic assay for beta-glucuronidase using microchip-based capillary electrophoresis" *J Chromatogr B* **2001**, *762*, 33-41.

Sun, Y. M.; Yu, C. W.; Liang, H. C.; Chen, J. P. "Temperature-sensitive latex particles for immobilization of alpha-amylase" *J Disper Sci Technol* **1999**, *20*, 907-920.

Szumski, M.; Buszewski, B. "State of the art in miniaturized separation techniques" *Crit Rev Anal Chem* **2002**, *32*, 1-46.

Szurdoki, F.; Michael, K. L.; Walt, D. R. "A duplexed microsphere-based fluorescent immunoassay" *Anal. Biochem.* **2001**, *291*, 219-228.

Takahashi, T.; Ogata, S.; Nishizawa, M.; Matsue, T. "A valveless switch for microparticle sorting with laminar flow streams and electrophoresis perpendicular to the direction of fluid stream" *Electrochem. Comm.* **2003**, *5*, 175-177.

Takei, Y. G.; Aoki, T.; Sanui, K.; Ogata, N.; Sakurai, Y.; Okano, T. "Dynamic Contact-Angle Measurement of Temperature-Responsive Surface-Properties for Poly(N-Isopropylacrylamide) Grafted Surfaces" *Macromolecules* **1994**, *27*, 6163-6166.

Takei, Y. G.; Matsukata, M.; Aoki, T.; Sanui, K.; Ogata, N.; Kikuchi, A.; Sakurai, Y.; Okano, T. "Temperature-responsive bioconjugates. 3. Antibody-poly (N-isopropylacrylamide) conjugates for temperature-modulated precipitations and affinity bioseparations" *Bioconjug Chem* **1994**, *5*, 577-582.

Taki, M.; Sawata, S. Y.; Taira, K. "Specific N-terminal biotinylation of a protein in vitro by a chemically modified tRNA(fmet) can support the native activity of the translated protein" *J Biosci Bioeng* **2001**, *92*, 149-153.

Taniguchi, T.; Duracher, D.; Delair, T.; Elaïssari, A.; Pichot, C. "Adsorption/desorption behavior and covalent grafting of an antibody onto cationic amino-functionalized

poly(styrene-N-isopropylacrylamide) core-shell latex particles" *Colloid Surface B* **2003**, *29*, 53-65.

Taylor, G. "Dispersion of soluble matter in solvent flowing slowly through a tube" *Proc. Royal Soc., A* **1953**, *219*, 186-203.

Teal, H. E.; Hu, Z. B.; Root, D. D. "Native purification of biomolecules with temperature-mediated hydrophobic modulation liquid chromatography" *Anal. Biochem.* **2000**, *283*, 159-165.

Templin, M. F.; Stoll, D.; Schrenk, M.; Traub, P. C.; Vohringer, C. F.; Joos, T. O. "Protein microarray technology" *Trends Biotechnol* **2002**, *20*, 160-166.

Thorsen, T.; Maerkl, S. J.; Quake, S. R. "Microfluidic large-scale integration" *Science* **2002**, *298*, 580-584.

Tiktopulo, E. I.; Bychkova, V. E.; Ricka, J.; Ptitsyn, O. B. "Cooperativity of the Coil-Globule Transition in a Homopolymer - Microcalorimetric Study of Poly(N-Isopropylacrylamide)" *Macromolecules* **1994**, *27*, 2879-2882.

Timoshenko, E. G.; Basovsky, R.; Kuznetsov, Y. A. "Micellesation vs aggregation in dilute solutions of amphiphilic heteropolymers" *Colloid Surface A* **2001**, *190*, 129-134.

Tsao, G. T.; Belfort, G. *Bioseparation*; Springer-Verlag: Berlin ; Hong Kong, 1992.

Umeno, D.; Kawasaki, M.; Maeda, M. "Water-soluble conjugate of double-stranded DNA and poly(N-isopropylacrylamide) for one-pot affinity precipitation separation of DNA-binding proteins" *Bioconjugate Chem* **1998**, *9*, 719-724.

Unger, M. A.; Chou, H.-P.; Thorsen, T.; Scherer, A.; Quake, S. R. "Monolithic microfabricated valves and pumps by multilayer soft lithography" *Science* **2000**, *288*, 113-116.

Vaidya, A. A.; Lele, B. S.; Deshmukh, M. V.; Kulkarni, M. G. "Design and evaluation of new ligands for lysozyme recovery by affinity thermoprecipitation" *Chem Eng Sci* **2001**, *56*, 5681-5692.

Vaidya, A. A.; Lele, B. S.; Kulkarni, M. G.; Mashelkar, R. A. "Thermoprecipitation of lysozyme from egg white using copolymers of N-isopropylacrylamide and acidic monomers" *J Biotechnol* **2001**, *87*, 95-107.

Van Holde, K. E.; Johnson, W. C.; Ho, P. S. *Principles of physical biochemistry*; Prentice Hall: Upper Saddle River, N.J., 1998.

Verpoorte, E. M. J.; Vanderschoot, B. H.; Jeanneret, S.; Manz, A.; Widmer, H. M.; Derooij, N. F. "3-Dimensional Micro-Flow Manifolds for Miniaturized Chemical-Analysis Systems" *J Micromech Microeng* **1994**, *4*, 246-256.

Wahlund, P. O.; Galaev, I. Y.; Kazakov, S. A.; Lozinsky, V. I.; Mattiasson, B. ""Protein-like" copolymers: Effect of polymer architecture on the performance in bioseparation process" *Macromol Biosci* **2002**, *2*, 33-42.

Wang, C.; Oleschuk, R. D.; Ouchen, F.; Li, J. J.; Thibault, P.; Harrison, D. J. "Integration of immobilized trypsin bead beds for protein digestion within a microfluidic chip incorporating capillary electrophoresis separations and an electrospray mass spectrometry interface" *Rap. Comm. Mass Spec.* **2000**, *14*, 1377-1383.

Wang, J. "Electrochemical detection for microscale analytical systems: a review" *Talanta* **2002**, *56*, 223-231.

Wang, J.; Pumera, M.; Chatrathi, M. P.; Escarpa, A.; Konrad, R.; Griebel, A.; Dorner, W.; Lowe, H. "Towards disposable lab-on-a-chip: Poly(methylmethacrylate) microchip electrophoresis device with electrochemical detection" *Electrophoresis* **2002**, *23*, 596-601.

Wang, P. C.; Gao, J.; Lee, C. S. "High-resolution chiral separation using microfluidics-based membrane chromatography" *J Chromatogr A* **2002**, *942*, 115-122.

Waters, L. C.; Jacobson, S. C.; Kroutchinina, N.; Khandurina, J.; Foote, R. S.; Ramsey, J. M. "Microchip device for cell lysis, multiplex PCR amplification, and electrophoretic sizing" *Anal Chem* **1998**, *70*, 158-162.

Weber, P. C.; Ohlendorf, D. H.; Wendoloski, J. J.; Salemme, F. R. "Structural Origins of High-Affinity Biotin Binding to Streptavidin" *Science* **1989**, *243*, 85-88.

Weigl, B. H.; Bardell, R. L.; Cabrera, C. R. "Lab-on-a-chip for drug development" *Adv. Drug Delivery Rev.* **2003**, *55*, 349-377.

Weigl, B. H.; Yager, P. "Microfluidics - Microfluidic diffusion-based separation and detection" *Science* **1999**, *283*, 346-347.

Wilbur, D. S.; Chyan, M. K.; Pathare, P. M.; Hamlin, D. K.; Frownfelter, M. B.; Kegley, B. B. "Biotin reagents for antibody pretargeting. 4. Selection of biotin conjugates for in vivo application based on their dissociation rate from avidin and streptavidin" *Bioconjugate Chem* **2000**, *11*, 569-583.

Wilchek, M.; Bayer, E. A. "Applications of avidin-biotin technology: literature survey" *Methods Enzymol* **1990**, *184*, 14-45.

Wilchek, M.; Miron, T.; Kohn, J. In *Methods in Enzymology, v. 104*; Jakoby, W. B., Ed.; Academic Press: New York, 1983, p 3.

Winnik, F. M. "Fluorescence studies of aqueous solutions of poly(N-isopropylacrylamide) below and above their LCST" *Macromolecules* **1990**, *23*, 233-242.

Winnik, F. M. "Quenching of fluorescence from pyrene-labeled poly(N-isopropylacrylamide) solutions heated above their lower critical solution temperature" *Macromolecules* **1990**, *23*, 1647-1649.

Woolley, A. T.; Mathies, R. A. "Ultra-High-Speed DNA-Sequencing Using Capillary Electrophoresis Chips" *Anal Chem* **1995**, *67*, 3676-3680.

Wu, C.; Zhou, S. Q. "Laser-Light Scattering Study of the Phase-Transition of Poly(N-Isopropylacrylamide) in Water .1. Single-Chain" *Macromolecules* **1995**, *28*, 8381-8387.

Wu, X. S.; Hoffman, A. S.; Yager, P. "Synthesis and characterization of thermally reversible macroporous poly(N-isopropylacrylamide) hydrogels" *J Polym Sci Pol Chem* **1992**, *30*, 2121-2129.

Xiong, L.; Regnier, F. E. "Channel-specific coatings on microfabricated chips" *J Chromatogr A* **2001**, *924*, 165-176.

Xu, Y.; Vaidya, B.; Patel, A. B.; Ford, S. M.; McCarley, R. L.; Soper, S. A. "Solid-phase reversible immobilization in microfluidic chips for the purification of dye-labeled DNA sequencing fragments" *Anal Chem* **2003**, *In press, published on www.*

Yakovleva, J.; Davidsson, R.; Lobanova, A.; Bengtsson, M.; Eremin, S.; Laurell, T.; Emneus, J. "Microfluidic enzyme immunoassay using silicon microchip with immobilized antibodies and chemiluminescence detection" *Anal Chem* **2002**, *74*, 2994-3004.

Yakushiji, T.; Sakai, K.; Kikuchi, A.; Aoyagi, T.; Sakurai, Y.; Okano, T. "Effects of cross-linked structure on temperature-responsive hydrophobic interaction of poly(N-isopropylacrylamide) hydrogel-modified surfaces with steroids" *Anal Chem* **1999**, *71*, 1125-1130.

Yamanaka, H.; Yoshizako, K.; Akiyama, Y.; Sota, H.; Hasegawa, Y.; Shinohara, Y.; Kikuchi, A.; Okano, T. "Affinity chromatography with collapsibly tethered ligands" *Anal Chem* **2003**.

Yang, H. H.; Zhu, Q. Z.; Chen, S.; Li, D. H.; Chen, X. L.; Ding, M. T.; Xu, J. G. "Fluorescence immunoassay system based on the use of a pH-sensitive phase-separating polymer" *Anal. Biochem.* **2001**, *296*, 167-173.

Yang, T. L.; Jung, S. Y.; Mao, H. B.; Cremer, P. S. "Fabrication of phospholipid bilayer-coated microchannels for on-chip immunoassays" *Anal Chem* **2001**, *73*, 165-169.

Yasui, M.; Shiroya, T.; Fujimoto, K.; Kawaguchi, H. "Activity of enzymes immobilized on microspheres with thermosensitive hairs" *Colloid Surface B* **1997**, *8*, 311-319.

Yoshizako, K.; Akiyama, Y.; Yamanaka, H.; Shinohara, Y.; Hasegawa, Y.; Carredano, E.; Kikuchi, A.; Okano, T. "Regulation of protein binding toward a ligand on chromatographic matrixes by masking and forced-releasing effects using thermoresponsive polymer" *Anal Chem* **2002**, *74*, 4160-4166.

Yu, C.; Davey, M. H.; Svec, F.; Frechet, J. M. J. "Monolithic porous polymer for on-chip solid-phase extraction and preconcentration prepared by photoinitiated in situ polymerization within a microfluidic device" *Anal Chem* **2001**, *73*, 5088-5096.

Yu, C.; Mutlu, S.; Selvaganapathy, P.; Mastrangelo, C. H.; Svec, F.; Frechet, J. M. J. "Flow control valves for analytical microfluidic chips without mechanical parts based on thermally responsive monolithic polymers" *Anal Chem* **2003**, *75*, 1958-1961.

Yu, C.; Xu, M. C.; Svec, F.; Frechet, J. M. J. "Preparation of monolithic polymers with controlled porous properties for microfluidic chip applications using photoinitiated free-radical polymerization" *J Polym Sci Pol Chem* **2002**, *40*, 755-769.

Yu, Q.; Bauer, J. M.; Moore, J. S.; Beebe, D. J. "Responsive biomimetic hydrogel valve for microfluidics" *Appl Phys Lett* **2001**, *78*, 2589-2591.

Zareie, H. M.; Bulmus, E. V.; Gunning, A. P.; Hoffman, A. S.; Piskin, E.; Morris, V. J. "Investigation of a stimuli-responsive copolymer by atomic force microscopy" *Polymer* **2000**, *41*, 6723-6727.

Zhan, W.; Alvarez, J.; Sun, L.; Crooks, R. M. "A multichannel microfluidic sensor that detects anodic redox reactions indirectly using anodic electrogenerated chemiluminescence" *Anal Chem* **2003**, *75*, 1233-1238.

Appendix A: Software

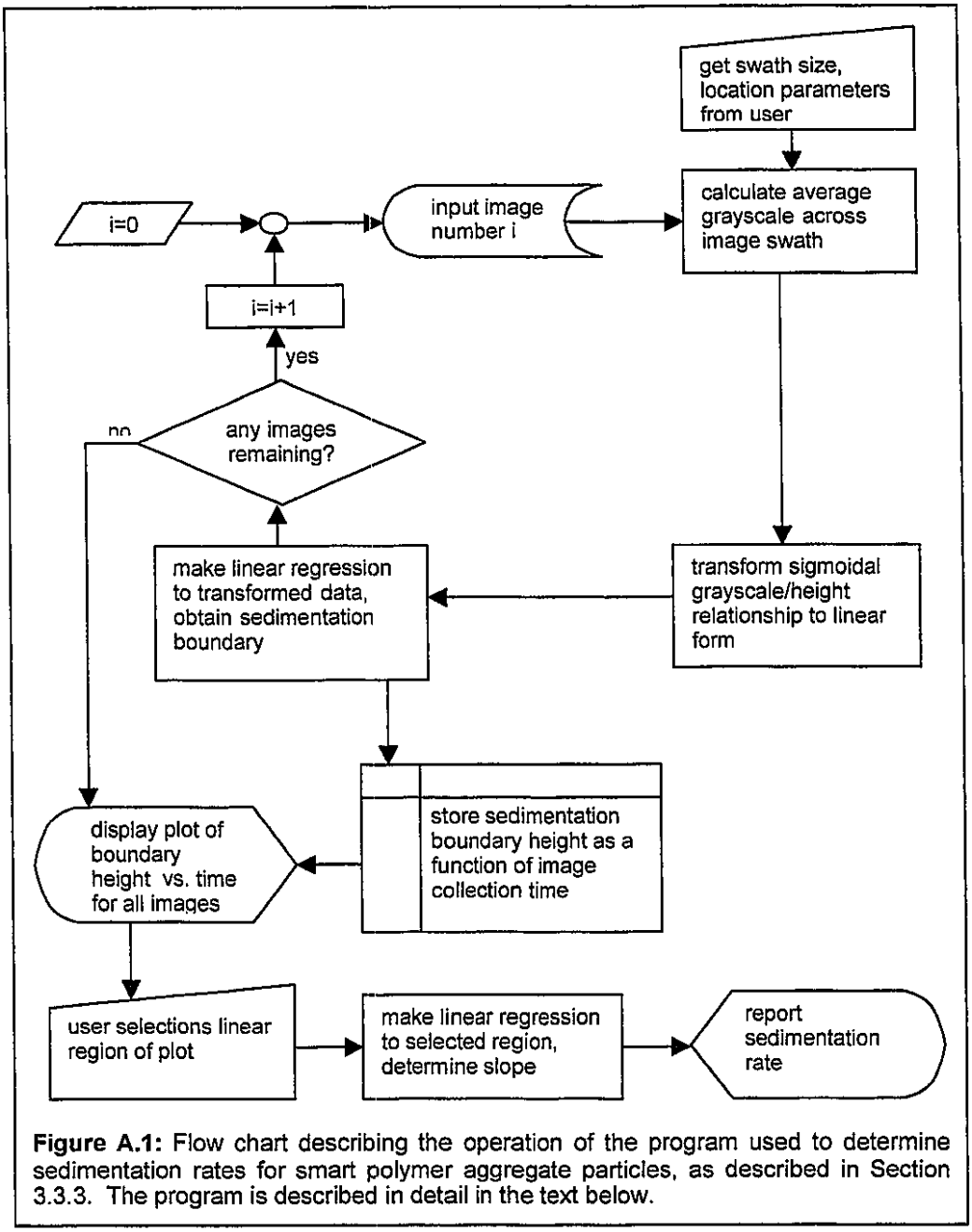

Figure A.1: Flow chart describing the operation of the program used to determine sedimentation rates for smart polymer aggregate particles, as described in Section 3.3.3. The program is described in detail in the text below.

Figure A.1 is a flowchart describing the operation of the program that was used to analyze polymer aggregate sedimentation data from the experiments described in Section 3.3. Section 3.3.3 describes this analytical process in some detail. The program was written in the C programming language to operate on a GNU/Linux system. Functions from the ImageMagick image-processing library (http://www.imagemagick.org) were used to input the images and reduce them to numerical data. Each sedimentation experiment produced a time series of images; as the particles settled, the sedimentation boundary height as determined from the images decreased. To quantify change in sedimentation boundary height with time during a single experiment, the images produced during that experiment were processed as follows: First, the grayscale values of the pixels in a single image were averaged across a user-selected swath (see Figure 3.9), yielding data that represented mean grayscale value as a function of height. These data were transformed from a sigmoidal function of height to a linear function of height, as described in Section 3.3.3. A linear regression was then performed for the transformed grayscale/height data, and the transformed grayscale midpoint (the inflection point of the pre-transformation sigmoid) was selected as the sedimentation boundary point, allowing for the determination of a sedimentation boundary height. After a sedimentation boundary height was determined for each imaged produced during an experiment, sedimentation boundary height was plotted for the user as a function of image collection time. The user was then allowed to select from this plot the linear region of the sedimentation curve (see Figure 3.3). A linear regression was performed for this region, yielding a sedimentation rate.

Table A.1: Commands for pump-control software developed for use in conjunction with Kloehn syringe pumps. In the experiments described in Chapters 3, 4, and 5, flow through microfluidic devices was driven by a bank of five syringe pumps. The software described in this table allows the user to address these pumps individually via a "pump number" assigned to each pump. Each pump was connected by a valve to both the microfluidic system and a reservoir containing working fluid (deionized water). The software controlled the valves such that clean working fluid was always drawn into the syringes from the reservoir and injected into the microfluidic system to drive flow. In this table, the term "steps" refers to pump motor steps: each pump can operate its syringe over a range of 40,000 steps. With 100 μL syringes installed in the pumps, this range represented about 60 μL. The "speed" parameter was entered by the user in units of "steps per second"; in main text of this document, these speeds have been translated to volumetric flow rates.

Command	Description	User-specified parameters
load	Pump withdraws fluid from reservoir into syringe.	• pump number • speed • number of steps
dispense	Pump dispenses fluid from syringe into system.	• pump number • speed • number of steps
handshake	Two pumps are operated simultaneously such the as one pump is injecting fluid into the system, the other is withdrawing fluid from the reservoir. Fluid can thereby be continuously driven through the system for an arbitrary length of time.	• two pump numbers • speed • number of syringe volumes to pump through system
inject	Two pumps operate in handshake mode, providing continuous flow through the system. A third pump is filled with fluid from the reservoir. At the command of the user, the fluid from this third pump is injected into the system.	• pump numbers for two handshaking pumps and one injection pump • speed • total number of samples to be collected from system • volume of each sample • volume of injection
reset_all	All pumps are initialized.	none
help	A description of commands is displayed.	none
exit	Program is terminated.	none

Appendix B: Instrument Settings

Table B.1: Settings for fluorescence spectrophotometers used to analyze samples from various experiments. For each target analyte, this table lists the excitation wavelength (λ_{ex}), emission wavelength (λ_{em}), excitation slit width, emission slit width, wavelength scan speed, and instrument model used.

Labeled species	λ_{ex}	λ_{em}	Excitation slit width	Emission slit width	Scan speed	Instrument
Texas Red-labeled IgG in affinity precipitation experiments (see sections 2.4.7, 2.4.8)	582 nm	603 nm	5.0 nm	5.0 nm	240 nm/s	Hitachi F-4500
Fluorescein-labeled streptavidin in affinity precipitation experiments (see section 2.5.2)	492 nm	518 nm	5.0 nm	5.0 nm	240 nm/s	Hitachi F-4500
Fluorescein-labeled DNA in affinity precipitation experiments (see section 2.4.9)	492 nm	518 nm	2.5 nm	2.5 nm	200 nm/s	Perkin-Elmer LS50B
Alexafluor 488-labeled streptavidin in affinity chromatography experiments (see section 4.3.6)	492 nm	518 nm	2.5 nm	2.5 nm	200 nm/s	Perkin-Elmer LS50B
Bodipy FL-labeled digoxigenin in immunoassay experiments (see section 5.3.4)	492 nm	511 nm	8.0 nm	5.0 nm	200 nm/s	Perkin-Elmer LS50B

Table B.2: Serial port settings for interfacing with Kloehn syringe pumps. The computer that controlled the pump rack (see sections 3.3.6 and 4.3.5) communicated with the pumps over as standard RS232 (serial) port. This table describes the serial port settings that made this communication possible. In a Linux system serial port settings can be viewed using the command "stty –F <device name> -a", where <device name> is the path of the device file corresponding to the appropriate serial port (/dev/ttyS1, for instance). The "stty" and "setserial" commands can be used to set serial communication parameters, as can functions in the "termios" standard C library.

Parameter	Value
speed	9600 baud
rows	0
columns	0
line	0
intr	^C
quit	^\
erase	^?
kill	^U
eof	^D
eol	undefined
eol2	undefined
start	^Q
stop	^S
susp	^Z
rprnt	^R
werase	^W
lnext	^V
flush	^O
min	1
time	5
options	-parenb, -parodd, cs8, hupcl, -cstopb, cread, clocal, -crtscts, ignbrk, -brkint, -ignpar, -parmrk, -inpck, -istrip, -inlcr, -igncr, -icrnl, -ixon, -ixoff, -iuclc, -ixany, -imaxbel, -opost, -olcuc, -onlcr, -onocr, -onlret, -ofill, -ofdel, n10, cr0, tab0, bs0, vt0, ff0, -isig, -icanon, -iexten, -ech, -echoe, -echonl, -noflsh, -xcase, -tostop, -echoprt, -echoctl, -echoke

Vita

Education

Doctor of Philosophy, Bioengineering — University of Washington
August 2003 — Seattle, Washington, USA

Bachelor of Science, Chemical Engineering — California Institute of Technology
June 1997 — Pasadena, California, USA

Research Experience

Graduate Research Assistant — **March 1998 to Present**
Department of Bioengineering
University of Washington
Professors Patrick S. Stayton and Allan S. Hoffman, Advisors

- A study of two-dimensional protein crystallization under lipid monolayers.
- Development of a temperature-controlled method for reversibly immobilizing biomolecules in microfluidic devices.

Research Assistant — **June 1997-Sept. 1997**
Department of Environmental Engineering
California Institute of Technology
Professor Michael Hoffmann, Advisor

- A study of the degradation of Pentachlorophenol (PCP) environmental contaminants by sonication and ozonation.

Research Assistant — **Jan. 1995-June 1997**
Department of Chemical Engineering
California Institute of Technology
Professor Frances Arnold, Advisor

- Directed evolution of a thermostable protease.

Awards, Scholarships, Fellowships, Prizes, Grants

- Bachelor of Science with Honors
- Recipient of Caltech Summer Undergraduate Research Fellowship, 1995 and 1996
- Selection to NSF Summer Institute in Japan, 2000
- Student poster prizes: *LabAutomation 2003* and University of Washington Bioengineering 2003 Robert F. Rushmer Lecture graduate poster session

Publications

- "Smart poly(*N*-isopropylacrylamide)-coated beads as a controlled immobilization substrate for a heterogeneous microfluidic immunoassay." Noah Malmstadt, Allan S. Hoffman, and Patrick S. Stayton. Manuscript in preparation.
- "A smart microfluidic affinity chromatography matrix composed of poly(*N*-isopropylacrylamide)-coated beads." Noah Malmstadt, Paul Yager, Allan S. Hoffman, and Patrick S. Stayton. *Analytical Chem.* **75**(13):2943-2949. 2003.
- "Affinity thermoprecipitation and recovery of biotinylated biomolecules via a mutant streptavidin-smart polymer conjugate." Noah Malmstadt, David E. Hyre, Zhongli Ding, Allan S. Hoffman, and Patrick S. Stayton. *Bioconjugate Chem.* **14**(3):575-580. 2003.
- "Molecular basis for asymmetrical growth in two-dimensional streptavidin crystals." Todd C. Edwards*, Noah Malmstadt*, Sandy Koppenol, Masahiko Hara, Viola Vogel, and Patrick S. Stayton. *Langmuir.* **18**(20):7447-7451. 2002. *Joint First Authors
- "Kinetics and mechanism of pentachlorophenol degradation by sonication, ozonation, and sonolytic ozonation." Linda K. Weavers, Noah Malmstadt, and Michael R. Hoffmann. *Environmental Science & Technology.* **34**(7):1280-1285. 2000.

Poster Presentations

- "Temperature-dependant smart bead adhesion: A versatile platform for biomolecular immobilization in microfluidic devices." Noah Malmstadt, Allan S. Hoffman, and Patrick S. Stayton. Presented at the Gordon Research Conference on the Physics and Chemistry of Microfluidics, August 2003.
- "Microfluidic affinity chromatography using a temperature-responsive smart polymer matrix." Noah Malmstadt, Allan S. Hoffman, and Patrick S. Stayton. Presented at *LabAutomation 2003*, February 2003.
- "Microfluidic affinity chromatography using a temperature-responsive smart polymer matrix." Noah Malmstadt, Allan S. Hoffman, and Patrick S. Stayton. Presented at *Gels, genes, grafts & giants: Transitioning biomaterials into the 21st century, A symposium in honor of the 70th birthday of Professor Allan S. Hoffman*, December 2002.
- "Atomic force microscopy of two-dimensional crystals of a novel streptavidin mutant." Noah Malmstadt, Todd C. Edwards, Viola Vogel, Masahiko Hara, and Patrick S. Stayton. Presented at the Biomedical Engineering Society 2000 Fall Meeting.